TECHNICKÁ UNIVERZITA V LIBERCI
Fakulta strojní

Mechanical Properties of Geopolymer Based Composite Thin-plate Reinforced with Textile Meshes

Disertační práce

Studijní program:	P2301 Strojní inženýrství
Studijní obor:	Materiálové inženýrství
Autor práce:	**Ing. Hiep Le Chi**
Školitel práce:	prof. Ing. Petr Louda, CSc. Katedra materiálu

Liberec 2020

Prohlášení

Prohlašuji, že svou disertační práci jsem vypracoval samostatně jako původní dílo s použitím uvedené literatury a na základě konzultací s vedoucím mé disertační práce a konzultantem.

Jsem si vědom toho, že na mou disertační práci se plně vztahuje zákon č. 121/2000 Sb., o právu autorském, zejména § 60 – školní dílo.

Beru na vědomí, že Technická univerzita v Liberci nezasahuje do mých autorských práv užitím mé disertační práce pro vnitřní potřebu Technické univerzity v Liberci.

Užiji-li disertační práci nebo poskytnu-li licenci k jejímu využití, jsem si vědom povinnosti informovat o této skutečnosti Technickou univerzitu v Liberci; v tomto případě má Technická univerzita v Liberci právo ode mne požadovat úhradu nákladů, které vynaložila na vytvoření díla, až do jejich skutečné výše.

Současně čestně prohlašuji, že text elektronické podoby práce vložený do IS/STAG se shoduje s textem tištěné podoby práce.

Beru na vědomí, že má disertační práce bude zveřejněna Technickou univerzitou v Liberci v souladu s § 47b zákona č. 111/1998 Sb., o vysokých školách a o změně a doplnění dalších zákonů (zákon o vysokých školách), ve znění pozdějších předpisů.

Jsem si vědom následků, které podle zákona o vysokých školách mohou vyplývat z porušení tohoto prohlášení.

27. května 2020 Ing. Hiep Le Chi

ACKNOWLEDGMENTS

I take this opportunity with immense pleasure to express my deep sense of gratitude to my thesis supervisor Prof. Petr Louda for offering me the opportunity to undertake my PhD study after I have completed my master's program in this University, for providing the project for this study, for the trust he put in me during these years and for his urging, patience, which motivated me to complete this thesis. I do sincerely acknowledge the freedom rendered to me by him for independent thinking, planning and executing the research.

I am also very thankful to Ing. Vladimír Kovačič for many supports during all the time I study here.

I would like to thank to Ing. Vladimír Nosek for helping me in correcting the grammar of Czech language, revising and correcting the format of the bibliography, and list of my publications.

I also wish to extend my thanks to PhD. Lukáš Voleský, Ing. David Pospíšil, PhD. Totka Bakalová, Ing. Le Van Su and PhD. Pavel Kejzlar for their assistance in handling some of the work that is involved in my research.

I thank profusely all the staff of the department of material science, the Technical University of Liberec for their kind help and co-operation throughout my study period.

Last but definitely not least, I am grateful to my family especially my parents and my wife for their boundless support with their patience and prayer for accomplishing this study.

In God I Trust

Hiep Le Chi

ABSTRAKT

Je známo, že portlandský cement je stavebním stavebním materiálem, který má prokazatelně velmi dobré mechanické vlastnosti. Proces výroby Portlanského cenmentu však vyžaduje vysokou spotřebu energie a vyvolavá velké množství emisí CO_2. Tato vlastnost je považována jako jedna z hlavních příčin globálního oteplování. Z tohoto důvodu se stavební průmysl stále více obrací na používání materiálů šetrných k životnímu prostředí, aby splnil cíle udržitelnosti potřebné pro moderní infrastruktury.

Geopolymery jsou novou třídou stavebních materiálů vyvinutých primárně jako ekologická a udržitelná alternativa ke konvenčním stavebním materiálům na bázi cementu. Vzrůstající zájem o oblast kompozitních materiálů vyrobených geopolymerní matricí a textilními výztuhami. Tato disertační práce popisuje experimentální zkoumání ohybového chování tenkovrstvých kompozitů z geopolymerní malty a textilních výztuží, o který lze uvažovat s ohledem na jejich možné využití v budoucích budovách. Geopolymerová malta se nejprve optimalizuje na základě kombinace geopolymerního pojiva a různých plniv s přiměřeným mísícím poměrem, aby se dosáhlo konečného produktu s požadovanou mechanickou pevností. Poté jsou vybrány dva typy malty pro použití jako matrice s proměnlivým přidáním nasekaných čedičových vláken pro textilem vyztužený geopolymerní kompozit. Bylo zkoumáno několik parametrů, jako jsou textilní typy, míra vyztužení, druh malty, dávkování a délka nasekaných čedičových vláken, aby se zjistil jejich vliv na ohybové vlastnosti kompozitů na tenké desce. Byly provedeny zkoušky čtyřbodovým ohybem a rázovou zkouškou Charpyho kladivem a byly prezentovány experimentální výsledky. U kompozitů geopolymeru vyztuženého čedičovou textilií výsledky ukazují, že k vyztužení vzorků by mělo být použito vícevrstvého a malosíťového typu čedičové textilie, aby bylo dosaženo vysoké účinnosti zpevnění. Naproti tomu použití uhlíkových textilií při výrobě kompozitů s geopolymerní matricí s vysokou pevností jim umožňuje dosáhnout relativně vysoké mechanické pevnosti. Hodnota pevnosti v ohybu a houževnatosti v ohybu je silně ovlivněna mírou vyztužení a mechanickými vlastnostmi vláknité příze uhlíkové textilie. Navíc přídavek nasekaného čedičového vlákna (BF) hraje důležitou roli jak ve zlepšené mechanické pevnosti, tak v režimu porušení geopolymerních textilních kompozitů. Experimentální výsledky z nárazového testu Charpyho také ukázaly, že použití jak nasekaných čedičových vláken, tak textilních vláken zlepšilo absorpční kapacitu energie výsledných vzorků.

***Klíčová slova*:** *geopolymerová malta, geopolymer vyztužený textilem, čtyřbodový ohybový test, režim porušení, sekané čedičové vlákno, uhlíkový textil, čedičový textil, mechanická pevnost, rázová pevnost.*

ABSTRACT

It is well-known that Portland cement is a construction building material with admirable mechanical properties which are proven. However, the Portland cement production process requires high energy consumption and it involves a large amount of CO_2 emission. This binder is attributed to one of the major causes behind global warming. For this reason, the construction industry is increasingly turning to the use of environmentally friendly materials in order to meet sustainability goals needed for modern infrastructures.

Geopolymers are a new class of construction materials developed primarily as an eco-friendly and sustainable alternative to conventional cement-based construction materials. Due to the increasing interest in the area of composite materials made by geopolymer matrix and textile reinforcements. This dissertation reports on the experimental investigation of the flexural behavior of geopolymer composite thin-plates made of geopolymer mortar and fiber reinforcements that keeping in mind for their possible use for future buildings. Geopolymer mortar is firstly optimized based on a combination of geopolymer binder with various fillers that is mixed in various mixing ratios to achieve the final product with the desired mechanical strength. Geopolymer mortar is then selected to use as a matrix considering varying addition of chopped basalt fibers for producing textile reinforced geopolymer composite. Several parameters such as textile types, reinforcement ratio, mortar type, and different fiber lengths of chopped basalt fibers inclusion dosage were studied to investigate their effect on the flexural properties of the composite thin-plates. The four-point bending test and impact Charpy test were performed; and the experimental results were presented. For basalt textile reinforced geopolymer composites, the results reveal that the multi-layer and small net size type of basalt textile should be used to reinforce the specimens in order to achieve high reinforcement effectiveness. In contrast, the use of carbon textiles in the production of high-strength geopolymer matrix composites makes it possible for them to achieve a relatively high mechanical strength. The value of the flexural strength and flexural toughness is strongly influenced by the reinforcement

ratio and the mechanical properties of the fiber yarn of the carbon textile. Besides, the addition of the chopped basalt fiber (BF) plays an important role in both the improved mechanical strength and the failure mode of the geopolymer textile composites. The experimental results from the Charpy impact test also showed that using both chopped basalt fiber and textile fiber has improved the energy absorption capacity of the resulting samples.

Keywords: *geopolymer mortar, textile reinforced geopolymer, four-point bending test, failure mode, chopped basalt fiber, carbon textile, basalt textile, mechanical strength, impact strength.*

TABLE OF CONTENTS

LIST OF FIGURES

LIST OF TABLES

1. INTRODUCTION

1.1 Background

For many decades now, the ordinary Portland cement-based concrete (PCC) has been most widely used as construction material, due to its outstanding properties, such as high durability, high compressiveness, desired mechanical strength concerning economic efficiency, ability to be cast into any desired shape, and that its ingredients are available in the most places. Besides this, an inherent disadvantage of PCC is that it contributes to environmental pollution due to CO_2 emission in the Portland cement production process. The production of a ton of cement is usually associated with the emission of 0.73 to 0.99 tons of CO_2, and the cement industry is one of the major distributions to the global CO_2 emissions, where these industries emit approximately 7% of the global share [1, 2]. In such a context, the development of innovative new building materials is needed to substitute Portland cement. A new binding material known as a geopolymer, developed by Davidovits in 1978 [3], is being considered as a possible substitute to Portland cement. Geopolymers are produced by a combination of rich source materials in silica and alumina such as metakaolin, fly ash, etc. with alkali activators that have been emerged as a novel building material for civil engineering more than three decades ago, and they are in recent years becoming an interesting topic in research for both the international scientific community and industrial firms. It is well-known that these materials could potentially offer an effective alternative over ordinary Portland cement concrete (OPC) for a variety of applications. The main reason for replacing OPC is that OPC contributes to environmental pollution due to CO_2 emission in the Portland cement production process from the calcination of limestone and the combustion of fossil fuel.

Due to the increasing need for new materials to be produced with low energy consumption thatoffer sustainability, economy, feasibility, and particularly good mechanical properties, textile-reinforced concrete has attracted the consideration of many scientists over the past three decades. Composites resulting from a combination of multi-axial textile reinforcement and a fine-grained aggregate-based cementitious matrix named textile reinforced concrete (TRC), bring the opportunity to repair/strengthen the old/new reinforced concrete structures. This is due to the favorable properties offered by TRC, such as its resistance to corrosion, its high strength to weight ratio, its ease and speed of

application, and the minimum change in geometry. Furthermore, TRC composites are also considered when manufacturing lightweight concrete structures or prefabricated sandwich panels with outstanding mechanical performance, thin-wall panels, and high-performance concrete construction with free-form designs [4-6].

Because of the increasing interest in the area of composite materials made by the geopolymer matrix and textile reinforcements, the present study aims to investigate the effectiveness of textile reinforcements made of basalt fiber and carbon fiber combined with chopped basalt fiber on flexural properties and failure modes of the textile geopolymer mortar.

1.2 Research Objectives of Dissertation

This dissertation deals with the design of the sample manufacturing process and the test the mechanical properties regarding four-point bending strength and Charpy impact strength of reinforced geopolymer composites – named textile reinforced geopolymer (TRG) – for a variety of the applications in civil infrastructure. Specific objectives of this research are detailed below:

- Optimization of the geomortar matrix with the highest mechanical strength based on incorporating various reinforcement materials.
- Experimental investigation of the effect of various parameters such as textile type, net size, reinforcement ratio on the mechanical properties and failure behaviour of textile geopolymer composite under four-point bending test.
- Experimental investigation of the effect of various parameters of chopped basalt fiber such as different fiber lengths, added dosages, mixing methods on the mechanical properties and failure behaviour of textile geopolymer composites under four-point bending test.
- Experimental investigation of the effect of textile types and added dosages of chopped basalt fiber on the impact strength of textile geopolymer composite under the Charpy impact test.

1.3 Organization of Dissertation

This dissertation is composed of 9 parts:

Part 1 provides an introduction and background, and objectives of the dissertation.

Part 2 represents a literature review on textile-reinforced concrete, geopolymers and their characterization, fiber geopolymer composites.

Part 3 describes the raw materials used in this thesis, the process of the geomortar mixing and casting samples, and test methods.

Part 4 evaluates the mechanical strength of the geomortar based on the incorporation of the various fillers.

Part 5 and 6 investigate the flexural behavior of geopolymer composite reinforced with basalt fiber and carbon fiber meshes.

Part 7 investigates the effect of chopped basalt fiber on the flexural behavior of textile geopolymer composites.

Part 8 investigates the impact resistance performance of textile reinforced geopolymer composites.

Part 9 represents the overall conclusion and recommendations for future research.

2. LITERATURE REVIEW

2.1 Textile reinforced concrete (TRC)

Although this thesis is focused on textile-reinforced geopolymer mortar composite, a brief review on textile-reinforced Portland cement-based concrete should be considered.

2.1.1 Introduction to textile reinforced concrete

Reinforced concrete with steel is the most successful building material in the past and today. Typical properties of concrete are high compressive strength and very low tensile strength. To improve the tensile strength, steel bar reinforcements are inserted into the concrete. Therefore, reinforced concrete with steel is very strong, durable, and cost-effective. But adding steel reinforcement to the structure will cause the reinforcement to corrode. Therefore, steel reinforcement needs a minimum cover layer between 20 and 70 mm against corrosion during the given service life of the structure. However, keeping in mind that some places of building structures do not require such strong concrete profiles, the question is what type of concrete could be lighter, more efficient, and more elegant. For this reason, textile-reinforced concrete was developed.

Textile Reinforced Concrete (TRC) is a composite material, which has been considered as a building material for more than a decade [7]. This composite material is fabricated using a fine-grained concrete matrix reinforced by multi-axial textile fabrics [7]. The textile reinforcements used as reinforced in concrete are alkali resistance glass, carbon, basalt, or aramid fabrics, et. The textile reinforcement plays a key role in carrying the bearing capacity and stiffness of composite materials. This type of composite can be used in a variety of applications, such as repairing and/or strengthening the structural elements of old structures, load-bearing elements in new structures, new thin-wall elements, and the lightweight concrete system [4–6].

- ***Cementitious matrix***

Fine-grained concrete is commonly used to improve the bond between the fiber yarns and the matrix by increasing the probability of penetration of concrete between filaments. The mixture needs to be able to penetrate the fiber yarns and filaments of the textile reinforcements. The geometry of the fabrics limits the maximum grain size of the matrix to values varying between 2 and 4 mm.

- ***Textile reinforcements***

In TRC applications, bi- or multi-axial 2D and 3D textile meshes can be used as reinforcement (see Figure 2.1). For a simple bi-axial case, the mesh comprises two groups of textile fiber yarns (threads), warp (0°) and weft (90°), interwoven perpendicularly to each other. Yarns are composed of multiple single fibers of continuous length, also designed as filaments; a grouping of continuous fibers is primarily done to obtain the desired thickness of the yarn. Filament yarns, consisting of drawn parallel fibers, are often used for reinforcing applications as they present smaller structural elongation in comparison to other forms of yarns, e.g. twisted and bonded. The fineness of yarn is measured in tex (g/1000 m) and is a function of the number of filaments, average filament diameter, and density. Moreover, the fabrication method and applied sizing to fibers have a significant effect on the interaction between the assembled filaments, as such, the mechanical properties of a fiber filament decrease when in yarn form [6].

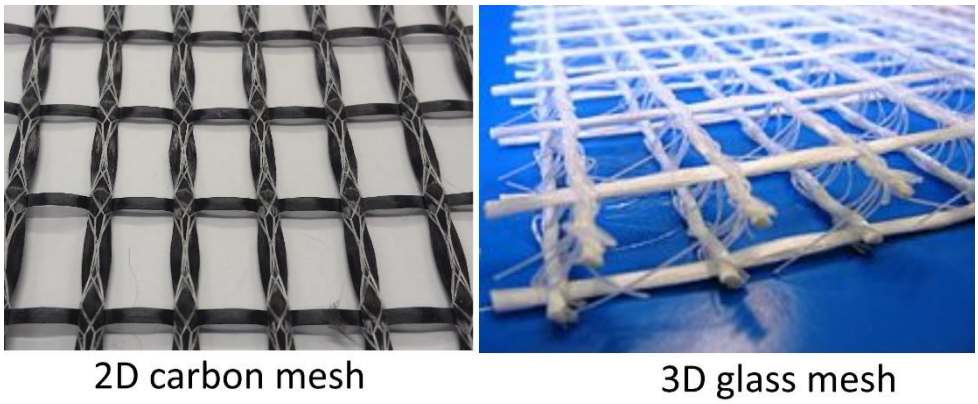

Figure 2.1 Overview of 2D mesh and 3D mesh structures reinforced in concrete.

2.1.2 Mechanical behavior of TRC composite

- ***Stress-strain behavior of TRC***

Textile reinforced concrete has different mechanical behaviour in tension and compression. In compression, the composite can be considered to behave linearly elastic up to fracture. In tension however, cracks initiate and propagate in the brittle matrix composite at very low-stress levels [8]. Figure 2.2 shows the nonlinear stress-strain behaviour in tension of TRC.

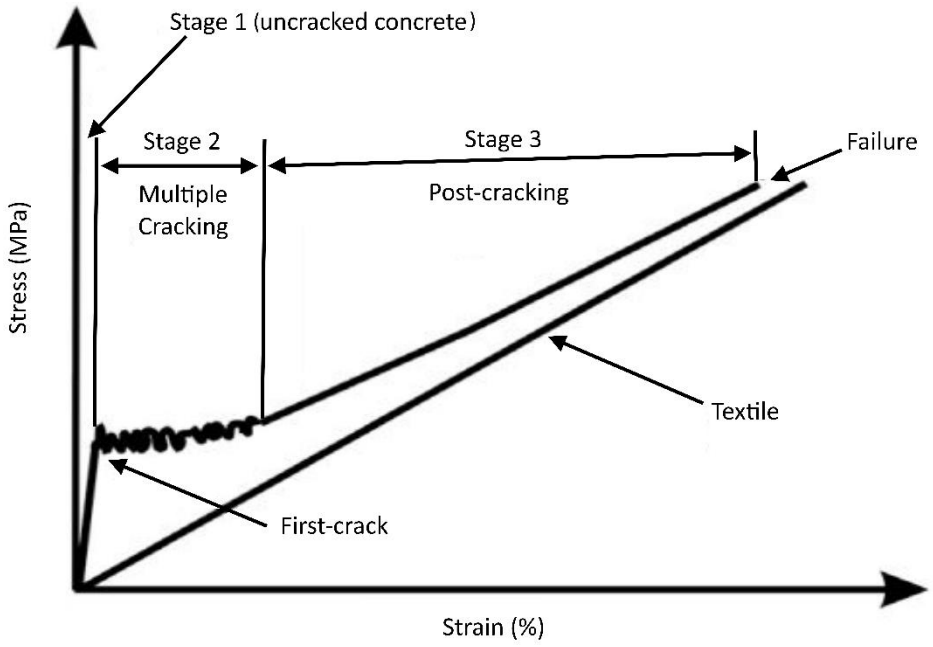

Figure 2.2 Typical stress-strain diagram of textile reinforced concrete under uniaxial tensile loading [8].

It can be seen that the curve behavior can be divided into three stages, as in Figure 2.2.

Stage I – This stage is identified by a linear increase in the load until the first crack in the matrix happened. This stage is called an elastic linear pre-cracking stage resulting from a combination of the geopolymer matrix and textile reinforcement.

Stage II – Multiple cracking stage occurs when the tensile strength of the cementitious matrix is reached as the proven oscillation of the curve when the applied load continues to increase, leading to the obvious pseudo-ductility behaviour of the composite. The rate of oscillation and slope of this phase depend strongly on the mechanical properties of the fiber yarn, reinforcement ratio, and mortar matrix. The number of cracks that each specimen will have is originated in this stage.

Stage III – Post-cracking or crack-widening stage. In this stage the contribution of the geopolymer matrix is almost unaffected, the textile reinforcement governs the flexural behaviour of the composites. This stage ends once the load-bearing capacity of the composite cannot be carried out anymore through the ultimate load achieved.

Aveston, Cooper and Kelly (1971) developed a theoretical model for these phenomena, hereby referred to as the ACK theory. This model is described briefly below and displayed in Figure 2.3.

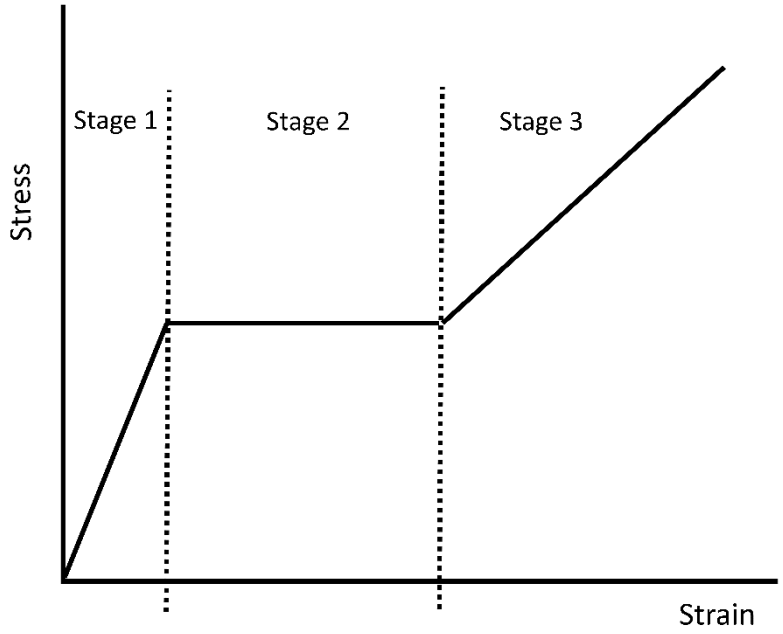

Figure 2.3 Stress-strain curve predicted by the ACK model [9].

During Stage I – Pre-cracking, the composite is uncracked, and both the matrix and the fibers contribute to the global stiffness following the "law of mixtures", assuming a perfect bond. The latter results in an equal strain in the fibers and the matrix, developing the following equation

$$\sigma_c = \sigma_m V_m + \sigma_f \eta V_f \qquad (2.1)$$

$$\sigma_c = \sigma_m (1 - V_f) + \sigma_f \eta V_f$$

where,

σ_c is the composite stress; σ_m is the matrix stress, $E_m\varepsilon_m$; σ_f is the fiber stress, $E_f\varepsilon_m$; ε_m is the matrix strain; E_m is the modulus of elasticity of the matrix; E_f is the modulus of elasticity of the fiber; V_f is the volume fraction of fiber; V_m is the volume fraction of the matrix; η is the efficiency factor ($0 \leq \eta \leq 1$) which accounts for the variation in composite properties with fiber architecture, Eq. 2.1. It must be said that these equations apply to the case of the one-dimensional direction of the fiber [9].

Stage II – Multiple cracking, the matrix's tensile failure stress σ_{mu} is reached and cracks start to initiate and propagate along the composite. The first crack occurs when the strain of the composite becomes greater than the ultimate matrix strain ε_{mu}. Thus, the composite does not fail if the ultimate load of the fiber is more than the ultimate load of the composite ($\sigma_{cu} > \sigma_c$).

$$\sigma_{fu}\eta V_f > E_m\varepsilon_{mu}V_m + E_f\varepsilon_{mu}V_f \qquad (2.2)$$

where ε_{mu} is the ultimate strain of matrix; σ_{fu} is the ultimate strength of the fiber.

After the cracking point, the post cracking behaviour depends on the critical volume fraction ($V_{f\,crit}$). As a result of the zero stress that can be carried by the matrix at the cracks, the volume fraction of fiber is drawn from Eq. 2.1, as follows:

At cracked section: $\sigma_m = 0$

The quantity of the fibers resists the load is: $\sigma_f = \sigma_{fu}$

Therefore,

$$V_{fcrit} = \frac{\sigma_c}{\eta\sigma_{fu}} \qquad (2.3)$$

Normally, the composite stress is similar to matrix stress before cracking ($\sigma_c \approx \sigma_{mu}$), thus:

$$V_{fcrit} = \frac{\sigma_{mu}}{\eta\sigma_{fu}} \qquad (2.4)$$

Therefore, if $\eta V_f \gg V_{f\,crit}$, and as a result of the increasing the applying load, the multiple cracking region forms. The mechanism of this stage is that the stress on the fibers at the first crack is transferred back into the matrix and, with an increase in the applied load, another matrix crack forms until the matrix is full of parallel spaced cracks [9].

Stage III – Post-cracking, the volume fraction of fibers is much greater than the critical volume fraction, the post cracking region forms once no further cracking occurs. In this stage, the additional load is completely carried by the fibers which results in pull out or rupture of fibers until the composite fails [9]

$$\sigma_{cu} = \eta V_f \sigma_{fu} \qquad (2.5)$$

where σ_{cu} is the ultimate composite strength; σ_{fu} is the ultimate fiber strength.

- ***Flexural behavior of TRC***

The behaviour of a reinforced concrete beam under bending performance is normally analyzed with respect to load and deflection rather than stress and strain. The typical flexural load-deflection curve is depicted in Figure 2.4, along with the indicated loading stages. In general, these behavioural stages are similar to those previously described for the tensile behaviour.

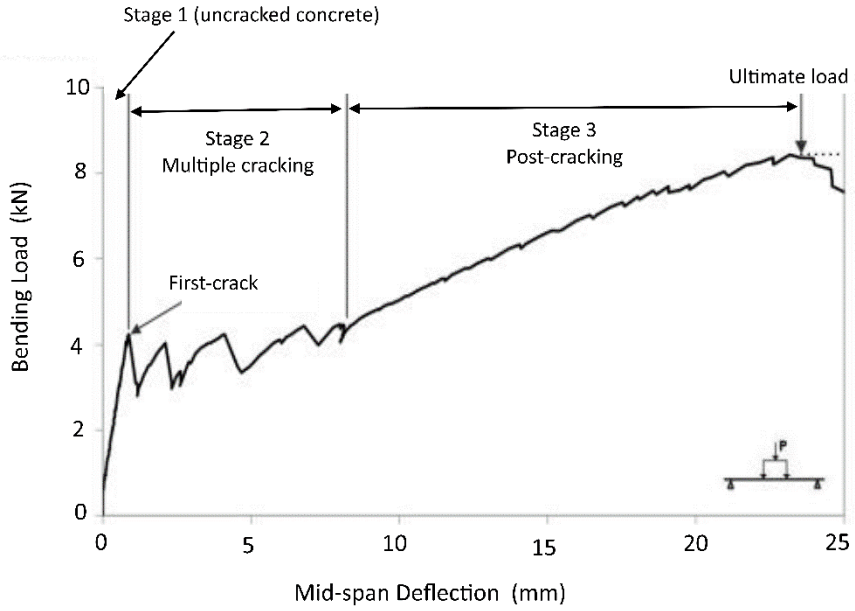

Figure 2.4 Typical bending load-deflection behaviour for a TRC under four-point bending [10].

It should be noted that the curve response does not always have to follow three distinct stages, regardless of any type of test setup. Behaviour of stage 2 and 3 depends strongly on textile type, reinforcement ratio, textile structure, etc. [11, 12]. Rambo et al. [11] investigated the mechanical behavior of basalt textile reinforced refractory concrete. The results showed that in the case of the TRC reinforced with only one fabric layer the stages II and III, typically seen in TRC, are absent, whereas the TRC produced with 3 and 5 fabric layers showed a strain hardening behavior with three different stages (see in Figure 2.5). Peled and Bentur [12] found the flexural behaviour of the TRC composites reinforced by crimped structure textile is better than woven fabric, and the woven structure textile is better than the straight roving, all at the same volume fraction, as shown in Figure 2.6. This good behaviour in crimped geometry can be accounted for by bonding as they found that crimped

yarn contributed significantly to the bond due to the anchoring effect. It can be seen that the flexural strength of woven fabric is almost double that of straight yarn.

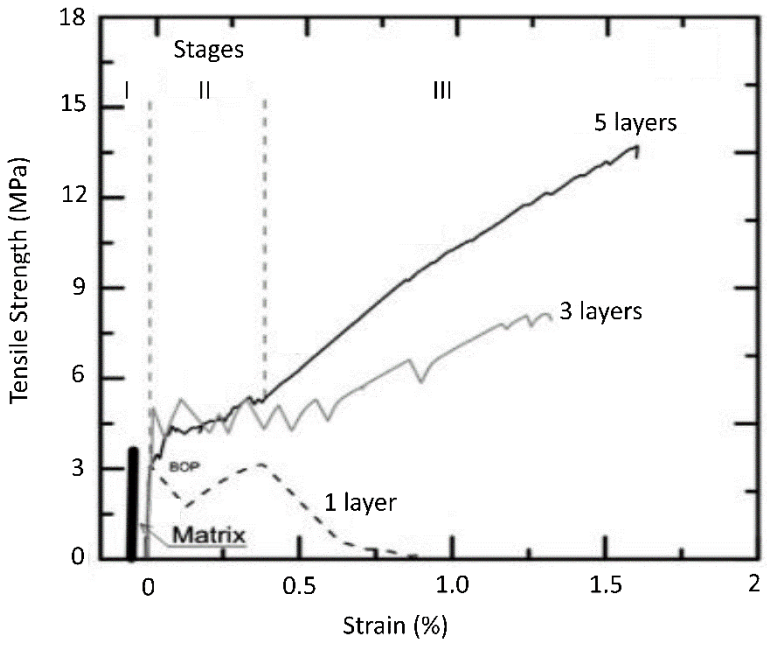

Figure 2.5 Effect of basalt textile reinforcement on the tensile behaviour of the TRC [11].

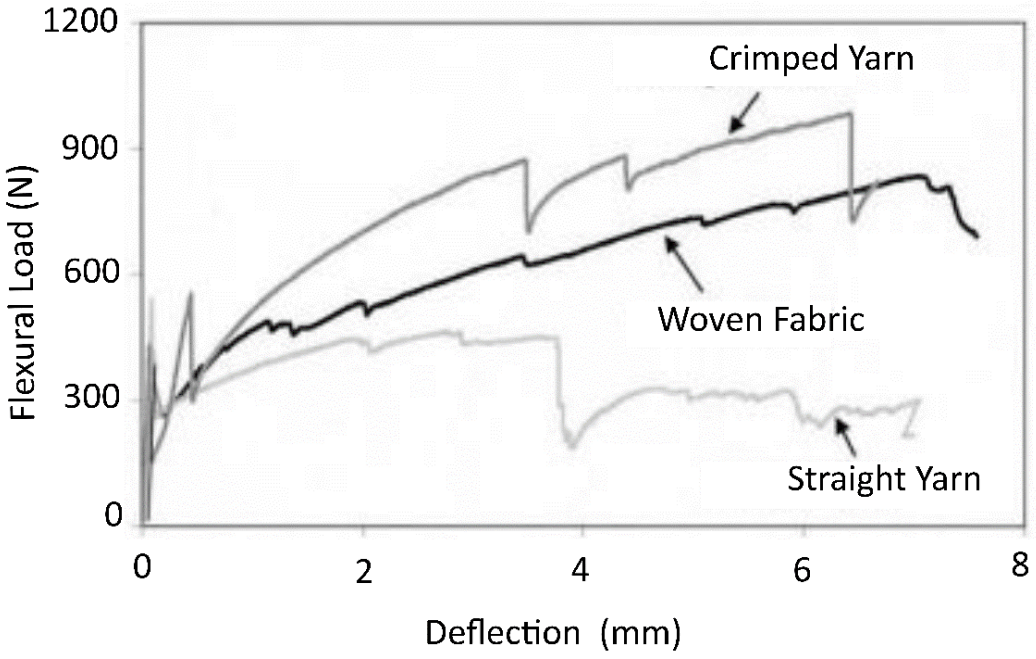

Figure 2.6 Flexural response of the TRC with fabric woven, untied crimped yarns and straight yarns, all from Polyethylene at V_f = 7.5 % [12].

2.2 Geopolymers

2.2.1 Term geopolymer and geopolymerization process

Geopolymers are inorganic aluminosilicate polymers belonging to the group of alkali-activated materials with non-crystalline networks, which are ceramic-like in their structures and properties. The term geopolymer was originally introduced by the France scientist Prof. Joseph Davidovits in the 1970s [3]. Geopolymers are synthesized from a two-component blend, including an alkaline solution primarily based on potassium or sodium and solid alumino-silicate materials based on metakaolin or fly ash at the room, or slightly higher, temperature. The polysialate terminology was suggested in the early 1980s by Davidovits to design the chemical structure of geopolymers. The sialate bond is termed by a Si – O – Al linkage-type, whereas a Si – O – Si linkage-type called a siloxo bond. The polysialate network is believed to consists of tetrahedral SiO_4 and AlO_4 units linked alternatively by sharing oxygen atoms, and alkali metal cations (Na^+, K^+, e.g.). The existence of the cations in the framework cavities is responsible for balancing the negative charge of Al^{3+} in IV-fold coordination. Polysialate has this empirical formula:

$$M_n \{-(SiO_2)_z\text{-}AlO_2\}_n, wH_2O$$

where M is an alkali cation such as potassium or sodium, and n is a degree of polycondensation; z is 1, 2, 3. Polysialates are chain and ring polymers with Si^{4+} and Al^{3+} in IV-fold coordination with oxygen and range from amorphous to semi-crystalline. So, based on Si/Al ratio some types of geopolymer were described in Figure 2.7, whereas Figure 2.8 showed the overall final structure of geopolymer proposed by Barbosa [13].

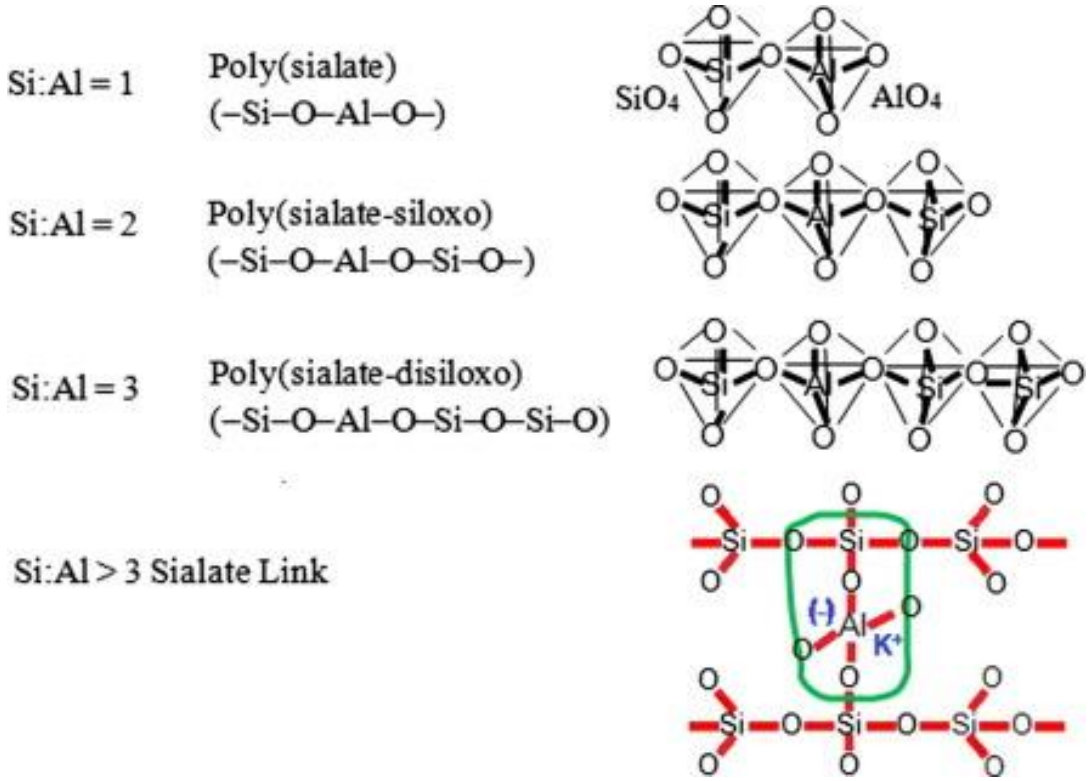

Figure 2.7 Geopolymer terminology proposed by J. Davidovits [3]

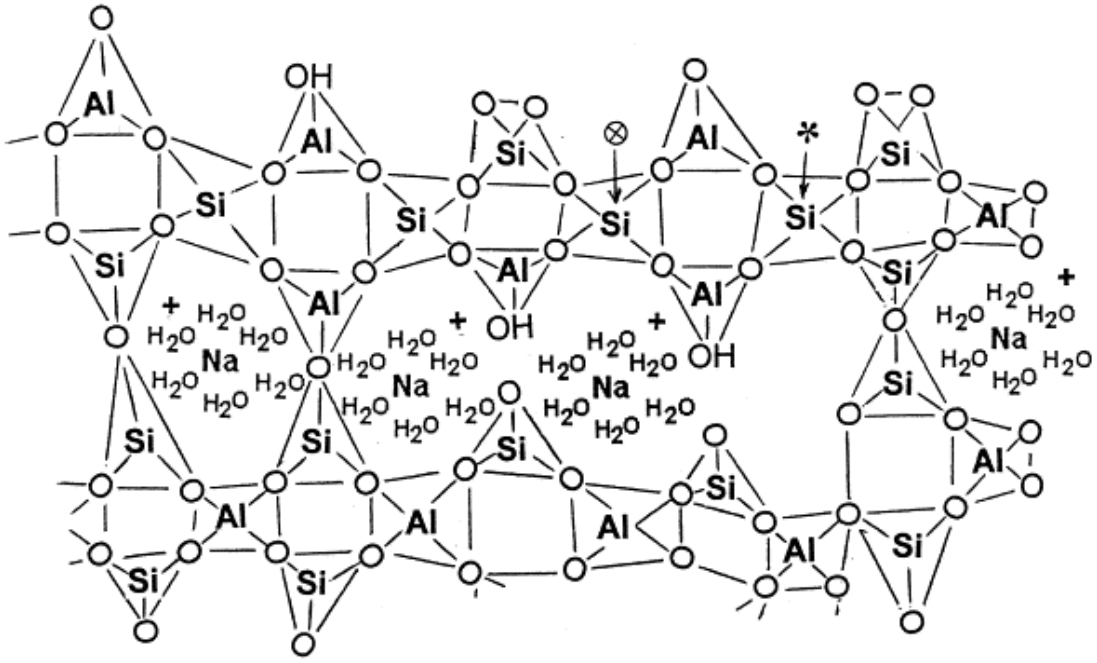

Figure 2.8 Semi-schematic structure for Na – polysialate polymer proposed by Barbosa, Mackenzie, and Thaumaturgo [13].

The reactions that occur during the geopolymer formation and solidification processes are generally named by the overall term geopolymerization. This process is very complicated and currently not fully understood. Glukhosky was the first researcher who proposed a general mechanism for the alkali activation of materials primarily comprising silica and reactive alumina in the 1950s. Gluhhovsky model divides the process into three stages: (a) destruction – coagulation; (b) coagulation – condensation; (c) condensation – crystallization. More recently, different authors have elaborated on and extended the Glukhovsky theories and applied the accumulated knowledge about zeolite synthesis in order to explain the geopolymerization process as a whole, leading to Duxson et al. to publish a reaction mechanism mode for geopolymerization (Figure 2.9) [14]. In the conceptual model by Duxon et al., the geopolymerization process is described in the following way. Dissolution of alumina and silica due to contact with alkali activating solution leads to the formation of individual alumina and silicate species (probably as monomers). It is the first step in geopolymerization. These monomers interact to form dimers, and further trimers, tetramers and so on. The aluminosilicate gel precipitates when the solution reaches saturation. Since reactive aluminum dissolves faster than silicon, initially the precipitated gel (Gel 1) is aluminum-rich. As the reaction progresses, more silicon is dissolved from the aluminosilicate source, and the concentration of silicon in the gel increasing giving rise to Gel 2. All these stages including dissolution, speciation, equilibrium, gelation, reorganization, polymerization, and hardening go on simultaneously. It requires an alkaline solution for the dissolution of aluminosilicate source, as well as for catalysis of the condensation reaction [15].

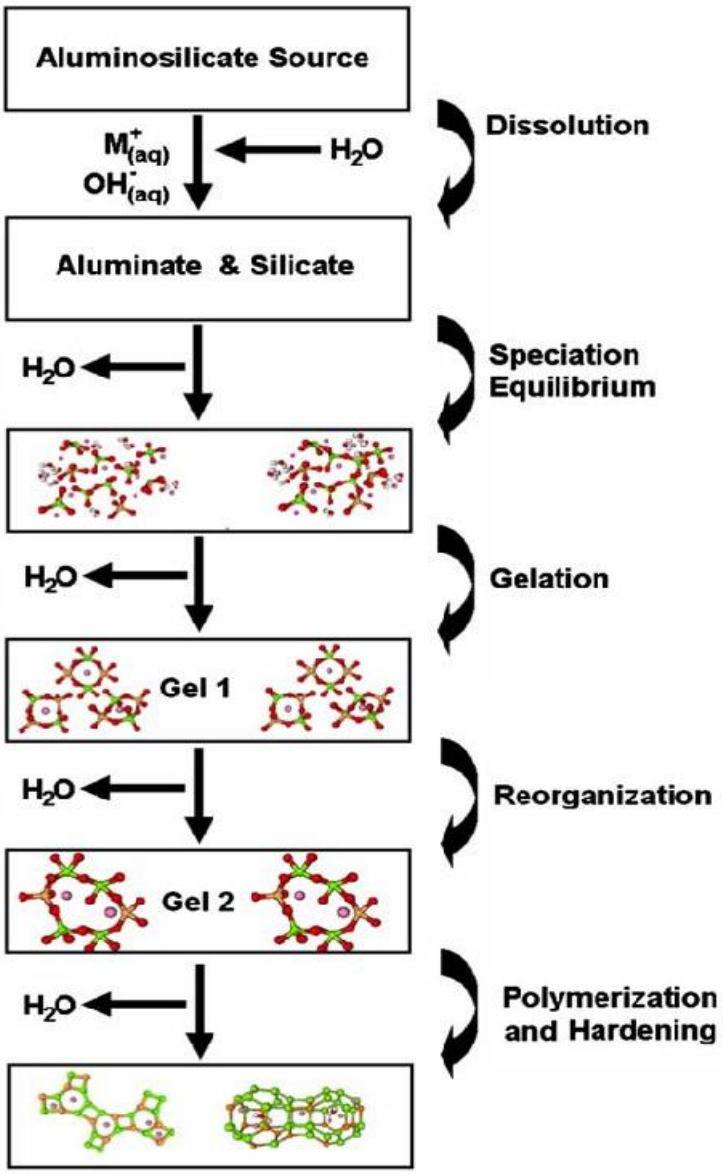

Figure 2.9 Reaction mechanism model for geopolymerization [14].

2.2.2 Raw materials and activating solutions

Various source materials that are rich in silica and alumina can be dissolved in an alkali solution that can act as a geopolymer precursor. The possible raw materials include natural minerals, calcined clays, metakaolin, industrial and by-products, such as fly ash, slag, red mud or waste glass or the mixture of these materials, but the most commonly used alumino-silicate source materials are class F fly ash and metakaolin, which have the different mass content of SiO_2 and Al_2O_3 with a very low rate of CaO. The selection and preparation of the raw materials establish the properties of the final geopolymer products. These

characteristics may include the good mechanical properties, high compressive strength, low shrinkage, high fire resistance, low thermal conductivity and acid resistance [14, 16–19]. Besides the alumino-silicate source, an alkali solution commonly based on sodium and/or potassium is required to induce the geo-polymerization reaction. Therefore, the resultant structure of geopolymer depends greatly on both the quantity and concentration of the alkali solution. In general, the aluminosilicate materials are activated by an alkali solution with high-pH concentration. The influence of alkali solution on the properties of geopolymers has been largely studied in the literature. For example, the study of Duxson, et al. in 2007 presented the effect of the concentration of the alkali, the amount of silica on the strength development of geopolymer based metakaolin or fly ash [20]. The results were found that the strength increased with the increasing Si/Al molar ratio from 1.15 to 1.90, regardless of the alkali ratio. However, the strength value of geopolymer decreased for all the specimens beyond Si/Al = 1.90. This finding indicates that the mechanical strength of geopolymer is better when alkali solution contains some silicates, and the lowest strength is obtained for the Si/Al = 1.15 molar ratio with respect to geopolymers synthesized by alkali hydroxide only. However, the amount of silica in the alkali solution is not too high, which cause a decrease in strength. Concerning the different alkali contents, geopolymers show the similar compressive strength for a given Si/Al ratio, suggesting that the difference in mechanical strength between samples having various alkali contents is of 10 – 20%, see in Figure 2.10.

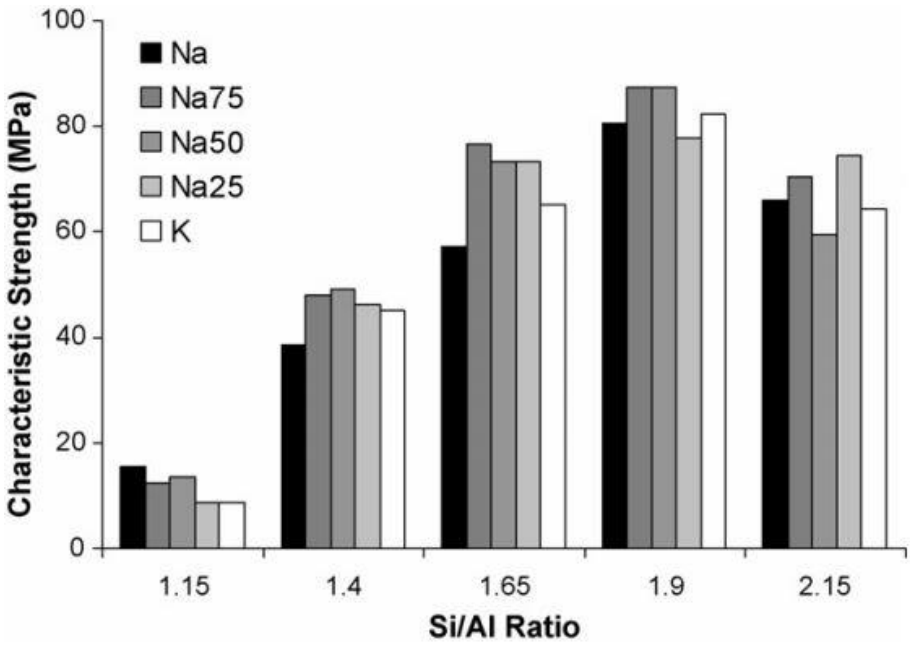

Figure 2.10 The compressive strength of geopolymer made by five different Si/Al ratios from alkali solutions with five different alkali cation ratios Na/(Na + K) = 0.00, 0.25, 0.50, 0.75 and 1.00 [20].

2.2.3 Mechanical performance and microstructure

Mechanical performance and microstructure of geopolymers strongly depend on the combined effects of SiO_2/Al_2O_3, Na_2O/Al_2O_3, Na_2O/H_2O, and Na/[Na + K] molar ratios in the alumina silicate and alkali solutions compositions. It was found that geopolymer gel structures with the desirable properties can be achieved when geopolymers are synthesized only at specific ranges of molar ratios [13, 19, 21]. Some researchers [22, 23] have gathered data in the literature to estimate the optimum formulation of geopolymers by artificial neutral networks resulting in the highest mechanical performance. Kamalloo et al. [22] used more than forty data items from the literature to create the filled contour plots which show the effect of R_2O/Al_2O_3 (where R = Na or K), SiO_2/Al_2O_3, and H_2O/R_2O molar ratios on the compressive strength of geopolymers based metakaolin (Figure 2.11). The finding shows that the optimized value for compressive strength is approximately about 80 MPa when the optimized SiO_2/Al_2O_3, R_2O/Al_2O_3, Na_2O/K_2O and H_2O/R_2O ratios were determined to be 3.6-3.8, 1.0-1.2, 0.6-1 and 10-11, respectively. Also from Figure 2.11 it could be obtained that optimum value of H_2O/R_2O ratio is about 10-11 to achieve high compressive strength. In the case of a high H_2O/R_2O ratio leads to the high amount of OH-

groups resulting in the fact that the amount of porosity tends to increase after condensation and this phenomenon induce a decrease in compressive strength of geopolymers. In other word, water provides the suitable media for geo-polymerization reaction and in low level of H_2O/R_2O ratios the rate of geo-polymerization reaction is low. Therefore, mechanical strength of geopolymer is decreased in low level of H_2O/R_2O ratios. Superposition of these mechanism make an optimum value of compressive strength in H_2O/R_2O =10-11 [22].

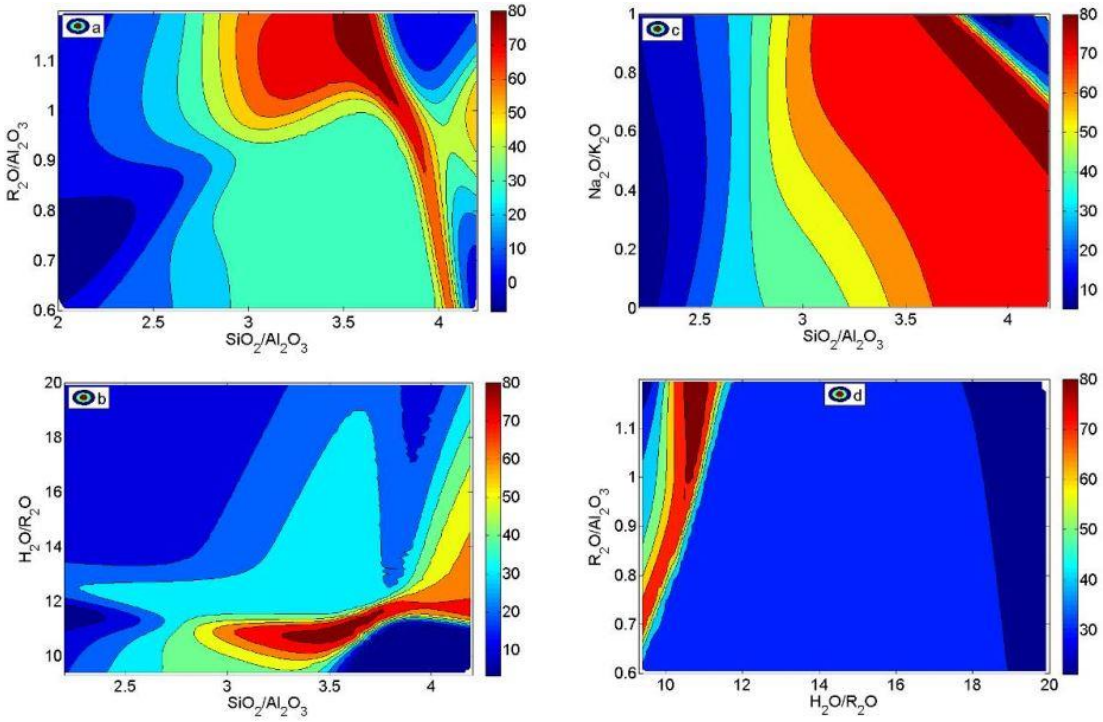

Figure 2.11 Filled contours plot of compressive strength that shows the effect of R_2O/Al_2O_3, SiO_2/Al_2O_3, Na_2O/K_2O and H_2O/R_2O ratios on compressive strength. The contours are in units of MPa [22].

It was observed that these molar ratios affect the mechanical performance of geopolymers, and also other properties, such as the microstructure and the porous network. Duxson et al. [19] have studied the relationship between microstructure and mechanical properties of metakaolin based geopolymers containing Si/Al molar ratios between 1.15 and 2.15 (2.3 < SiO2/Al2O3 < 4.3). The authors published SEM images of geopolymers exhibiting essential changes in microstructure by varying Si/Al molar ratio (Figure 2.12). The change in microstructure appears most dramatic between Si/Al ratios of 1.40 and 1.65. Specimens with Si/Al ≤ 1.40 exhibit a microstructure comprising large interconnected pores, loosely structured precipitates and unreacted material. Specimens with Si/Al ≥1.65 are classified

by a largely homogeneous microstructure containing unreacted particles and some smaller isolated pores. Moreover, geopolymers with Si/Al ratio ≥1.65 do not change significantly in microstructure with increasing Si/Al ratio. However, the specimens with Si/Al ratio of 1.90 show a slight decrease in the observed porosity. Therefore, improvement in microstructural homogeneity provides strong reasoning for the increase in mechanical properties at lower Si/Al ratios, but there is nothing directly observable in the SEM micrographs that can explain what is responsible for the decrease in strength above the maximum. Theoretically, Si-O-Si linkages are stronger than Si-O-Al and Al-O-Al bonds [21], meaning that the strength of geopolymers should increase with Si/Al ratio since the density of Si-O-Si bonds increases with Si/Al ratio [24]. The decrease in mechanical strength between specimens with Si/Al ratio of 1.90 and 2.15 suggests that other factors begin to affect the mechanical properties.

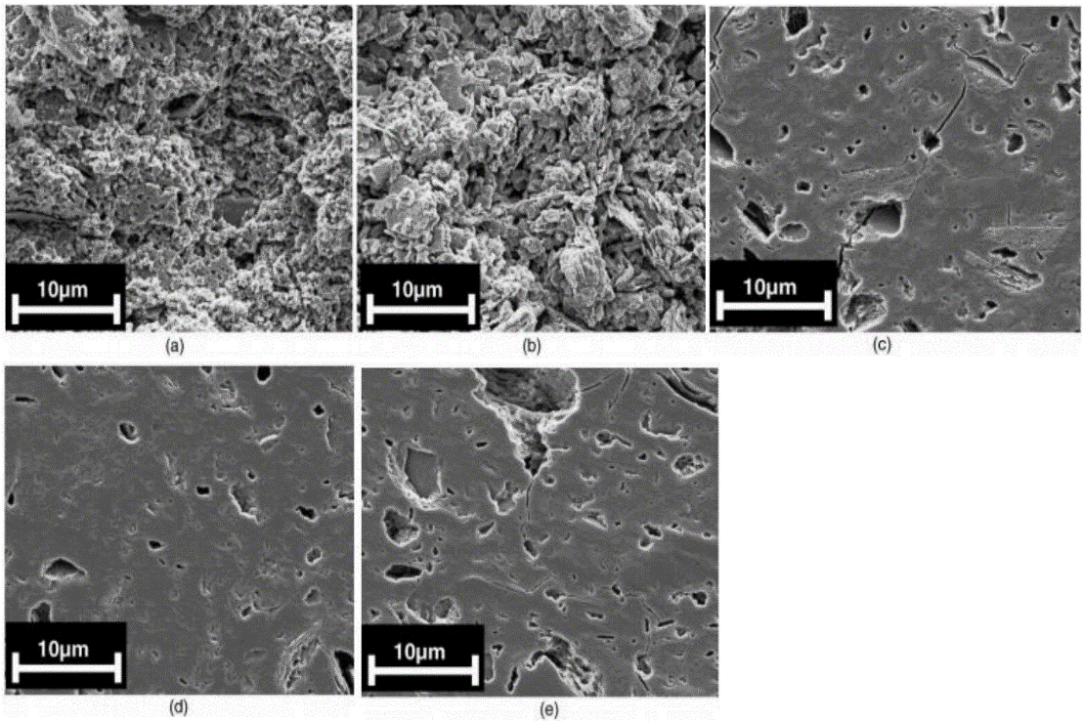

Figure 2.12 SEM micrographs of Na-geopolymers: Si/Al ratio of (a) 1.15, (b) 1.40, (c) 1.65, (d) 1.90 and (e) 2.15 [19].

2.3 Geopolymer matrix composites.

As previously outlined in the above section, the reasonable choice of molar ratios is a key factor to synthesis geopolymer binder with the desired mechanical properties. A basic understanding of these parameters for the fabrication of geopolymer binder should be

known when studying this material. However, this thesis does not focus on the production of geopolymer binder but focuses on the production of geopolymer matrix-based composite by incorporating reinforcement materials. It is well-known that the brittle nature of geopolymers, like most ceramics, make them difficult to be accepted as an engineering material. Although they show high compressive strength, their tensile strength and flexural strength are so low. Moreover, a pure geopolymer presents many defects and micro-cracks in its microstructure due to high shrinkage during the curing process. They are very sensitive to crack formation under loading [24]. Cracks continue to propagate as the load increases; as a result, geopolymers fail when faced with extra loads. Consequently, geopolymers should exist in the system of the multi-component materials through the addition of a variety of reinforcements into them, to form the geopolymer composites with improved mechanical properties and structures.

The particle reinforcements provide several advantages when being incorporated in geopolymer composites, particularly as they offer desirable material properties while geopolymer resin acts as a binding intermediate essential for structural applications. Depending on their properties, the addition of a new type of filler materials could improve one or more properties of geopolymer through chemical reaction or physical changes. Compared to fiber reinforcements, particle reinforcements in composites are less effective in flexural and tensile strengthening; but they mainly achieve gains in stiffness, compression, and wear-resistance, et. Moreover, the other benefit of these reinforcements is their low cost and ease of production and forming. The mortar prepared with geopolymerization process is known as geopolymer mortar. The core reinforcement of geopolymer mortar is sand. The sand acts as a filler material in making of mortar and also increases crushing strength and reduces shrinkage [25]. Sand also increases the volume of mortar which results in a reduction of the cost of the final products. In other words, micro or nano-grained fillers are often considered to be added to mortar to enhance its physico-mechanical properties since they act as both an excellent pore-filling material and a highly reactive pozzolanic material [26–32]. Silica fume (SF) is a by-product from ferrosilicon industry which contains extremely small particle sizes that act as micro-fillers. The average particle size of SF is relatively small, with good filling effect and can be filled between the cement particle gaps which improves the microstructure and decreases the porosity. Moreover, SF is comprised of amorphous spherical particles that enhance the rheological properties of the fresh mixture. At the fresh state of the mixture, silica fume reduces the

bleeding and segregation rate. At the same time, it contains a high percentage of amorphous silicon dioxide making it a highly reactive pozzolanic material. However, the overdose of silica fume had hindered the geopolymerization due to an increase in Si/Al affecting to mechanical and durability properties of the final product, accompanied by microstructures with high porosity. This high porosity, which is responsible for weaknesses in the specimen, is related to the amount of unreacted silica fume [30, 32, 33]. At the same time, the overdose of micro or nano-grained fillers had also engaged too much water, denying aluminosilicate sources around them water enough, resulting in decrease geo-polymerization reaction; thus so the porosity is relatively increased [34]. The experimental results from references [35, 36] showed that the porosity, bulk density, and pore size distribution were significantly impacted by the amount of sand added to geopolymer paste.

The main objective of incorporation of fiber reinforcements in brittle materials can help to improve the plastic cracking characteristics, the tensile or flexural strength, the impact strength and toughness and to control cracking and the mode of failure by means of post-cracking ductility and to improve durability [37]. In other words, there are three major requirements to be considered in the selection of fiber as reinforcement in concrete: i) compatibility of material properties with the application; ii) sufficient fiber-matrix interaction to transfer stresses; iii) optimum aspect ratio to secure effective post-cracking behavior [38]. The addition of fiber reinforcements in geopolymer matrix composites was first investigated in the 1980s by Davidovits et al. with the objective to manufacture molding tools and patterns for the plastic processing industry [39–41]. Up to date, a wide variety of fiber reinforcements (both organic and inorganic types) have been used to reinforce geopolymers with the aim of improving mechanical properties suitable for specific types of engineering application, including nanofibers [42], short fibers [43–51], continuous fibers [52–55], woven fabrics [56–60], among others. In the following sections, only basalt short fibers and fibers in the form of textile which are used as reinforcements in production of geopolymer matrix composites are summarised and discussed in some more details due to their involvement in this thesis work.

2.3.1 Basalt short fibers geopolymer composites

Short fiber reinforced composites are an important group of materials for engineering applications due to their adaptability to conventional manufacturing techniques and low

cost of fabrication. When mixed into concrete, randomly distributed fibers can bridge these cracks and arrest their development. By this mechanism, it has been well established that the addition of fibers can enhance the mechanical behaviour of plain concrete. The difficulty that fiber inclusion causes during the initial mixing, including balling of fibers and compacting problems, results in inadequately compacted and air-entrapped concrete. Nevertheless, the increase in fiber quantity results in a significant increase in strain energy density and thus imparts increased ductility to the composite.

Basalt fibers are environmentally friendly material made from natural volcanic basalt rocks through their melting process at a high temperature of about 1500 ºC. The quality and strength characteristic of basalt fiber depends mainly on the type of raw material and the manufacturing conditions [61]. Chemical compositions of basal fiber are rich in oxides of alumina and silica along a small amount of magnesium, calcium, sodium, potassium, silicon and iron [62]. It is observed that basalt is an inorganic fiber that is like glass fiber, has better tensile strength than the glass fiber, broader failure strain than the carbon fiber. Basalt fiber is a novel type of inorganic fiber that is considered as an effective alternative material for glass fiber. Both of these products have a similar manufacturing process, but basalt fiber obtains more economical and improved mechanical properties. Alkaline resistance of basalt fiber under accelerated aging or short-term aging conditions was investigated by some authors in previous studies [63–66]. Jongsung Sim et al. assessed the alkali resistance of the basalt fiber. Three different types of fibers including basalt, glass, and carbon were immersed in a 1M NaOH solution for 7, 14, 21, and 28 days. The experimental results showed that the basalt and the glass fibers lost their volumes significantly under alkali conditions. On the surface of these two fibers, reaction products developed and fell apart as the immersion period increased, consequently, decreasing a sound part or volume of the fibers. Those reaction products were assumed to be from the reaction between SiO_2 in the fibers and alkali solution [63]. In the carbon fiber, no such reaction product was observed, and the calculated volume reduction was less than 20% at 28 days of immersion. The basalt and the glass fibers lost their strength about more than 80% at 28 days of the immersion period, whereas about 13% of the strength reduction was measured for the carbon fiber after 28 days [63]. C. Scheffler et al. [64] also investigated the influence of the chemical composition of the aging solution (NaOH, cement) on the corrosion process of AR-glass and basalt fibers. The results show that the rate of this corrosion depends on the chemical constitution of the fiber and the alkaline solution as well as on the time and temperature.

Both solutions finally lead to highly corroded states after a few days at raised temperatures, but the manner of failure stress reduction strongly differs. In NaOH solution the failure stress steadily decreases, being interrupted by phases of increasing stresses. In contrast, the filaments in cement solution do not reveal decreasing failure stresses over a vast interval of temperature and time [64]. Portal et al. [66] investigated tensile behavior of textile reinforcements (AR-glass, basalt and carbon textile) under accelerated ageing conditions. Their study showed that the tested carbon textile reinforcement has a superior alkali and temperature resistance, while the standard conditions were found to be too aggressive for the tested basalt and AR-glass products causing them to have nearly unmeasurable capacity after ageing.

From the review of literature it was concluded that when basalt fiber is treated in the alkaline environment, although it is proved to have partial loss of strength, it is less likely to be damaged than glass fiber. However, reports that evaluate the alkaline resistance of basalt fiber under realistic alkali environments (fiber embedded directly in the cement composite for long-term aging) are scarce.

The investigation of the effectiveness of the chopped basalt fibers on the mechanical properties of geopolymer based composites was studied by some authors. Study based on a geopolymer paste matrix made of metakaolin with the addition of 1, 3, 5, 7 and 10% by weight of geopolymer paste were carried out in terms of flexural strength [67]. The fibers had about 6.4 mm length and 13 μm diameter. The strength properties increased with the fiber addition. For non-fiber geopolymer paste, the flexural strength was 1.7 MPa and increased with the addition of basalt fibers - it was respectively: 1% - 3.6 MPa, 3% - 8.6 MPa, 5% - 13.5 MPa, 7% - 16.5 MPa and 10% - 19.5 MPa. Anil Ronad et al. [68] investigated a study on mechanical properties of geopolymer concrete reinforced with chopped basalt fibers. Geopolymer concretes made of fly ash class F with the addition of slag, plasticizer, basalt fiber and two types of aggregates (fine and coarse) were prepared. The strength tests were carried out on geopolymer concretes with fiber addition of 0.0%, 0.5%, 1%, 1.5%, 2%, 2.5% by the weight of material (fly ash + slag). The experimental results showed that all the geopolymer concretes with basalt fiber addition has always higher mechanical strength compared to plain one. The compressive strength of plain concrete gains 30.82 MPa at 7 days and 43.35 MPa at 28 days. The best result was achieved for 2% fiber addition with compressive strength at 7 days of 40.1 MPa and at 28 days of

58.4 MPa. For the split tensile test, the strength values of the plain concrete were 2.2 MPa at 7 days and 2.4 MPa at 28 days. Best values were also achieved for concrete with 2% fiber addition: 3.2 MPa and 3.6 MPa. Arunagiri et al. [69] conducted a study concerning the mechanical properties of basalt fiber reinforced geopolymer concrete. They have achieved the highest compressive strength of geopolymer concrete at 2% basalt fiber addition. They have said that basalt fiber acts as a crack arrestor and prevents sudden failure of structures. They also confirmed that incorporating of basalt fiber within the geopolymer concrete can improve compressive as well as tensile strength at optimal dosage. Xiaolu Guo et al. [70] studied the mechanical properties of geopolymer mortar with the addition of short basalt fibers. The compositions of geopolymer mortar consists of fly ash class C, steel slag, sand and basalt fibers (diameter: 7 – 30 μm, lengths: 12 mm). The mechanical strength of geopolymer mortar was estimated based on various content of fibers: 0.0, 0.1, 0.2, 0.3, 0.4, 0.5 % by volume. The mortar specimens were tested at the age of 3, 7 and 28 days. From the experimental results, it was found that at the early ages of 3, 7 days the incorporation of basalt fiber decreased the compressive strength of the geopolymer mortars regardless of the added fiber content. However, all the specimens with fiber addition achieved higher compressive strength than control specimens at the age of 28 days. The highest compressive strength was obtained for 0.4% addition of basalt fibers, it was 40.3 MPa, which is 18.5% higher than the control sample. For bending strength, the highest value of 7.3 MPa at the age of 28 days was obtained for 0.3% addition, which improving 12.3% compared with the control sample. Based on the data, the authors concluded that the basalt fiber can improve the compressive and flexural strength to a certain extent, and the enhancement at the later stage is more obvious. Its suitable content is 0.3–0.4% according to the data. Giulia Masi et al. [45] has published an article on the effect of chopped basalt fibers on the mechanical and thermal properties of aluminate activated geopolymers. Short basalt fibers have a length of 5 mm and a diameter of 16 μm. Fiber reinforced geopolymers were synthesized by adding different dosages of fibers (0.5%, 1.0 % by volume). According to experimental results he stated that the presence of chopped basalt fibers in the geopolymer matrix was not found to affect the flexural strength and compressive strength of the geopolymer paste. However, adding 1 % of basalt fibers to the geopolymer matrix showed a slight increase in the energy absorbed during the three-point bending test. Basalt fiber geopolymer composites at elevated temperatures were also carried out. The basalt fibers did not degrade until 1000 ºC and the composites increased in flexural strength with increasing heated

temperature due to the improved bonding with the matrix after sintering. Their study confirmed that although chopped basalt fibers did not significantly improve mechanical properties of the geopolymer composites at low temperatures, they are more suitable for thermal applications in a range of higher temperatures from 600 ºC to 1000 ºC. In another study on behavior of chopped fibers reinforced fly ash geopolymer paste at elevated temperatures is observed by Faiz Shaikh et al [71]. In their study, basalt fibers with 12.7 mm length, 13 μm diameter were added in various dosages of 0.5, 1.0 and 1.5% by weight of fly ash. The tests were carried out at an ambient temperature and elevated temperatures of, 200 °C, 400 °C, 600 °C, 800 °C. The experimental result showed that the geopolymer containing 1 wt.% of basalt fibers displayed better compressive strength, lower volumetric shrinkage and mass loss than other fiber contents. No significant damage and change in fiber diameter at elevated temperatures are observed in SEM analysis. So, the results confirmed the resistance of basalt fiber at elevated temperatures. Daming Ren et al. [72] investigated geopolymer composites made of metakaolin with three mineral fillers: wollastonite, thermolite particles and chopped basalt fibers. The geopolymer composite with metakaolin replacement of 12% (5% WS + 5% TR + 2% SBF) is the optimum group, which leads to the most effective improvement in the compressive strength of the resulting product. The compressive strength of this composite increased to 33.5 MPa, compared to a value of 13 MPa for the pure geopolymer. Then, this geopolymer composite was tested for strength after 3, 7, 28 and 90 days for resistance against aggressive environments, i.e. 15% Na_2SO_4 solution and 15% NaCl solution. The results showed that fibre geopolymer composites maintained higher mechanical properties than pure geopolymer. Chopped basalt fibers with 12 mm length and 20 μm diameter were also used as fiber reinforcement in production of boron waste additive metakaolin based geopolymer mortar composite [73]. Basalt fiber was added as a volume fraction ratio of 0.4%, 0.8% and 1.2% and its addition effect on the geopolymer composites behavior was carried out. The experimental results showed that both flexural strength and compressive strength increased with increasing fiber content and the samples reinforced with 1.2% basalt fiber had the best value of mechanical strength. Their study revealed that addition of basalt fibers also improves the other characteristics of the geopolymer composites such as water absorption, voids ratio, flexural toughness factor and abrasion resistance. For example, the basalt fiber composites raised from 154.55% to 287.01% in terms of flexural toughness factor or reductions of between 2% and 18% in abrasive wear, compared to control samples. The behaviour of geopolymer

materials at high temperatures were also be researched, i.e. 300 °C, 600 °C and 900 °C. Significant degradation of mechanical properties was found at temperatures of 600 °C and 900 °C, however basalt fiber reinforced samples still had higher values than the control samples. Weimin et al. [74] investigated the impact of mechanical properties of basalt fiber reinforced geopolymer concrete (BFRGC). Geopolymer concrete is made from fly ash/slag, limestone rubble, river sand, sodium-based activator and chopped basalt fiber (18 mm length, 16 μm diameter). Some parameters such as dynamic compressive strength, deformation and energy absorption capacity, were studied using a 100 mm diameter split Hopkinson pressure bar (SHPB) system. The SHPB system is an apparatus for testing the dynamic stress-strain response of materials. Impact properties of BFRGC exhibit strong strain rate dependency and increase approximately linearly with the strain rate. The addition of basalt fiber can significantly improve deformation and energy absorption capacities of geopolymer concrete (GC), while there is no notable improvement in dynamic compressive strength. In addition, the optimum volume fraction of basalt fiber of 0.3 % was presented for BFRGC. Dias and Thaumaturgo conducted a study on the basalt fiber reinforced geopolymer concrete in terms of fracture toughness. They compared to geopolymer concrete with ordinary Portland cement concrete, their study revealed that using basalt fibers proved to in benefit of improving the characteristics of the resulted concretes in terms of deformation and energy absorption [75].

From the review of literature it has been explored that the effect of adding chopped basalt fibers on the mechanical properties of geopolymers appears to depend on the type of geopolymer matrix (metakaolin, fly ash, or slag, et.) and with or without any aggregates. As reviewed literature above, some researchers confirmed the chopped basalt fibers do not positively affect on flexural and compressive strength of resulting samples. Others revealed that the mechanical strength of samples after adding these fibers improved significantly. It can be seen that the effect of the addition of chopped basalt fiber to geomortar should be continued to study.

2.3.2 Textile fabric geopolymer composites

Textile reinforcements have many advantages over short fiber reinforcements because only a certain small amount of short discrete fibers can be added to the cementitious materials due to the clustering effect and uneven distribution of fibers in the mixture. Textile reinforcements provide a higher amount of fibers incorporated in cementitious materials

compared to short fibers and show significantly greater load capacity as fibers are arranged in the form of bundles or yarns and due to easy position where the required load. These materials can be used for applications in load-bearing structural members such as structural panels, impact and blast-resistance structures, repair and retrofit and strengthening of unreinforced masonry walls. Textile reinforcements combined with geopolymer matrix are simply named textile reinforced geopolymer (TRG). Up to date, many works have been performed to evaluate the effectiveness of the use of a textile reinforced geopolymer matrix composite for the external strengthening layer of existing structure members [76–83]. For example, Vasconcelos et al. [79] carried out a study on the use of reinforcing carbon fiber sheets and metakaolin based geopolymer mortar as an external strengthening layer for concrete prisms. The carbon fiber sheets were pre-impregnated with epoxy resin and placed within the geopolymer mortar before the setting of the resin. The use of geopolymer mortars as a binding agent to bond the carbon reinforced polymer sheets to the concrete substrate. Their study observed that metakaolin geopolymer mortars show a high mechanical resistance and a relevant adhesion to the concrete substrate. Although their adhesion strength is lower than the one present by commercial pre-pack repair mortars, they are very cost-effective (5–10 times less expensive). On the other hand, the adhesion strength between CFRP and geopolymer mortars proved to be lower than expected which could be due to the fact that the composition of the geopolymer mortars was not optimized and also to the fact that the CFRP used was not prone to this kind of application. Costantino Menna et al. [80] observed poor adhesion of the geopolymer carbon fabric composites so that a negligible strengthening of the reference reinforced concrete beams was obtained. The poor performance of the CFRG system could be due to the sizing of the used carbon fibers, that was designed to have an optimal adhesion with epoxy resin. Sergio Tamburini et al. [78] performed an experiment on the use of metakaolin based geopolymer mortar combined with different types of textile reinforcements for the strengthening layers of brick masonry substrates. Excellent adhesion of all fiber reinforced geopolymers on soft mud clay bricks was found. Very interesting pull-off strength values were also found for fiber reinforced geopolymers coupled to strong extruded clay bricks. Hai Yan Zhang et al. [83] investigated the mechanical behavior of reinforced concrete beams shear strengthened with carbon textiles reinforced geopolymer mortar through static load tests. From the experimental results it was observed that textile reinforced geopolymer mortar is a very promising solution for retrofitting and strengthening RC members, due to its superior fire resistance,

excellent corrosion resistance and good weatherability. It is worth to notice that the reason for choosing geopolymer matrix composites is that they are more stable at elevated temperatures than a polymeric resin, while compared to a Portland cement matrix, they are better at anticorrosion in a chemical environment and have a lower CO_2 footprint [84].

It can be concluded that the research results in the current literature on TRG composites are presented in terms of the strengthening layers for reinforced concrete. Moreover, the majority of studies prefer to use carbon fiber reinforcement instead of other fibers. The reason may be that although carbon fibers are expensive, they have been found to promote a good load-bearing capacity of the reinforced composite due to the high tensile strength and Young's modulus. In other words, basalt is another type of fiber that has been used to some extent for geopolymer composites, however, mostly in the form of short fiber reinforcement. Only a few studies have used basalt textiles in combination with geomatrix as the strengthening layers. Despite many efforts in using the TRG composites as the strengthening layers for reinforced concrete, no research work reported on the experimental investigation of mechanical properties of geopolymer composites which are produced by textile reinforcements and geomortar in the current literature. This approach of research is quite interesting because it is possible more easily to assess the effectiveness of some key parameters including textile type, net size, reinforcement ratio, geomortar type, additional reinforcements on mechanical properties of resulting composites. Finally, for each specific application consideration can be given to the appropriate selection of reinforcement type as well as geomortar matrix.

3. RAW MATERIALS AND METHODS OF THE EXPERIMENTATION

This part provides information about the raw materials and their properties, molds used for producing the samples, curing regime of the samples, the testing methods used in the research. The whole work of this thesis was carried out in the geopolymer lab of Technical University of Liberec, Czech Republic.

3.1 Raw materials

3.1.1 Geopolymer binder

Commercial geopolymer binder Baucis LNa based on metakaolin provided by České Lupkové závody, Czech Republic was used as the aluminosilicate source for producing geopolymer mortar (in weight percent: SiO_2—47.4; Al_2O_3—29.7; CaO—14.5; MgO—2.6; TiO_2—1.8; Fe_2O_3—0.5; K_2O—0.3; Na_2O—1) along with sodium silicate activator of modul 1.73 (in weight percent: SiO_2—20.72; Na_2O—12.33; H_2O—66.68) (see in Figure 3.1). Geopolymer cement was synthesized from calcined kaolin and shale fly dust burnt in a rotary kiln (for 10 h at 750 °C) with a Si/Al molar ratio of 2.0. In order to prepare geopolymer paste, the mixing ratio of two components (solid, liquid) was taken out according to the requirement of the manufacturer.

3.1.2 Sand

Two different types of silica sand, supplied by Sklopísek Střeleč, a.s. Czech Republic, were used as the fine aggregates for geopolymer mortar matrix (grain size in mm: ≤ 0.063 and 0.6–1.25) (see in Figure 3.1).

3.1.3 Silica fume

Powder additive (microsilica or silica fume) based on amorphous SiO_2 for concrete and mortar was purchased from Kema Mikrosilika-sanační centrum s.r.o., Sviadnov Czech Republic (see in Figure 3.1). The chemical composition of microsilica as follows (wt.%): SiO_2 – 90, CaO – 0.8, MgO – max. 1.5, Al_2O_3 – max. 1, Na_2O – 0.5. This additive was added into geopolymer mortar to improve both the workability of the fresh mortar and the mechanical strength of the hardened mortar.

Figure 3.1 Raw materials used in this work.

3.1.4 Chopped basalt fiber

The chopped basalt fiber (BF) was provided by Kamenny Vek, and the three types with the approximate lengths are 6 mm. 12 mm, 24 mm, respectively, which have individual fiber diameters of 13 μm, a density of 2.67 g/cm^3, tensile strength in the range of 2700–3200 MPa, and tensile modulus of 85–95 GPa, as shown in Figure 3.2. Basalt has a softening and melting point of 1060 ºC and 1250 ºC, respectively. It is non-combustible, making it useful for high-temperature applications.

Figure 3.2 Three types of the chopped basalt fibers (BF) with different fiber lengths used in this work, from left to right: fiber length of 24 mm (24 mm BF), the fiber length of 12 mm (12 mm BF), the fiber length of 6 mm (6 mm BF).

3.1.5 Textile reinforcements

Two types of textiles were used in this study. One is the basalt fiber mesh corresponding to three net sizes (10 x 14 mm, 22 x 22 mm, 36 x 36 mm) (see in Figure 3.3a) and the second is the carbon fiber mesh corresponding to three net sizes (10 x 15 mm, 21 x 21 mm, 34 x 34 mm) (see Figure 3.3b). These textiles were provided by Aligard company, Czech Republic and their mechanical properties are shown in Table 3.1.

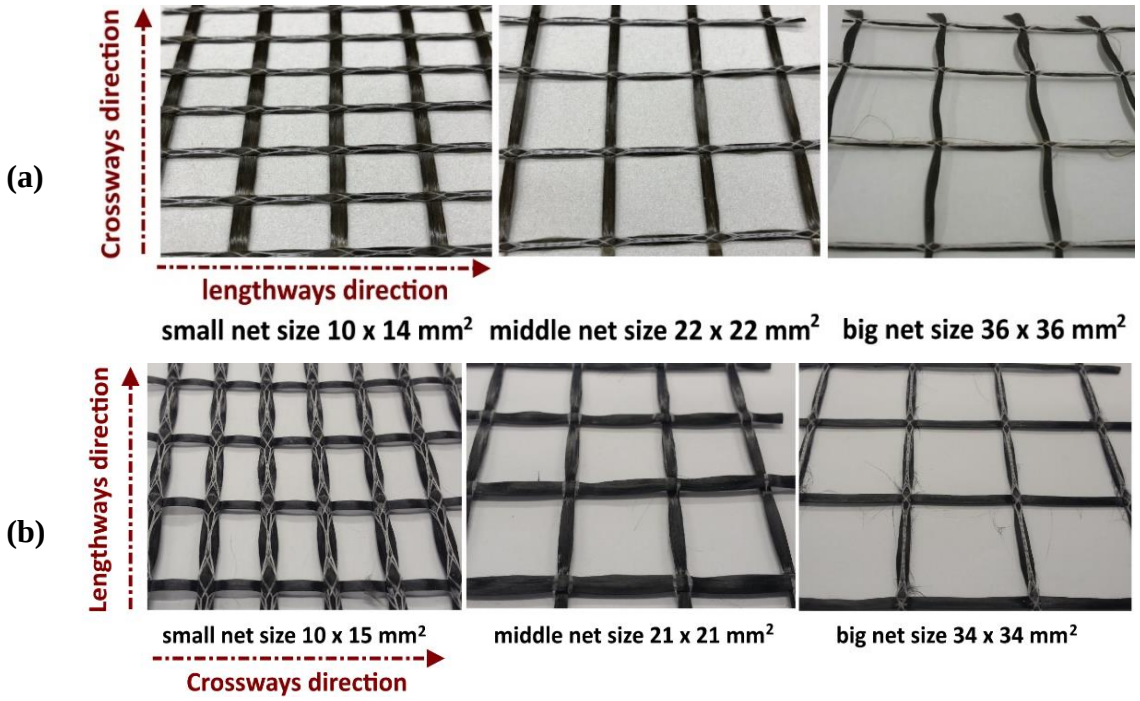

Figure 3.3 Images of textile reinforcements: (a) basalt fiber meshes; (b) carbon fiber meshes

Table 3.1 Material characteristics of textile reinforcements provided by the manufacturer.

Form	**Carbon Fiber Mesh**		
Fiber type	Carbon HTC 10/15–40	Carbon HTC 21/21–40	Carbon HTC 34/34–40
Fiber density	1.77 g/cm^3	1.77 g/cm^3	1.77 g/cm^3
Number of threads/m	78 (lengthways); 55 (crossways)	39 (lengthways); 39 (crossways)	26 (lengthways); 26 (crossways)
Weight	350 g/m^2	330 g/m^2	212 g/m^2
Tex	3200 g/km	3200 g/km	3200 g/km
Stitch spacing	10 × 15 mm^2 (center to center distance)	21 × 21 mm^2 (center to center distance)	34 × 34 mm^2 (center to center distance)
Tensile strength	2847 MPa (lengthways); 2551 MPa (crossways)	2531 MPa (lengthways); 2841 MPa (crossways)	2544 MPa (lengthways); 2720 MPa (crossways)
Young's Modulus	252 GPa (lengthways) 228 GPa (crossways)	229 GPa (lengthways) 252 GPa (crossways)	242 GPa (lengthways) 250 GPa (crossways)
Elongation	1.17% (lengthways) 1.24% (crossways)	1.71% (lengthways) 1.47% (crossways)	1.47% (lengthways) 1.34% (crossways)
Form		**Basalt fiber mesh**	
Fiber type	Basalt HBT 10/14–40	Basalt HBT 22/22–40	Basalt HBT 36/36–40
Fiber density	2.75 g/cm^3	2.75 g/cm^3	2.75 g/cm^3
Number of threads/m	84 (lengthways) 61 (crossways)	43 (lengthways) 42 (crossways)	26 (lengthways) 25 (crossways)
Weight	375 g/m^2	229 g/m^2	153 g/m^2
Tex	2400 g/km	2400 g/km	2400 g/km
Stitch spacing	10 x 14 mm^2	22 x 22 mm^2	36 x 36 mm^2
Tensile strength	1335 MPa (lengthways) 1251 MPa (crossways)	1068 MPa (lengthways) 1347 MPa (crossways)	1141 MPa (lengthways) 1279 MPa(crossways)
Young's Modulus	81.20 GPa (lengthways) 84.50 GPa (crossways)	75.10 GPa (lengthways) 74.20 GPa (crossways)	83.40 GPa (lengthways) 85.61 GPa (crossways)
Elongation	1.86 % (lengthways) 1.50 % (crossways)	1.61 % (lengthways) 1.63 % (crossways)	1.62 % (lengthways) 1.54 % (crossways)

3.2 Sample preparation process

3.2.1 Mixing process of the geomortar

Geopolymer mortars are a mixture that consists of geopolymer binder and different fillers including rough silica sand, micro-milled silica sand, silica fume and chopped basalt fiber. Thus, geopolymer mortar was prepared according to the following steps. Firstly, geopolymer cement and activator solution with a given ratio were mechanically stirred for about 5 min to gain a homogenous binder. Geopolymer binder is preferably mixed separately to ensure the best possible dissolution of alumina and silica in the alkali environment leading to the attainment of the good geopolymerization process of geopolymer paste. Secondly, fine-particle reinforcements such as silica fume and micro-milled sand, were added to the slurry, and mixture was stirred for about 3 min more. Finally, the addition of chopped basalt fibers to geomortar is performed in two ways depending on the fiber dose level. With a low dose level, the BFs were added after step 2 completed, and

the mixture was mixed for about a minute so that the fibers were evenly distributed in the geomortar, followed by the rough sand being added and mixed. After adding sand, the geomortar must be mixed at a slow speed to minimize breaking the initial length of the BFs. This approach of mixing is to assess the effect of the fiber length of the BF on the mechanical properties of the geomortar. With a high dose level, the rough silica sand along with chopped basalt fibers was added simultaneously to the prepared mixture followed by mixing for a few minutes depending on various BF dosages to ensure a homogenous mortar. It should be noted that due to the high dose level of the BF added into the geomortar, to achieve the homogeneous mixture and good workability, the initial length of the BF must be changed, and it was chopped into smaller dimensions during mixing. Thus, in this approach the original length of the BF does not affect the mechanical strength of the geopolymer mortar, but the fiber dosage does. During the mixing process of the geomortar containing the chopped basalt fibers, observing by the naked eye is seen that the fresh geomortar with a low dose level has the worse workability than one with a high dose level. So, it should be manually vibrated after casting the geomortar into the molds in order to fix the compacting problems, results in inadequately compacted and air-entrapped mortar. Geomortars were mixed using either of the two mixers depending on the amount of mortar produced that is shown in Figure 3.4.

Figure 3.4 Two mixers are available for the geomortar mixing, TUL-KMT

3.2.2 Fabrication of the geomortar samples

The selection of a suitable mortar composition for use as a matrix to manufacture the geopolymer composite reinforced with the textile reinforcements should be carried out. The geomortar must ensure two desired criteria: i) having good workability, which is able to help a good penetration of the mortar between fiber yarns of textile layers; ii) it must also achieve the highest mechanical strength as well as possible. After preliminary trials, a number of the different geomortars were selected for further work to identify the most suitable geomortar composition for the fabrication of the textile reinforced geopolymer composite (Table 3.2). The content of rough silica sand in geomortar is fixed at a constant ratio of 1.5 by weight mass of geopolymer cement. Its higher content is not considered because of both low workability of mortar and limiting the incorporation of other fillers. So, an optimized matrix composition will be determined based on varying mixing ratios between the three different fillers such as silica fume, micro-milled silica, and chopped basalt fiber. Next, the various dosages of the chopped basalt fibers were added to geomortar to estimate the effect of the BF on the mechanical properties of the geomortar (Table 3.3). Three kinds of chopped basalt fiber with different lengths (6 mm, 12 mm, 24 mm) were used. As mentioned above, they were added to gemortar in two dose levels. The low dose level is applied to all three kinds of the BF with an increment of 0.25 % and up to 0.75%, except for the 6 mm BF up to 1.00 %. It is worth to notice that while the 6 mm BFs are dispersed easily in the mixture, by using 12 mm BFs and 24 mm BFs the difficulty of mixing has occurred due to the fiber entanglement that results in the presence of several clusters of fibers in the mixture as the BF content starts at 0.5 %. The high dose level is only applied to 6 mm BF with an increment of 2.50 % and up to 7.5 %. This is due to the fact that the fiber length has no impact on the mechanical properties as the BF used at a high dose level.

The specimens were produced by pouring the readily homogenized geomortar into 30 x 30 x 150 mm^3 prismatic molds, manually vibrated for a while followed by covering by polypropylene film and subsequent curing at the laboratory temperature. The label of geomortar was defined as following: GM means the geopolymer mortar, while S, F, B imply the micro-milled sand, the silica fume, and the chopped basalt fiber, respectively. For example, GM means that geopolymer mortar without the addition of the reinforcements, whereas GM-0.2S0.1F5B means that geomortar contains the micro-milled

sand and silica fume by mass ratio of 0.2 and 0.1 regarding geopolymer cement, respectively, and 5% of the BF by weight percentage regarding geopaste.

Table 3.2 Mixture of geomortar containing various doses of the fillers (by weight ratio).

No. sample	Cement	Activator	Rough silica sand	Micro-milled sand	Silica fume	BF (*)
GM	1	0.8	1.5	0.0	0.0	0
GM-0.2S	1	0.8	1.5	0.2	0.0	0
GM-0.2S0.1F	1	0.8	1.5	0.2	0.1	0
GM-0.2S5B	1	0.8	1.5	0.2	0.0	5
GM-0.2S0.05F5B	1	0.8	1.5	0.2	0.05	5
GM-0.2S0.2F5B	1	0.8	1.5	0.2	0.2	5
GM-0.1S0.1F5B	1	0.8	1.5	0.1	0.1	5
GM-0.2S0.1F5B	1	0.8	1.5	0.2	0.1	5
GM-0.3S0.1F5B	1	0.8	1.5	0.3	0.1	5
GM-0.4S0.1F5B	1	0.8	1.5	0.4	0.1	5

(*) chopped basalt fiber dosage by mass percentage of geopolymer paste.

Table 3.3 Mixture of geomortar containing various dosages of the BF (by weight ratio).

No. sample		Cement	Activator	Rough silica sand	Micro-milled sand	Silica fume	BF (*)
GM-0.2S0.1F0B		1	0.8	1.5	0.2	0.1	0.00
GM-0.2S0.1F0.25B	Low dose	1	0.8	1.5	0.2	0.1	0.25
GM-0.2S0.1F0.50B		1	0.8	1.5	0.2	0.1	0.50
GM-0.2S0.1F0.75B		1	0.8	1.5	0.2	0.1	0.75
GM-0.2S0.1F1.00B		1	0.8	1.5	0.2	0.1	1.00
GM-0.2S0.1F2.50B	High dose	1	0.8	1.5	0.1	0.1	2.50
GM-0.2S0.1F5.00B		1	0.8	1.5	0.2	0.1	5.00
GM-0.3S0.1F7.50B		1	0.8	1.5	0.3	0.1	7.50

(*) chopped basalt fiber dosage by the mass percentage of geopolymer paste.

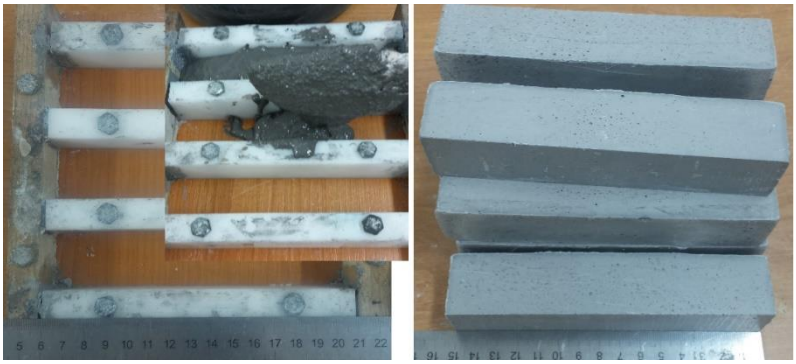

(a) (b)

Figure 3.5 (a) 30 x 30 x 150 mm^3 molds used to cast geomortar; (b) 28-day samples ready for test.

3.2.3 Fabrication of textile reinforced geopolymer samples for four-point bending test

The specimens are molded in the rectangular form with the dimensions of 400 × 100 × 15 mm^3. The textile layers were used as reinforced with geomortar matrix, and the specimens were manufactured by hand lay-up method. A mortar layer with desired thickness was poured on the bottom of the mold, followed by placing a textile layer. This operation is performed alternatively and ends up with a mortar layer on the mold top. The textile layers were positioned in the mold with the desired distance by using the thin metal plates at the ends of the mold. Next, the nut bolts were tightened together in order to fix the thin metal plates. The mold was manually vibrated for a while to ensure the good penetration of the fresh mortar between textile layers. Next, each fiber bundle will be stretched as well as possible using the adjustable wrench for the purpose of composite that ensuring tension state of fiber yarn embedded in mortar. Finally, the mold was manually vibrated again for a while, adding mortar into the mold if it is missing and it is covered by polypropylene plastic film for 24h. Figure 3.6 describes the detail components of the mold system 400 x 100 x 15 mm^3, whereas the manufacturing process of textile reinforced geopolymer mortar composites is described in Figure 3.7.

Figure 3.6 Photograph showing the detail components of the mold system of dimension 400 x 100 x 15 mm3.

Figure 3.7 The manufacturing process of textile reinforced geopolymer mortar composites.

Geopolymer mortar reinforced with three different types of basalt fiber meshes (BRG specimens)

The arrangement of textile layer in the mold was clearly described in Figure 3.8. It was found that four reinforcing layers were the eligible number in order to ensure easy penetration of geopolymer mortar between textile layers when the total thickness of the specimens was 15 mm. For instance, the distance between two adjacent layers should be bigger than the size of sand grains, so this distance was 2 mm in the case of four reinforcing layers because the distance from center to center between two adjacent layers was 3 mm while self-thickness of fiber yarn was about 1 mm. It should be said clearly that the number of fiber yarns per one textile layer in the bearing direction is: eight yarns for the B-10x14 mesh, four yarns for the B-22x22 mesh and three yarns for the B-36x36 mesh. In this work, the four-point bending performance of textile geopolymer composite was carried out based on the textile type and the different number of reinforcement ratios. The geopolymer mortar containing 5% of chopped basalt fiber (the label GM-0.2S0.1F5B) was selected for a matrix.

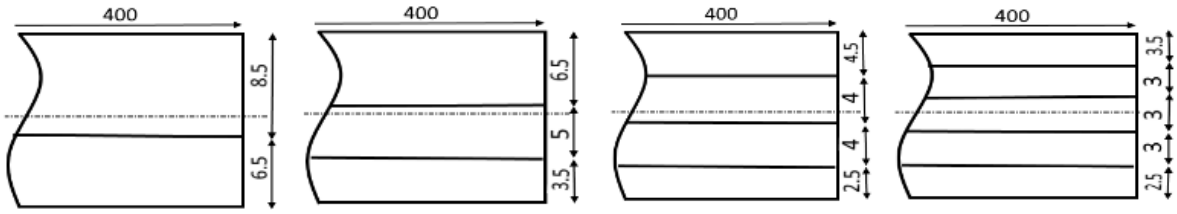

Figure 3.8 Schematic drawing of the arrangement of the basalt textile in the specimens (unit: mm).

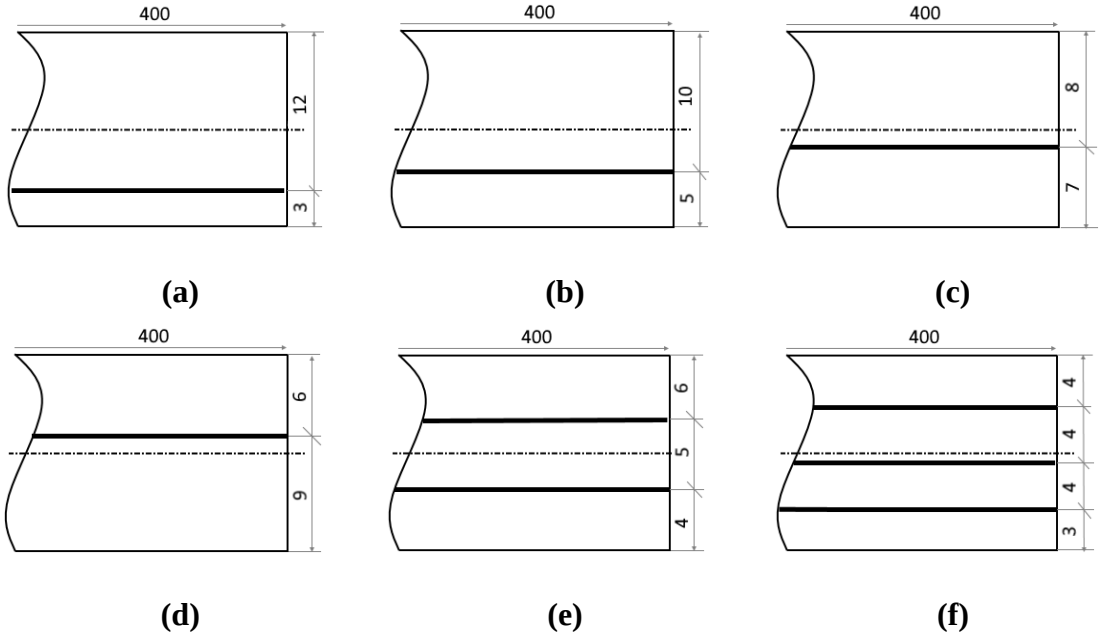

Figure 3.9 Schematic drawing of the arrangement of carbon textile in the specimens (unit: mm).

Geopolymer mortar reinforced with three different types of carbon fiber meshes (CRG specimens)

The layout of carbon textile in the mold was clearly described in Figure 3.9. Unlike basalt fiber meshes, because the self-thickness of carbon fiber yarn was about 2 mm, it was found that three reinforcing layers were the eligible number in order to ensure easy penetration of geopolymer mortar between textile layers when the total thickness of the specimens was 15 mm. Similar to basalt fiber meshes, the number of the fiber yarns per one textile layer in the bearing direction is: eight yarns for the C-10x15 mesh, four yarns for the C-21x21 mesh and three yarns for the C-34x34 mesh. Similar to the BRG specimens, the four-point bending performance of textile geopolymer composite was carried out based on the textile

type and the different number of reinforcement ratios, position of textile layer in the specimens, and used the same geopolymer mortar as used for the BRG specimens.

Geopolymer mortar reinforced with carbon meshes and containing various doses of chopped basalt fibers

When compared to basalt textiles, carbon textiles have been found to promote a better load-bearing capacity of the reinforced composite due to the high tensile strength and Young's modulus. So, one layer of C-10x15 mesh was considered to investigate the influence of the BF dosages on the flexural performance of the textile geopolymer composite. Figure 3.10 shows the experimental program of carbon textile geopolymer composite that demonstrates what type of sample is used regarding each key factor.

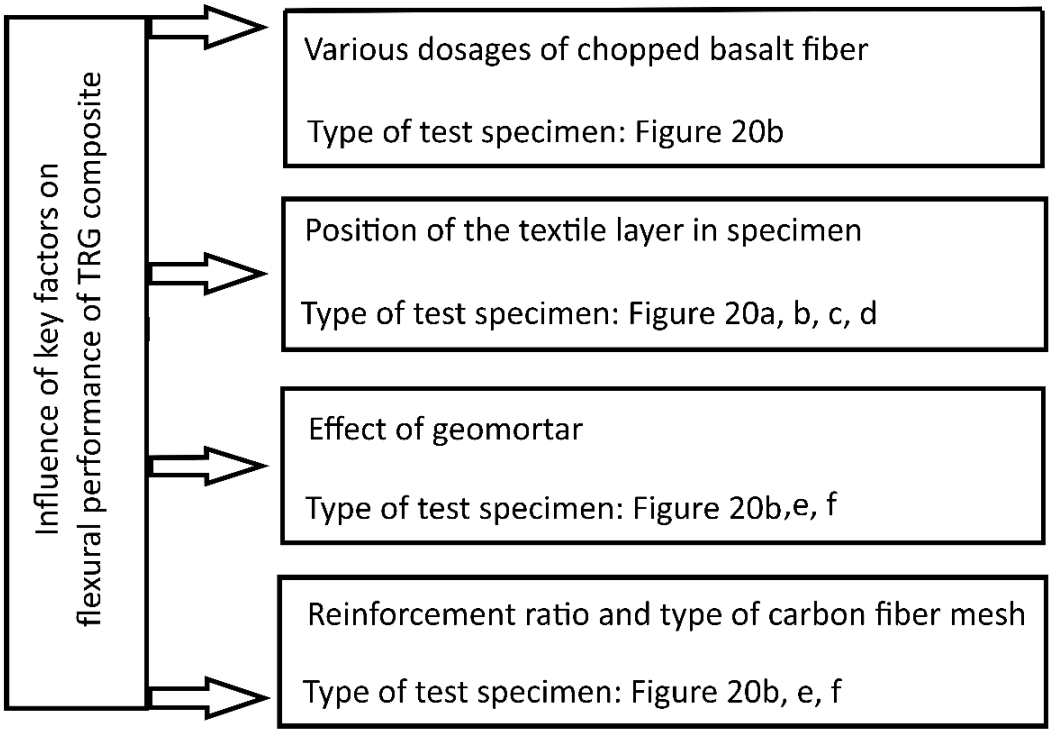

Figure 3.10 Schematic drawing of the experimental program of carbon fiber mesh reinforced geopolymer mortar.

Reinforcement ratio

The reinforcement ratio could be defined as the ratio of the area of the textile reinforcement to the area of the specimens. It can be expressed by the following Equation (1):

$$\rho_f = \frac{A_f}{A_c} \quad (1)$$

Where ρ_f is the reinforcement ratio, A_f is the cross-sectional area of the fiber yarn of the carbon textile in mm^2, A_c is the cross-sectional area of the BRG specimens in mm^2.

The cross-sectional area of the fiber yarn can be calculated by the following Equation (2):

$$A_f = \frac{Tex}{D_f} \quad (2)$$

Where D_f is the fiber density in g/cm^3, Tex is the linear density of the fiber yarn in g/km.

So, the BRG specimens that are reinforced with 1 – 4 layers of the basalt fiber meshes will have a reinforcement ratio of 0.47%, 0.93%, 1.40%, 1.86% for B-10x15 textile mesh; 0.23%, 0.47%, 0.70%, 0.93% for B-22x22 textile mesh; 0.17%, 0.35%, 0.52%, 0.70% for B-36x36 textile mesh, respectively.

The CRG specimens that are reinforced with 1 – 3 layers of the carbon fiber meshes will have a reinforcement ratio of 0.96%, 1.93%, 2.89% for C-10x15 textile mesh; 0.45%, 0.96%, 1.45% for C-21x21 textile mesh; 0.36%, 0.72%, 1.08% for C-34x34 textile mesh, respectively.

3.2.4 Fabrication of textile reinforced samples for Charpy impact test

The samples with dimension of 15 x 50 x 120 mm^3 were cut off from the full samples that were formerly prepared to test the four-point bending strength. Due to the limited size of the samples for Charpy impact test, only textile fiber meshes with small net size were used (Figure 3.11). The samples were cut using the machine shown in Figure 3.12.

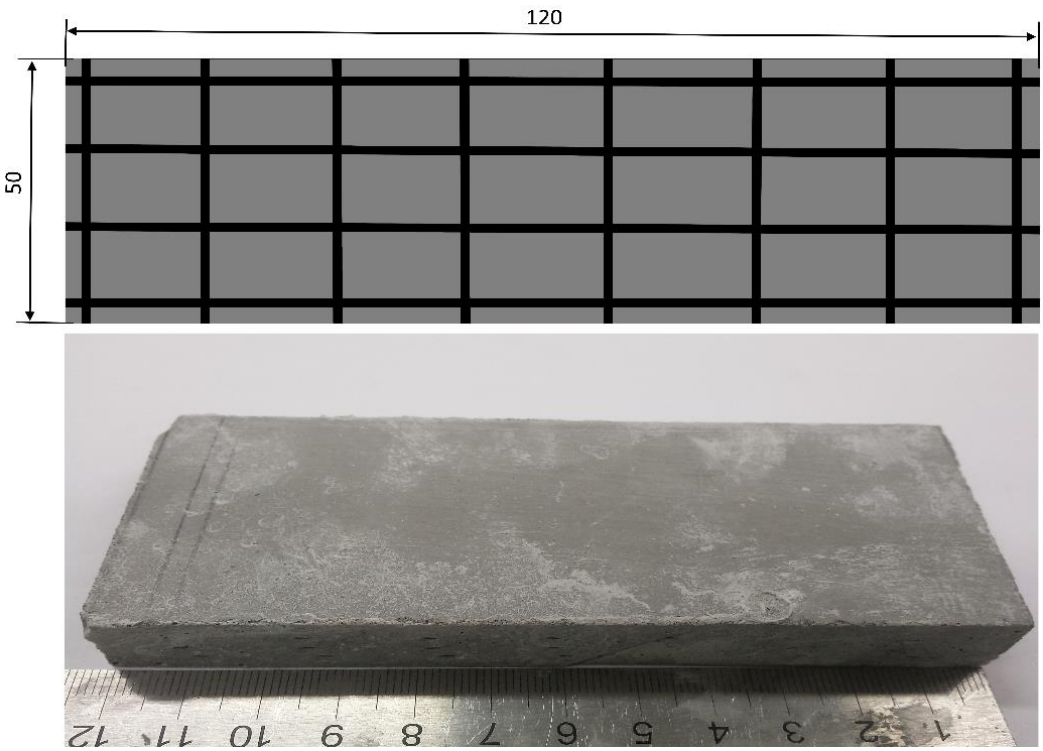

Figure 3.11 The sample size of textile geopolymer composites for Charpy impact test (unit: mm).

Figure 3.12 The cutting machine with diamond blade.

3.2.5 Curing regime of the test samples

After casting, all the specimens were wrapped using a polypropylene film and cured at room temperature, ~22 ºC, with 45% relative humidity for 24h. Afterward, the specimens were demolded, and wrapped again using a polypropylene film, and kept at room temperature until testing.

3.3 Test methods

3.3.1 The compressive strength and three-point flexural strength test

The compressive strength and three-point flexural strength tests of the 30 x 30 x 150 mm^3 samples were used to evaluate the mechanical strength of various geopolymer mortars. Three specimens for each mixture were prepared for the flexural test, and then the compressive strength was measured on both residual pieces obtained from flexural strength which is assumed according to EN 196-1 standard showing Figure 3.13 and were tested on universal testing machine LabTest II shown in Figure 3.14. The compressive strength and flexural strength can be calculated as per the Equation (3) and (4), respectively.

$$\sigma_c = \frac{F}{A} \qquad (3)$$

where σ_c is the compressive strength in MPa; F is the applied load at the fracture point in N; A is the area of the tested sample in mm^2.

$$\sigma_f = \frac{3Fl}{2bd^2} \qquad (4)$$

where σ_f is the flexural strength in MPa; F is the applied load at the fracture point in N; l is the length of the support (outer) span in mm; b is the width of the tested sample in mm; d is the thickness of the tested sample in mm.

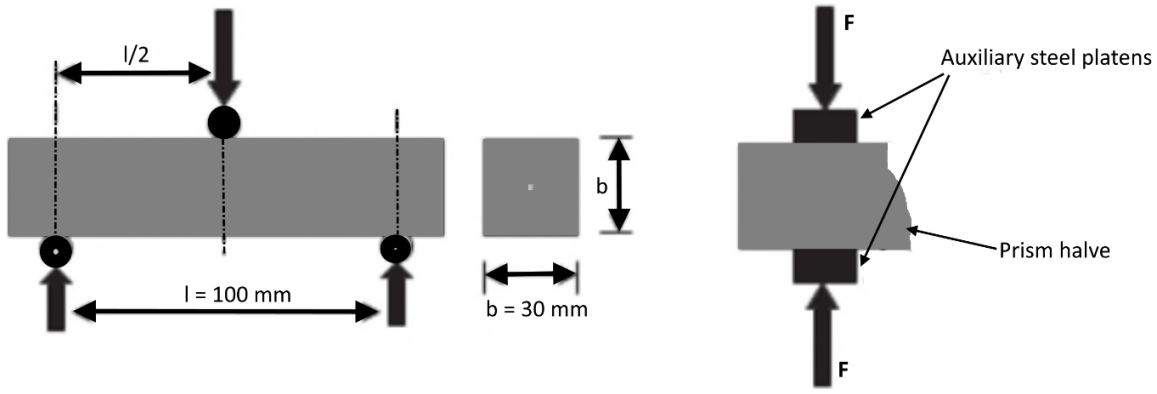

Figure 3.13 Three-point flexural test and uniaxial compressive test.

Figure 3.14 Universal testing machine P 100-LabTest II, TUL-KMT.

3.3.2 Four-point bending test

The four-point bending test method was used to evaluate the flexural performance of textile reinforced in geopolymer composites. The detailed description about the specimen arrangement and testing process was shown in Figure 3.15. The testing machine with a load cell capacity of 100 kN (FP Lab Test II, from LABORTECH s.r.o Opava, Czech Republic), located at the Technical University of Liberec Laboratory, with the applied load under displacement control at a loading rate of 4 mm/min, was used (see in Figure 3.14). The four-point flexural strength in the special case where the outer support span is equal to three times the inner support span can be calculated as per the Equation (5):

$$\sigma_f = \frac{Fl}{bh^2} \qquad (5)$$

where σ_f is the four-point flexural strength in MPa; F is the load at a given point on the load–displacement curve in N; b is the width of the tested sample in mm; h is the thickness of the sample in mm; and l is the support span in mm.

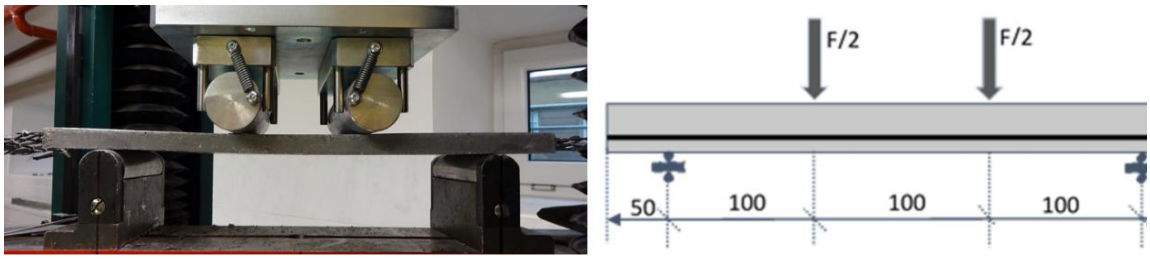

Figure 3.15 Four-point bending test for the 15 x 100 x 400 mm^3 specimens.

3.3.3 Charpy impact test

The Charpy impact test was carried out on the Charpy testing machine designed according to ČSN EN 10045 in order to evaluate the impact mechanical strength of textile reinforced geopolymer mortar. A Charpy impact tester with a 18kg pendulum hammer was employed to determine the impact strength (Figure 3.16). The specimen with size of approximately 15 x 50 x 120 mm^3 was used in this test. The impact strength can be calculated as per Equation (6):

$$KU = \frac{K}{S} \qquad (6)$$

where σ_i is impact strength in MPa; E is impact energy required to break the tested sample in Joule (J); A is the cross-section area of the tested sample in m^2.

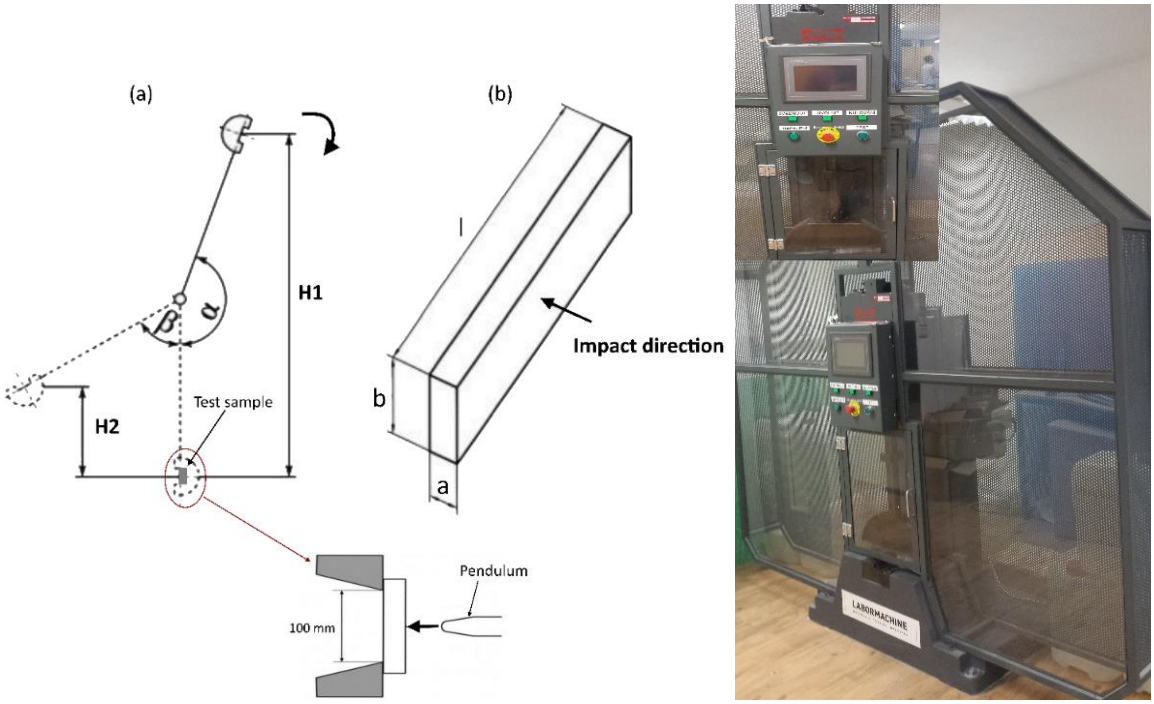

Figure 3.16 Left showing schematic of Charpy impact test: (a) schematic of Charpy machine, (b) sample shape and impact direction; Right showing Charpy tester, TUL-KMT

4. MECHANICAL STRENGTH OF THE GEOPOLYMER MORTAR

The main goal of doing this part was to find out the geomortar sample with the strongest mechanical strength performance, which will be used as a matrix in production of the geopolymer composite reinforced with the textile reinforcements in further work. Besides, it also assessed the mechanical strength of geomortar containing various dosages of chopped basalt fiber. Geomortar is made by combining geopolymer paste, rough silica sand, and the different fillers such as micro-milled sand, silica fume and chopped basalt fiber (BF). The optimization process was conducted based on varying the mixing ratios between these three fillers.

4.1 The effect of the different fillers on mechanical properties of the geomortar

The compressive strength test and three-point bending strength test were the methods of the choice for evaluation of the mechanical strength of the geomortar. Three samples with dimensions of $30 \times 30 \times 150$ mm^3 for each recipe were used for the flexural test, and then the compressive strength was measured on both residual pieces obtained from flexural strength, which described clearly in section 3.3.

Table 4.1 shows the effect of incorporating the fillers on mechanical strength of geomortar. After preliminary trials, the five different recipes of geomortar were selected to clarify the difference in strength between them (see in Table 4.1). The plain geomortar (GM mix) that contains geopolymer paste and rough silica sand shows the weakest mechanical strength with a value of 9.47 MPa in flexure and 60.05 MPa in compression at the age of 28 days. It was observed that the addition of micro-milled sand to geomortar (GM-0.2S mix) leads to a decent increase in strength, on the other way, this causes flowability of fresh geomortar to be significantly reduced, which was confirmed by the author's naked eye during mixing. When considering the 28-day mechanical strength, the GM-0.2S mix increases flexural strength by 11.40 % and compressive strength by 13.54 % respectively, compared to plain geomortar. However, when silica fume filler continues to be added to this geomortar (GM-0.2S0.1F mix), the flowability of fresh geomortar, as well as the mechanical strength of hardened geomortar, has increased significantly. The increase in mechanical strength of

geomortar incorporating silica fume, on the one hand, may be related to denser microstructure stems from the packing effect of the fine spherical particles of silica fume behave as micro-aggregate filler, which disperses in geopolymer paste and fills the inner space inside the microstructure of geopaste [30]. On the other hand, silica fume, as a highly reactive pozzolan, offers the active SiO_2 which helps to form siloxo bridges during geopolymerization leading to improvement in the mechanical strength of geomortar [30], [33]. When considering the 28-day mechanical strength, the GM-0.2S0.1F mix increases flexural strength by 23.39 % and compressive strength by 32.49 % respectively, compared to plain geomortar. For the GM-0.2S5B mix, this geomortar that replaced silica fume by chopped basalt fibers also showed significant improvement in strength, compared to the plain geomortar. Also, this geomortar showed a slight rise in bending strength and this increased to 8.4 % at the age of 28 days, compared to geomortar with silica fume addition (GM-0.2S0.1F mix), despite its compressive strength not being higher. This is due to the fact that the bridge effect of the BF is more useful in bending strength. For the GM-0.1S0.1F5B mix that contains all three fillers simultaneously, the geomortar strength continues to increase dramatically. When considering the 28-day mechanical strength, the average mechanical strength of the GM-0.2S0.1F5B mix increases flexural strength by 55.44 % and compressive strength by 61.32 % respectively, compared to plain geomortar. So, we can be concluded that geomortar containing different fillers with reasonable proportion can achieve relatively high mechanical strength. The mechanical strength results showed in Table 4.2 – Table 4.4 will be reported on how the sample strength will change when considering the change in mixing ratio by varied content of each type of the fillers.

Table 4.1 Mechanical strength of geopolymer mortar containing various types of fillers.

No. sample	**Flexural Strength [MPa]**		**Compressive Strength [MPa]**	
	7 days	**28 days**	**7 days**	**28 days**
GM	8.79 ± 0.61	9.47 ± 0.88	52.24 ± 3.40	60.05 ± 2.64
GM-0.2S	9.76 ± 0.45	10.55 ± 0.25	58.63 ± 2.99	68.18 ± 1.76
GM-0.2S0.1F	9.46 ± 0.35	11.78 ± 0.48	60.84 ± 2.34	79.56 ± 3.32
GM-0.2S5B	10.64 ± 0.43	12.77 ± 0.51	69.63 ± 3.81	78.52 ± 2.94
GM-0.2S0.1F5B	11.80 ± 0.67	14.72 ± 1.17	76.62 ± 5.74	98.87 ± 1.59

The effect on the mechanical strength of the geomortar aged 7 days and 28 days with varied micro-milled sand additions is shown in Table 4.2. These geomortar samples contain a

constant content of the BF and silica fume while varying the content of micro-milled sand from 0.1 to 0.4 by mass ratio regarding to geopolymer cement (see in Table 3.2). When the mass ratio increases from 0.1 to 0.2, the sample strength at the age of 28 days increases to 9.77 % in flexure and to 15.82 % in compression, however when mass ratio goes up from 0.2 to 0.3, the rate of strength development drops to 5.23 % in flexure and 6.36 % in compression; and this rate continues to drop to 17.2 % in flexure and 11.07 % in compression when mass ratio rises up from 0.3 to 0.4. It was observed that the highest mechanical strength found in GM-0.2S0.1F5B sample with mass ratio of 0.2. The decline in strength with increasing content of micro-milled sand is related to the increasing water demand with increasing filler content which resulted in a loss of mortar packing. Table 4.3 reported the results of the mechanical strength of the geomortar with varied silica fume additions. The results showed that no significant change in the mechanical strength of geomortar when the mass ratio of silica fume to geopolymer cement ranges from 0.05 to 0.2. However, it was found that the mass ratio of 0.1 (GM-0.2S0.1F5B mix) was an optimum level of silica fume added in geomortar; later on, the silica fume content increases leading to the decrease in sample strength. As previously reported, an overdose of silica fume has shown inauspicious effects on strength properties of geopolymer and also hinders the geopolymerization process. This is due to the increase of SiO_2 content present in the silica fume results in an increase of Si/Al ratio in the combination of binder [30].

Table 4.2 Mechanical strength of the geomortar with varied micro-milled sand additions.

No. sample	**Flexural Strength [MPa]**		**Compressive Strength [MPa]**	
	7 days	**28 days**	**7 days**	**28 days**
GM-0.1S0.1F5B	10.75 ± 0.89	13.41 ± 1.09	58.36 ± 5.40	83.64 ± 2.51
GM-0.2S0.1F5B	11.80 ± 0.67	14.72 ± 1.17	76.62 ± 5.74	98.87 ± 1.59
GM-0.3S0.1F5B	9.27 ± 0.62	13.95 ± 0.53	69.41 ± 4.30	90.71 ± 2.45
GM-0.4S0.1F5B	8.29 ± 0.59	11.55 ± 1.09	55.26 ± 5.10	80.67 ± 3.45

Table 4.3 Mechanical strength of the geomortar with varied silica fume additions.

No. sample	**Flexural Strength [MPa]**		**Compressive Strength [MPa]**	
	7 days	**28 days**	**7 days**	**28 days**
GM-0.2S0F5B	10.64 ± 0.43	12.77 ± 0.37	69.63 ± 3.81	78.52 ± 2.94
GM-0.2S0.05F5B	10.59 ± 0.53	13.69 ± 0.50	73.86 ± 3.70	94.07 ± 2.46
GM-0.2S0.1F5B	11.80 ± 0.67	14.72 ± 1.17	76.62 ± 5.74	98.87 ± 1.59
GM-0.2S0.2F5B	12.89 ± 0.39	13.69 ± 0.39	75.84 ± 3.78	93.79 ± 6.72

Table 4.4 represented the mechanical strength of the geomortar containing the varied percentage of the BF at high dose level. The 6 mm BF added to geomortar with three various dosages of 2.5 %, 5.0 % and 7.5 % by mass percentage of geopaste was used while the content of the remaining fillers was constant. The results showed that there is a significant difference in both bending strength and compressive strength between geomortars without the BF and those with the BF adding. When the BF content goes up from 0.0 % to 2.5 %, the sample strength increases to 17.49 % in flexure and 23.27 % in compression. When the BF content continues to increase from 2.5 % to 5.0 %, at the same time the sample tends to increase slightly in both compressive strength and bending strength. When the BF content continues to rise to 7.5 %, results showed that there is no significant difference in mechanical strength between 5% BF samples and 7.5% BF sample. It must be noted that at the sample preparation point of view, the more BF content the sample contains, the more time it will take to produce the samples. Also, the flowability of fresh geomortar, despite a large amount of the BF added to geomortar is still quite good.

Table 4.5 shows the geomortar containing varied dosages of the BF at low dose level. The low dose is applied to all three kinds of the BF with an increment of 0.25 % and up to 0.75 %, except for the 6 mm BF up to 1 %. As a general comment, using the BF at low dose level can clearly improve the flexural strength of geomortar, but there is no clear effect on compressive strength, compared to using the BF at high dose level. In some cases, the addition of the BF causes an increase in compressive strength, in other cases this induces a decrease in strength. All the samples also show a poor flowability of fresh mixture and this property is worse with increasing BF content accompanied by fiber clumping in mixture especially for geomortar using 12 mm BF and 24 mm BF. This result is consistent with findings from Santarelli et al. [85] that by increasing fiber content, a degradation in compressive strength is observed. This is mainly attributed to difficulties related to the dispersion of the fibers, which resulted in the marked occurrence of clusters of fibers. Another issue to be considered is linked to the increasing water demand with increasing fiber content which resulted in a loss of mortar packing [85]. The influence of the chopped basalt fiber on the microstructure of geopolymer mortar is clearly shown in Figure 4.1. The fibers are evenly distributed in all volumes of the material. It is clearly visible that they are oriented in different directions. The material is probably anisotropic, and the fiber distribution was regular. The fiber distribution in the matrix influences the properties of the

specific composite. It can be seen that the BF was randomly distributed in matrix and bridge over the micro-cracks resulting in enhancement of mechanical strength. In addition, there are matrix particles attached to the fibers, which indicates a sufficient level of adhesion between the fiber and matrix.

Table 4.4 Mechanical strength of the geomortar with varied BF additions.

No. sample		Flexural Strength [MPa]		Compressive Strength [MPa]	
		7 days	28 days	7 days	28 days
GM-0.2S0.1F0.0B	High dose	9.46 ± 0.35	11.78 ± 0.48	60.84 ± 2.34	79.56 ± 3.32
GM-0.2S0.1F2.5B		11.20 ± 0.49	13.84 ± 0.55	72.08 ± 3.75	92.37 ± 2.27
GM-0.2S0.1F5.0B		11.80 ± 0.67	14.72 ± 1.17	78.85 ± 5.74	98.87 ± 1.59
GM-0.2S0.1F7.5B		12.77 ± 0.59	14.92 ± 1.74	78.18 ± 4.88	98.35 ± 3.39

Table 4.5 Mechanical strength of the geomortar with respect to different fiber lengths, inclusion dosage at the age of 28 days.

Fibre length [mm]		No. sample	Flexural Strength [MPa]	Compressive Strength [MPa]
6 mm BF	Low dose	GM-0.2S0.1F0.25B	11.96 ± 0.27	80.05 ± 5.67
		GM-0.2S0.1F0.50B	13.43 ± 0.85	77.01 ± 3.13
		GM-0.2S0.1F0.75B	12.28 ± 0.33	76.56 ± 4.68
		GM-0.2S0.1F1.00B	13.33 ± 0.56	75.24 ± 4.01
12 mm BF		GM-0.2S0.1F0.25B	12.96 ± 0.50	77.18 ± 1.27
		GM-0.2S0.1F0.50B	11.85 ± 0.13	83.37 ± 1.31
		GM-0.2S0.1F0.75B	12.65 ± 0.15	83.77 ± 1.06
24 mm BF		GM-0.2S0.1F0.25B	12.25 ± 0.78	81.82 ± 1.08
		GM-0.2S0.1F0.50B	13.05 ± 0.65	82.47 ± 3.10
		GM-0.2S0.1F0.75B	14.10 ± 0.77	78.51 ± 2.25

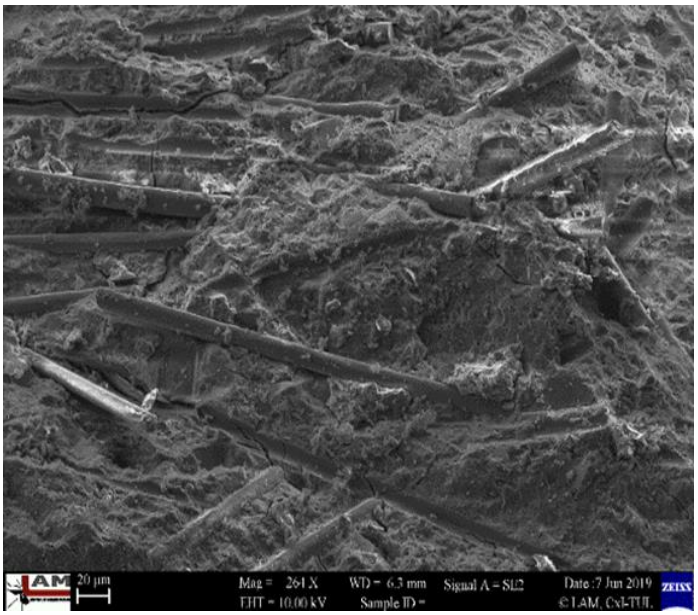

Figure 4.1 SEM microstructure of the 28-day geomortar with the 5% BF additions.

4.2 The development of the mechanical strength of the geomortar

Figure 4.2 – Figure 4.3 provide the information about the development of the mechanical strength of geomortar at the various periods of aging time. Figure 4.2 describes the strength development of the geomortar without the BF addition, whereas the geo-mortar filled by the 5% BF is shown in Figure 4.3. The 28-day specimens were named as a reference sample. A number of these specimens were then kept at the lab room (~26 °C, with 45% relative humidity) in order to observe the strength development at the further ages, such as 60 days, 90 days, 150 days, 180 days and 365 days. From Figure 4.2, after 28 days of curing age it can be observed that both bending strength and compressive strength show a constant trend with increasing aging time. This behavior is believed that the geomortar strength without the BF addition is almost stable over time. In the contrast, the strength development of geomortar with the BF addition shown in Figure 4.3 is strongly dependent on this fiber.

While the samples show a slight decrease in compressive strength, the increasing aging time affects samples to have a more pronounced decrease in their flexural strength. This phenomenon is believed to be due to the degradation of basalt fiber in alkaline environment [63, 64, 66]. When degradation of basalt fiber occurs, bond strength at the matrix/fiber interface will decrease; as a result, it can lead to poor bending resistance of the sample due to the reduction of bridge effect of the chopped fiber in the matrix. However, the result also

showed that degradation of basalt fiber appears to occur only in a certain period of time up to 150 days, beyond this time the sample strength remains almost unchanged. When compared to reference 28-day samples, the average mechanical strength of the samples with the BF additions with the increasing aging time of 60 days, 90 days, 150 days, 180 days, 360 days decreases the compressive strength by 4.72%, 5.74%, 7.90%, 8.35%, 6.38% respectively, whereas decreases the flexural strength by 11.07%, 11.41%, 22.42%, 22.48%, 21.54%, respectively.

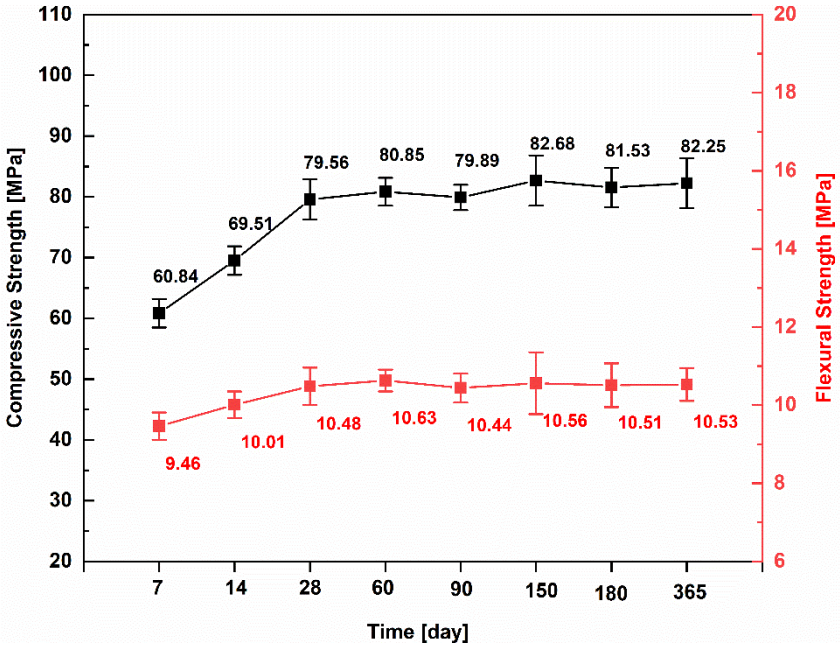

Figure 4.2 The development of mechanical strength of geopolymer mortar without chopped basalt fiber addition (GM-0.2S0.1F0B mix) at the different periods of time.

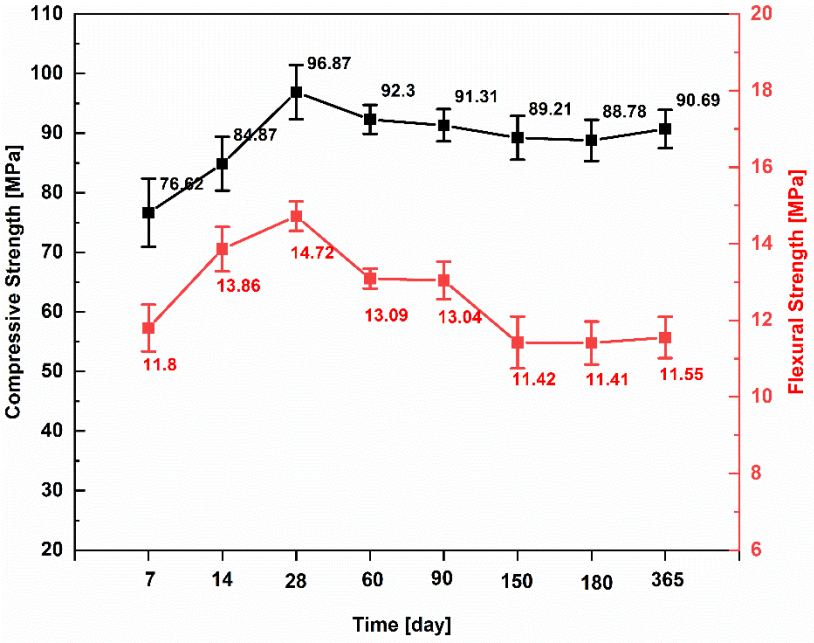

Figure 4.3 The development of mechanical strength of geopolymer mortar with chopped basalt fiber addition (GM-0.2S0.1F5B mix) at different periods of time.

4.3 Summary

It can be seen that geomortar containing different fillers with reasonable proportion can achieve relatively high mechanical strength. The best mix causes samples to increase flexural strength approximately by 55.44 % and compressive strength by 61.32 % respectively, compared to plain geomortar.

The fact that the BF addition at low dose level to geomortar does not indicate a marked increase in mechanical strength compared to that at high dose level.

The reported data on the strength development of the geomortar revealed that the geomortar without the BF additions almost remains unchanged strength over time up to 365 days. In contrast, the mechanical strength of the geomortar with the BF addition has been reduced. However, a decrease of the sample strength lasts only up to 150 days, beyond this time the mechanical strength is almost unchanged.

Finally the GM-0.2S mix and GM-0.2S0.1F along various dosages of the BF will be used as a mortar matrix in production of textile reinforced geopolymer composite in the following parts.

5. FLEXURAL PERFORMANCE OF VARIOUS BASALT FIBER MESHES REINFORCED GEOPOLYMER MORTAR

This part investigates the effect of basalt fiber meshes on the flexural performance of textile geopolymer composites. Three types of basalt fiber meshes as described in the previous materials section are used as reinforcement materials in production of textile reinforced geomortar composites. The GM-0.2S0.1F5B mix is selected as geomortar matrix. The flexural behaviour of the BRG specimens was analyzed based on a different number of textile layers and various types of basalt fiber meshes.

5.1 The flexural behavior of the basalt fiber mesh reinforced geomortar (BRG specimens).

The BRG specimens made of geomortar reinforced with one to four layers of each type of basalt mesh were tested at the age of about 40 days after casting by the four-point bending test method. Figure 5.1 represents the typical curves of flexural load-displacement behaviour of textile reinforced concrete composite under the four-point flexural test, whereas the response of the flexural load-displacement curves of all the tested BRG specimens was described in Figure 5.2 – Figure 5.5. As demonstrated in Figure 5.1, there are two distinctly different types of the load-displacement response of the specimens under flexure which consist of displacement-softening behavior and displacement-hardening behavior. In the field of fiber reinforced concrete, the materials refer to displacement-softening behavior (Figure 5.1a); when the first crack initiates, the specimen is then destroyed due to localization of this crack. As further load continues to increase, the presence of the fiber is unable to produce the post-crack strength higher than the first-crack strength, however, it helps to restrict sudden brittle failure. Depending on the number of fiber yarns, fiber characteristics, and fiber alignment, the figure of the load-displacement curves softens down differently. In this case, BRG 10 × 14-1 L, BRG 22 × 22-1 L, BRG 22 × 22-2 L and BRG 36 × 36-1-4 L produced a displacement-softening behavior with low load-bearing capacity, see in Figure 5.2 – Figure 5.5. The remaining reinforced specimens, in contrast, show a displacement-hardening behavior, see in Figure 5.1b. This kind of behavior is accompanied by multiple cracks and further load-bearing capacity after the formation of the first crack. In this behavior, the first crack stress is maintained, and the load is transferred to the other weak parts of the matrix through the fiber yarns. So the first

crack does not localize to the increasing applied load. Instead, new cracks will be developed somewhere else in the matrix. Consequently, the increase in applied load results in formation of multi-cracks and higher load-bearing capacity. For these specimens, load-displacement curves were illustrated in three obvious parts corresponding to the stages in the bending test, which demonstrated clearly in the introduction part. The first stage is the elastic-linear pre-cracking stage which is established by the combination of geopolymer matrix and reinforcement through a linear increase in load until the first crack appears. The second stage is a multiple-cracking phase, as proven fluctuation of the curve when the load continues to apply. The number of cracks in each specimen almost results in this stage and the profile of this phase strongly relates to the number of textile layers, the stiffness of matrix, the organization of textiles in the matrix, and the bond strength at the interface between fiber yarn and matrix. The third stage is the post-cracking or crack-widening phase. It is indicated by the expansion of the cracks; the present cracks continue to become broader until the specimens break down by rupturing or slipping of the fiber yarns of the textile.

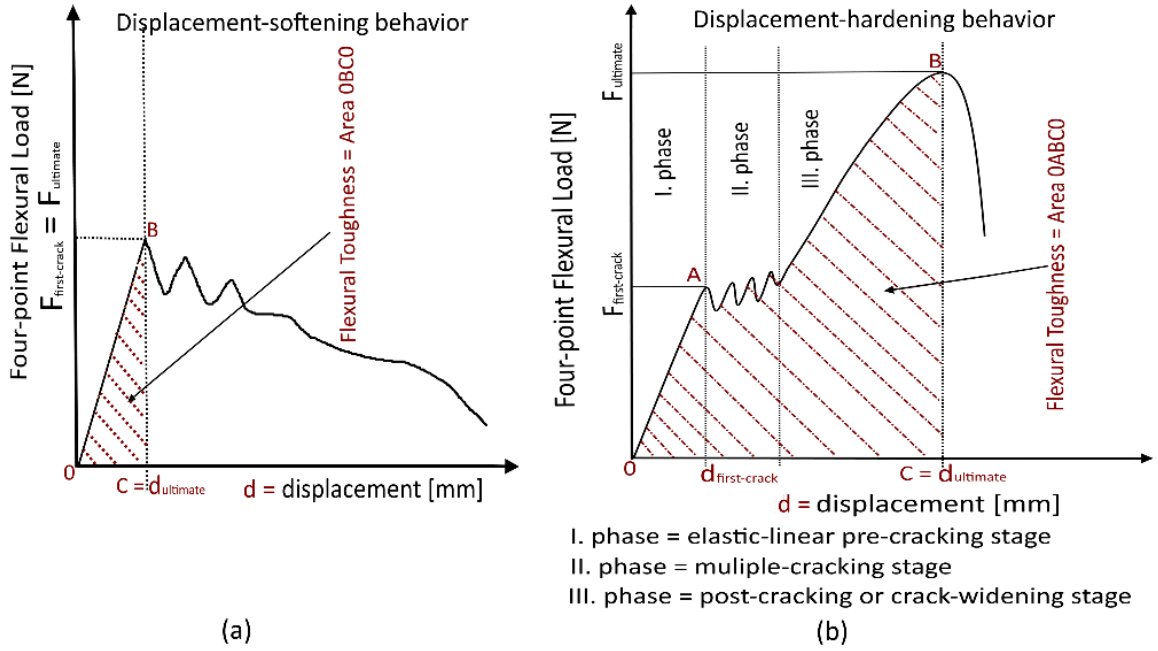

Figure 5.1 Flexural load – displacement behavior of textile reinforced concrete composite under flexural test: (a) displacement-softening behavior; (b) displacement-hardening behavior.

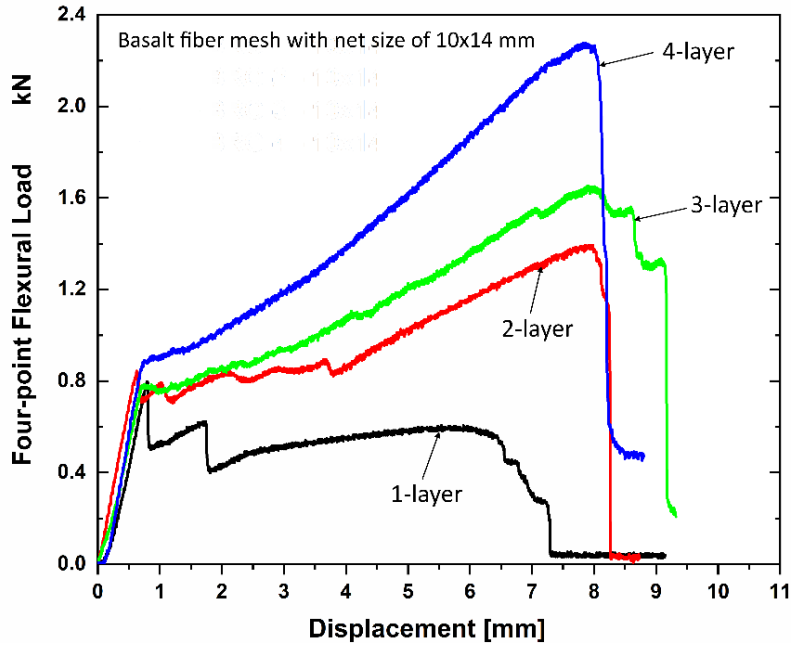

Figure 5.2 Flexural load-displacement curves of the B-10x14 composites reinforced with the basalt textile having a net size of 10 x 14 mm.

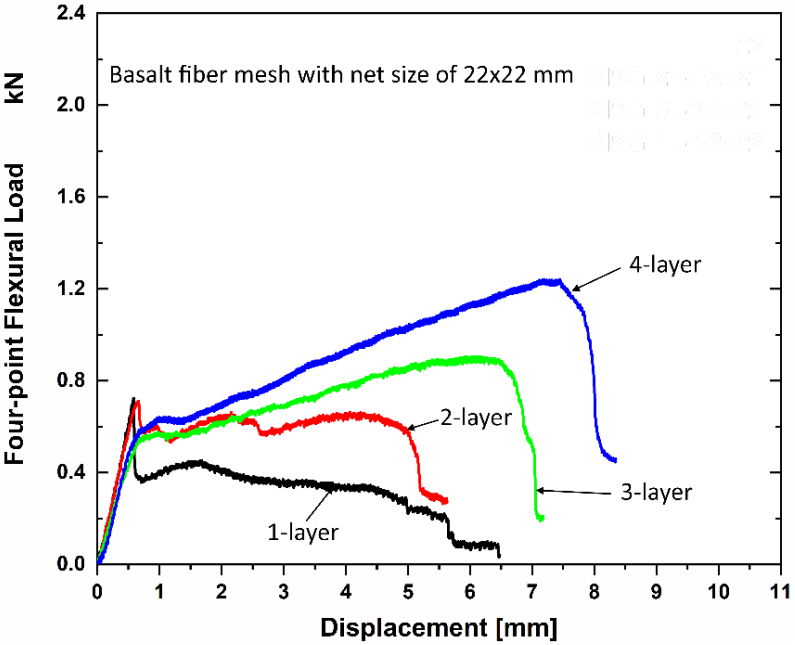

Figure 5.3 Flexural load-displacement curves of the B-22x22 composites reinforced with the basalt textile having a net size of 22 x 22 mm.

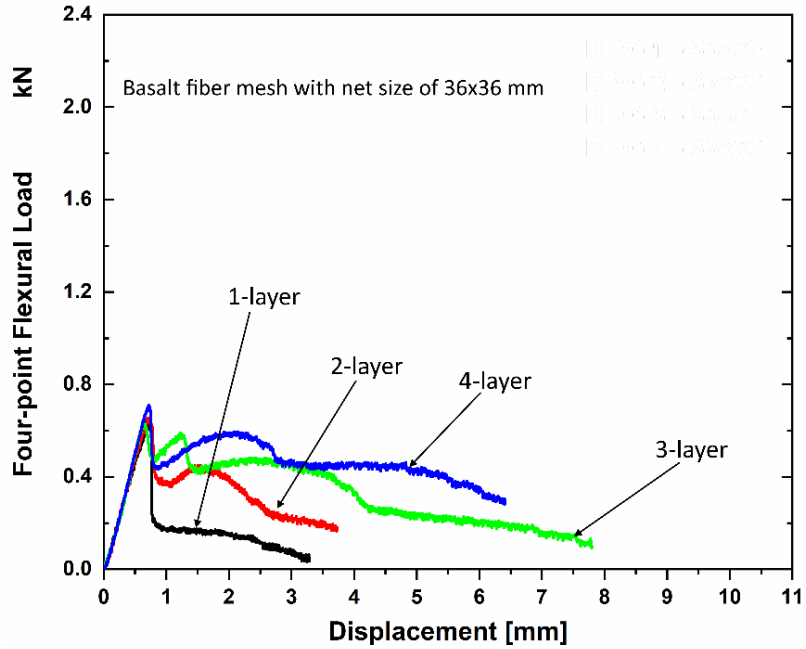

Figure 5.4 Flexural load-displacement curves of the B-36x36 composites reinforced with the basalt textile having a net size of 36 x 36 mm.

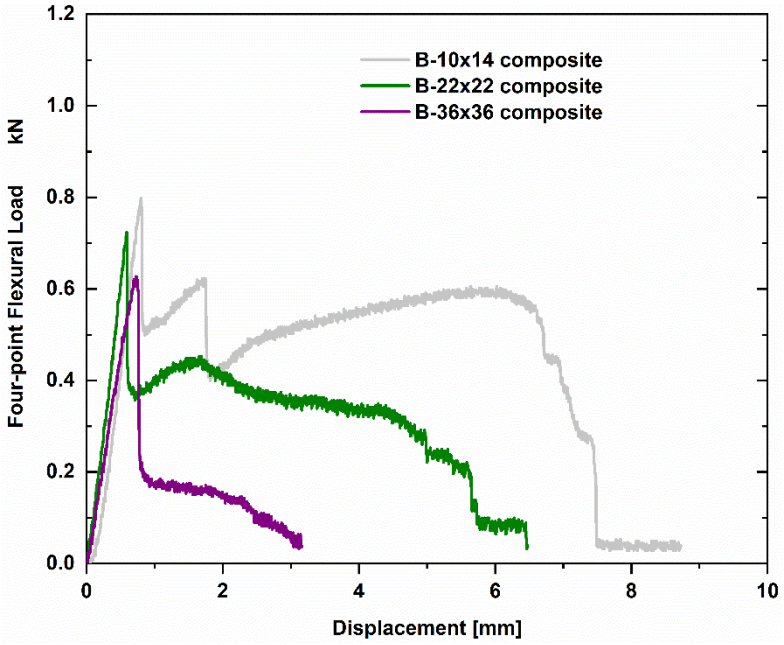

Figure 5.5 The comparison of flexural load-displacement curves between the BRG specimens reinforced with one textile layer and geomortar.

The effect of different layers of basalt textile having a small net size on the flexural performance of the BRG specimens is described over the flexural load-displacement curves

in Figure 5.2. With the increasing reinforcement ratio in the composite, its bearing load capacity obviously increases. The figure of the curves changed positively when the textile layer increased from one layer to four layers. While specimens reinforced with one textile layer broke down due to localization of the first crack, the increasing number of textile layers affect specimens having the failure manner into a more brittle fracture, i.e., a sudden loss of bearing load capacity after reaching the maximum load. Moreover, the dropping length of the second stage is also precisely related to the reinforcement ratio, and the figure of this stage of the curve is significantly different. The higher the number of the reinforcement ratio, the less fluctuation of the curve. This leads to a higher slope and flexural stiffness of specimens in this second stage. A similar conclusion is also represented for specimens reinforced with basalt textile having a middle net size, as seen in Figure 5.3. On the other hand, the specimens are required to be reinforced with a minimum of three layers in order to achieve a clear displacement-hardening behavior. Figure 5.4 exhibits the flexural load-displacement curves of specimens which are reinforced with basalt textile of a big net size. Unexpectedly, even when using reinforcing four layers; the specimens could not produce a displacement-hardening behavior. At this point, we can be concluded that the number of fiber yarns per each textile layer plays a key role in the composite behavior of the specimens. For instance, with the same reinforcement ratio in the specimen, B-22x22 composite with reinforcing three layers showed a displacement-hardening behavior, whereas B-36x36 composite with reinforcing four layers was unable to do so. Figure 5.5 gives a clear view of the effect of the net size on the response of flexural load-displacement curves of the BRG specimens, in which specimens reinforced with one textile layer are taken as a representation. Although these specimens show a displacement-softening behavior, the specimens reinforced with basalt textile having higher reinforcement ratio restrict the longer failure as well after the end of the first stage.

5.2 The mechanical properties of the BRG specimens

Table 5.1 detailed the results of the mechanical properties of the tested BRG specimens obtained from the four-point bending test, such as first-crack load, first-crack stress, ultimate-crack load, ultimate-crack stress, ultimate displacement, the number of cracks, flexural toughness and reinforcement ratio, whereas Figure 5.6 – Figure 5.10 show a few graphs representing the mechanical properties of these BRG specimens.

It should be noted that at this kind of composite material, mechanical properties extremely depend on both the arrangement of textile layer in matrix and direction of the applied load. For instance, the specimens reinforced with one layer do not always gain a stable value of flexural strength assuming that this textile layer is changed the position of the arrangement, and it would bring higher bearing load capacity in case that textile layer is positioned closer to tension edge with respect to ensuring the anchoring capability of textile [86]. Subsequently, the first-crack stress depends in part on the process of specimen production. Due to the insertion of textile layer in specimens, the fresh mixture should be carefully cast into the mold in order to gain a good penetration of matrix between textile layers. As shown in Figure 5.6, the green dashed line shows the significant variation of first-crack stress between the tested specimens. The B-22x22 composites with 2 – 3 reinforcing layers show the worst values in strength, for this reason it can be explained by the fact that those specimens were badly produced which resulted in the formation of many cavities surrounding the fiber yarn over the remaining specimens, as shown in Figure 5.6. The specimens reinforced with a greater number of reinforcement ratios, on the other hand, obviously lead to higher ultimate-crack stress, expect for those reinforced with basalt textile of a big net size, as shown in Figure 5.7. For basalt textile of a small net size, the specimens reinforced with two, three, four layers increased in ultimate-crack stress by 61.40% MPa, 110.75% MPa, 172.99% MPa, respectively, compared to one-layer reinforced specimens. For basalt textile of a middle net size, the specimens reinforced with three to four layers increased in ultimate-crack stress by 23.11% MPa, 72.09% MPa, compared to one-layer reinforced specimens. For the basalt textile of a big net size, although four textile layers were applied, the specimens were still unable to obtain the ultimate-crack stress over first-crack stress. This can be explained from three reasons: i) due to bigger net size makes the insufficient distribution of fiber yarns in the specimens, i)) low tensile strength of fiber yarn reflected the composite behavior (see in Table 1), iii) insertion of basalt textile in geopolymer mortar during aging has caused a partial reduction in its mechanical strength due to alkaline environment [22, 37]. Figure 5.8 shows the correlation between bending strength and reinforcement ratio of all the BRG specimens. Assuming that the fiber yarns of basalt textiles have the same mechanical properties, the use of the reinforcement ratio in the range of 0.17 to 0.7 is not able to improve the bending strength of the BRG specimens. However, the bending strength has changed markedly when the reinforcement ratio is above 0.7.

Table 5.1 The results of flexural behavior of the BRG specimens.

Samp. \ Value		F_1 [kN]	F_2 [kN]	R_{mo1} [MPa]	R_{mo2} [MPa]	y [mm]	Toughness [kN.mm]	Cr. [-]	Rr. [%]
B-10x14	1L	0.80 ± 0.05	0.80 ± 0.05	10.70 ± 0.07	10.70 ± 0.07	0.74 ± 0.04	0.30 ± 0.02	2	0.47
	2L	0.84 ± 0.01	1.29 ± 0.10	11.17 ± 0.07	17.27 ± 1.20	8.02 ± 0.07	7.18 ± 0.40	6	0.93
	3L	0.79 ± 0.07	1.69 ± 0.05	10.56 ± 0.90	22.54 ± 0.72	8.15 ± 0.14	8.37 ± 0.67	9	1.40
	4L	0.82 ± 0.10	2.19 ± 0.09	10.93±1.32	29.21 ± 1.22	8.30 ± 0.97	11.74±0.13	13	1.86
B-22x22	1L	0.74 ± 0.01	0.74 ± 0.01	9.82 ± 0.15	9.82 ± 0.15	0.67 ± 0.15	0.23 ± 0.04	2	0.23
	2L	0.65 ± 0.07	0.69 ± 0.04	8.62 ± 0.93	8.65 ± 0.56	1.06 ± 0.41	0.40 ± 0.14	2	0.47
	3L	0.57 ± 0.03	0.91 ± 0.04	7.53 ± 0.35	12.09 ± 0.52	6.43 ± 0.55	4.30 ± 0.41	5	0.70
	4L	0.59 ± 0.04	1.27 ± 0.06	7.86 ± 0.53	16.89 ± 0.79	7.45 ± 0.30	6.49 ± 0.48	8	0.93
B-36x36	1L	0.75 ± 0.10	0.75 ± 0.10	9.98 ± 1.43	9.98 ± 1.44	0.84 ± 0.18	0.27 ± 0.02	2	0.17
	2L	0.67 ± 0.07	0.67 ± 0.07	8.88 ± 0.98	8.88 ± 0.98	0.73 ± 0.02	0.24 ± 0.03	2	0.35
	3L	0.74 ± 0.10	0.74 ± 0.10	9.88 ± 1.35	9.88 ± 0.35	0.70 ± 0.06	0.29 ± 0.08	2	0.52
	4L	0.72 ± 0.01	0.72 ± 0.01	9.57 ± 0.10	9.57 ± 0.10	0.69 ± 0.08	0.27 ± 0.04	2	0.70

Note: The symbols such as F_1, F_2, R_{mo1}, R_{mo2}, y, Cr., Rr. stand for first-crack bending load, ultimate bending load, first-crack bending strength, ultimate bending strength, ultimate displacement, number of cracks and reinforcement ratio, respectively.

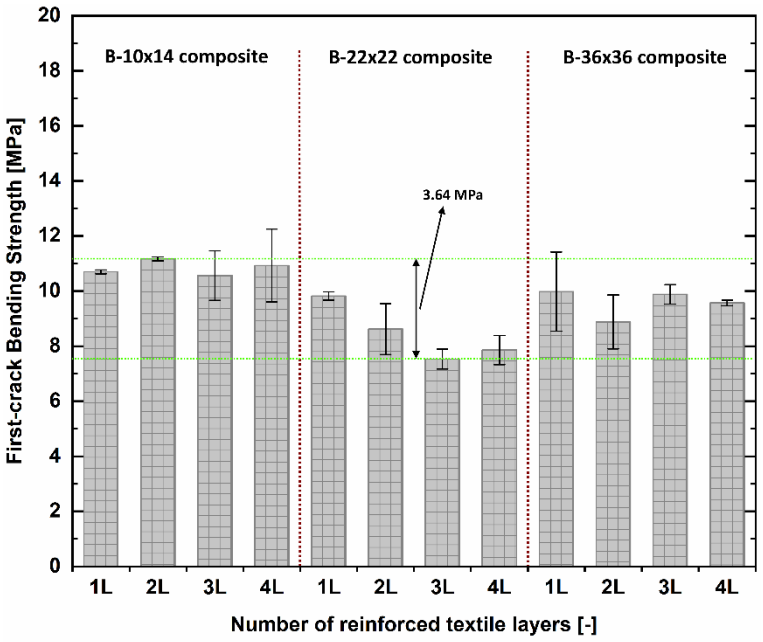

Figure 5.6 Average value of first-crack bending strength of basalt fiber meshes reinforced geomortar.

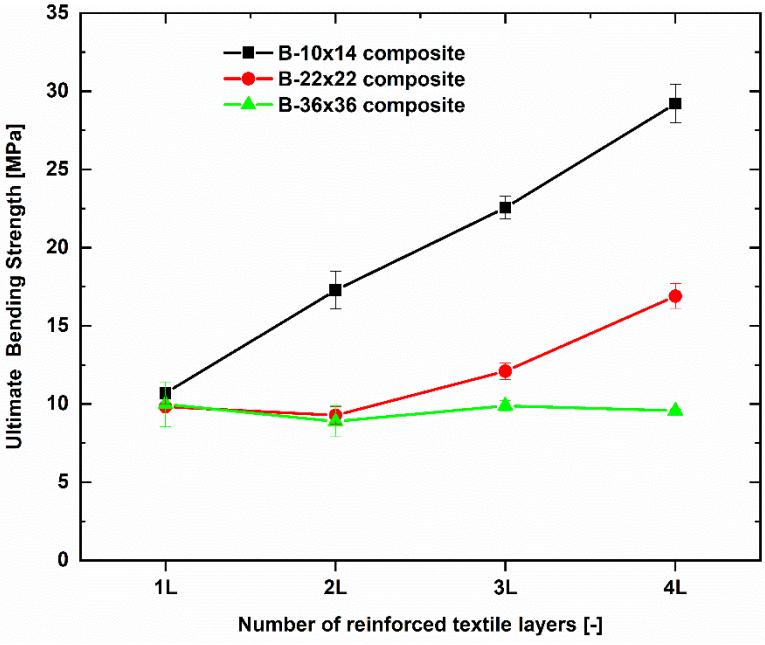

Figure 5.7 Average value of ultimate bending strength of basalt fiber meshes reinforced geomortar.

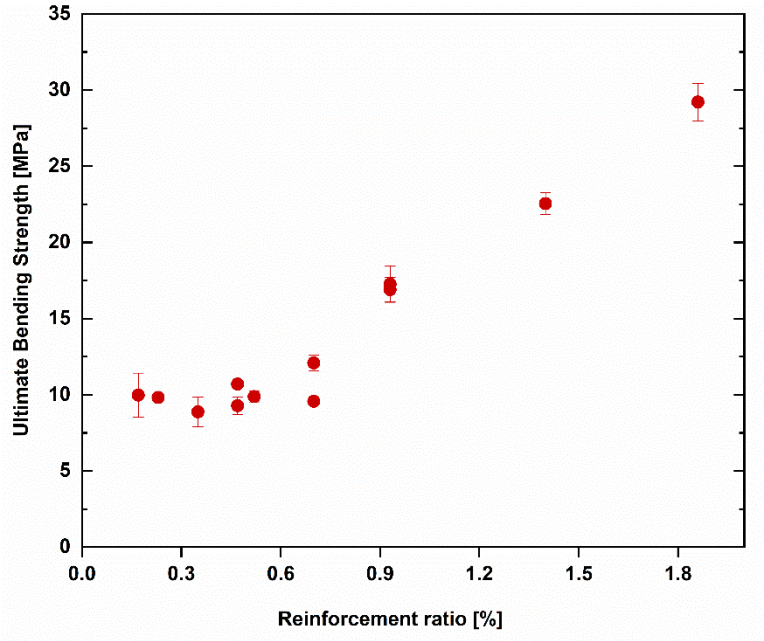

Figure 5.8 Correlation between bending strength and reinforcement ratio of the BRG specimens.

Figure 5.9 shows the average value of ultimate displacement of basalt fiber meshes reinforced geomortar. It can be observed that the large difference in displacement between samples led to a significant difference in energy absorption capacity between samples (see in Figure 5.10). The flexural toughness, so-called absorption energy capacity, is defined as the resistance of a material to failure or crack propagation. Toughness implies the amount of energy the specimen is able to absorb under loading up to a specified displacement, which clearly described in Standard ASTM/C 1609 [87]. In this work, it is measured as the area under the respective load-displacement curves up to peak load (ultimate load). Material with large energy absorption capacity obviously has higher energy to maintain crack propagation. Flexural toughness of the tested specimens is measured as area under respective load-displacement curves up to the peak load. According to the graphical representation of the toughness values in Figure 5.10, it was found that using basalt mesh of big net size results in very poor resistance of the BRG specimens to failure and their toughness value is almost the same with all BRG specimens. A similar conclusion is also represented for the BRG-10x14-1L, BRG-22x22-2L and BRG-22x22-2L. By contrast, the toughness value of the remaining BRG specimens improved obviously with the increasing number of textile layers and type of net size. For example, the BRG 10x14-2L has toughness value in 7.18 kN.mm, this value increased to 11.55% (8.36 kN.mm) with BRG 10x14-3L and increased to 63.61% (11.74 kN.mm) with BRG 10x14-4L. On the other hand, BRG 10x14-4L has toughness value in 1.17 kN.mm, this value decreased to 44.67% (6.49 kN.mm) with BRG 22x22-4L and decreased to 97.71% (0.27 kN.mm) with BRG 36x36-4L.

Figure 5.11 showed the strength development of the BRG specimens at different periods of time. In general, with increasing time the bending strength tends to decrease, but the difference in strength between the CRG specimens at the time after a half-year is not negligible. The reduction in strength of the BRG specimens is attributed to the presence of basalt fiber. As shown in Figure 5.11, compared to the 28-day samples the bending strength of the 180-day samples decreased by 21.46%, but the difference in strength between the 180-day samples and the 180-day samples was not significant. This result is consistent with the results of the mechanical strength development of geomortar samples shown in part 4.

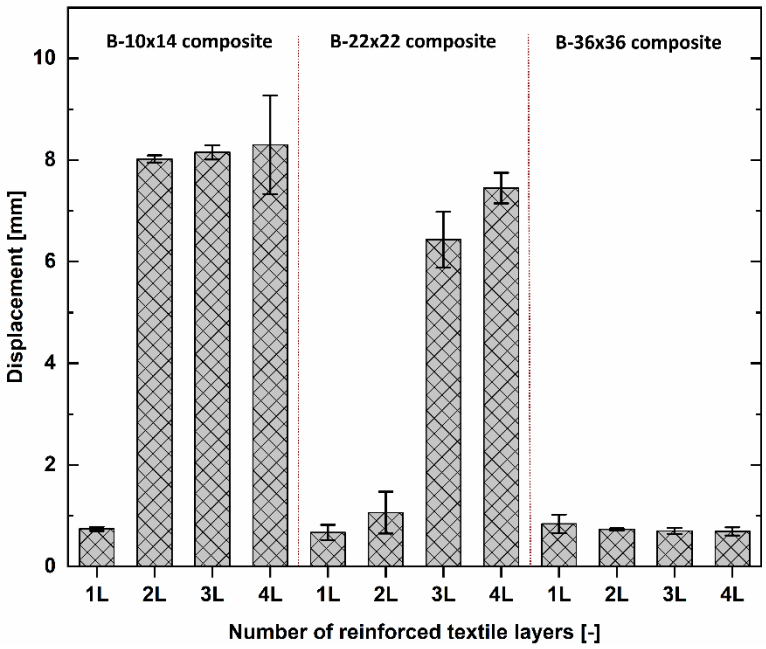

Figure 5.9 Average value of ultimate displacement of basalt fiber meshes reinforced geopolymer mortar.

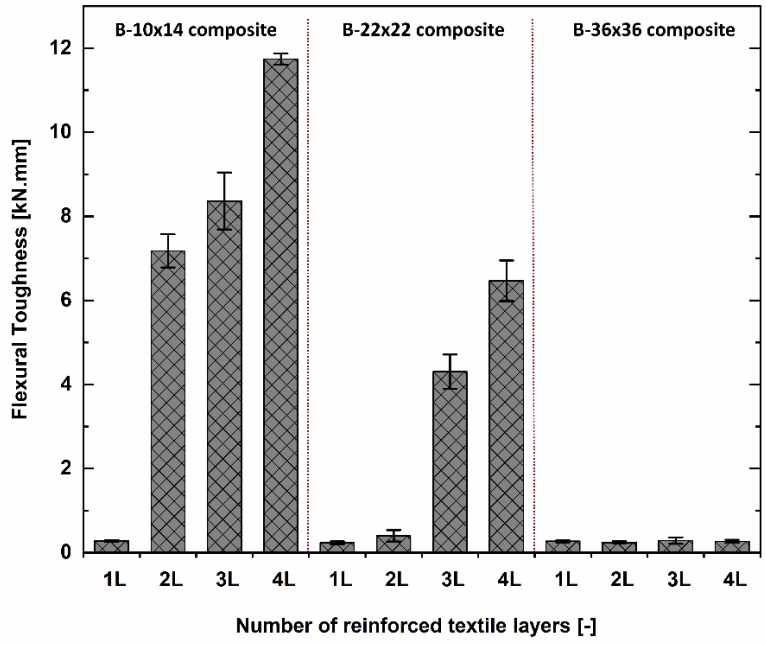

Figure 5.10 Average value of flexural toughness of basalt fiber meshes reinforced geopolymer mortar.

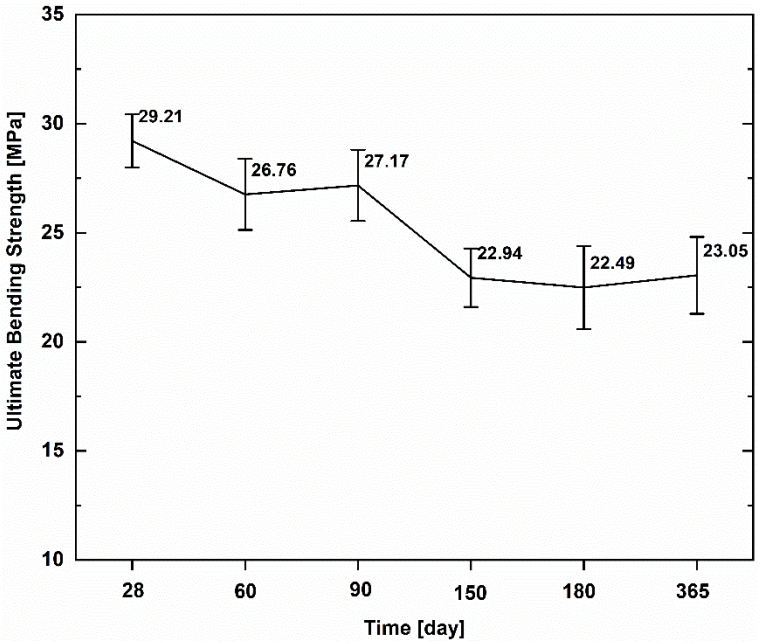

Figure 5.11 Development of flexural strength of the BRG specimens at various periods of time.

5.3 Failure mode of the BRG specimens

The imprint of fiber yarn embedded in geomortar matrix was clearly shown in Figure 5.12. It can be observed that good specimen production leads to better penetration of fresh mortar between textile layers resulting in a denser matrix structure with less cavities at the interface between mortar matrix and fiber yarn (Figure 5.12a). Additionally, the presence of filaments separated from fiber yarn indicates that there is a good bonding strength at the interface between fiber yarn and mortar matrix. In contrast, the image shown in Figure 5.12b points out a different view of the mortar matrix – fiber interface, which shows many cavities.

Figure 5.13 shows the failure modes of the BRG specimens under the four-point bending test. In general, all of the specimens had the same failure mode by the flexural failure due to the rupture of basalt fiber yarn in matrix, and no debonding of the fiber yarn or a gradual peeling process of mortar matrix happened during the testing. The difference can be seen clearly in the number of cracks and crack spacing between the reinforced specimens. With the increasing number of reinforcing layers, the BRG specimens displayed more cracks and narrow crack spacing, for this reason it is because the amount of energy that the specimens

absorb will be greater and accumulates faster during the multiple cracking stage. Moreover, the number of cracks also depends significantly on the number of fiber yarns per each layer (Figure 5.13). The failure with single crack results in the specimens BRG 10x14-1L, BRG 22x22-1L, BRG 22x22-2L, and all of the specimens reinforced with basalt textile of big net size. It can be said that using basalt textile of a big net size (shown in Figure 5.13c), even when using four strengthening layers also makes it impossible to help the BRG specimens achieving a multiple cracking behavior. The failure of these specimens is characterized by the widening of the first crack.

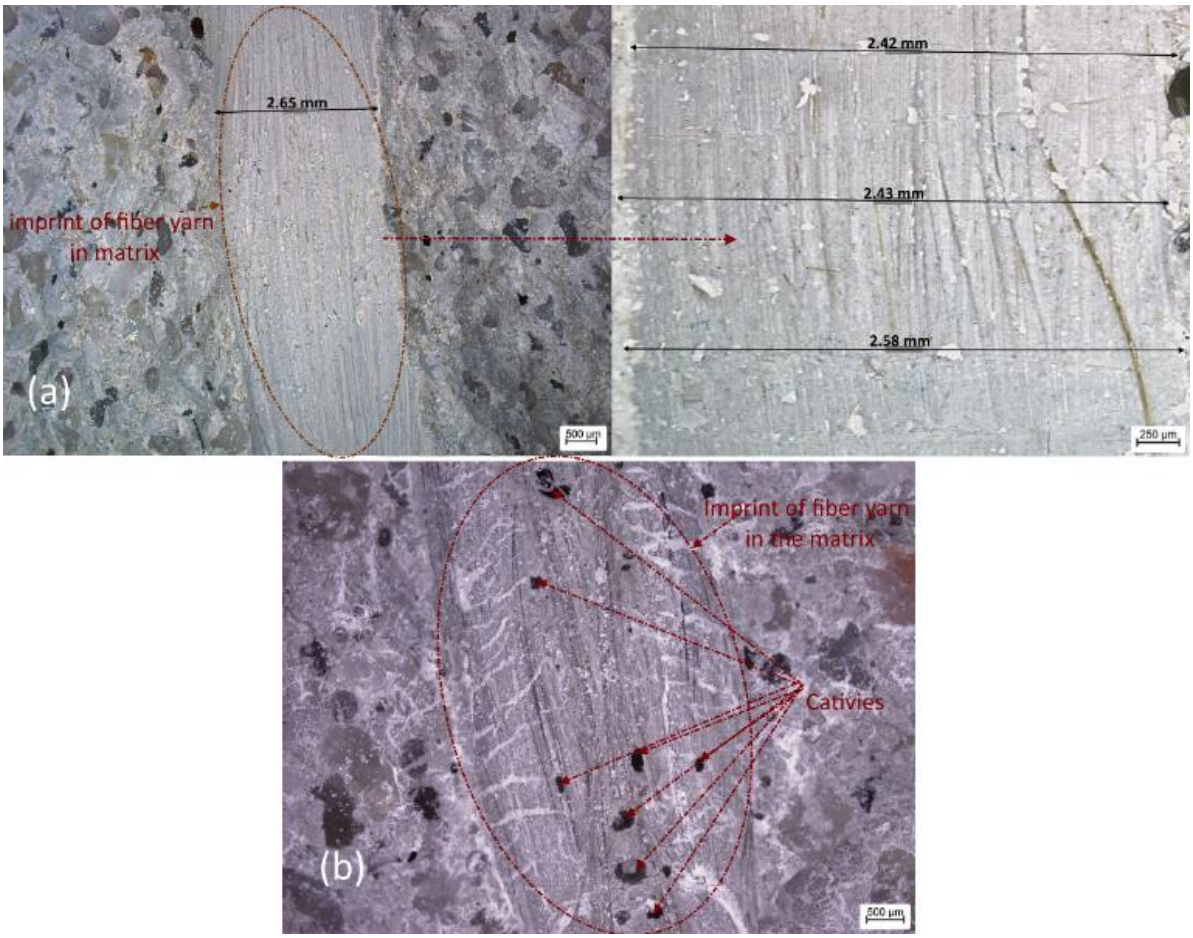

Figure 5.12 Geopolymer matrix/fiber yarn interface: (a) B-10x14 composite with reinforcing four layers; (b) B-22x22 composite with reinforcing three layers (500x magnification).

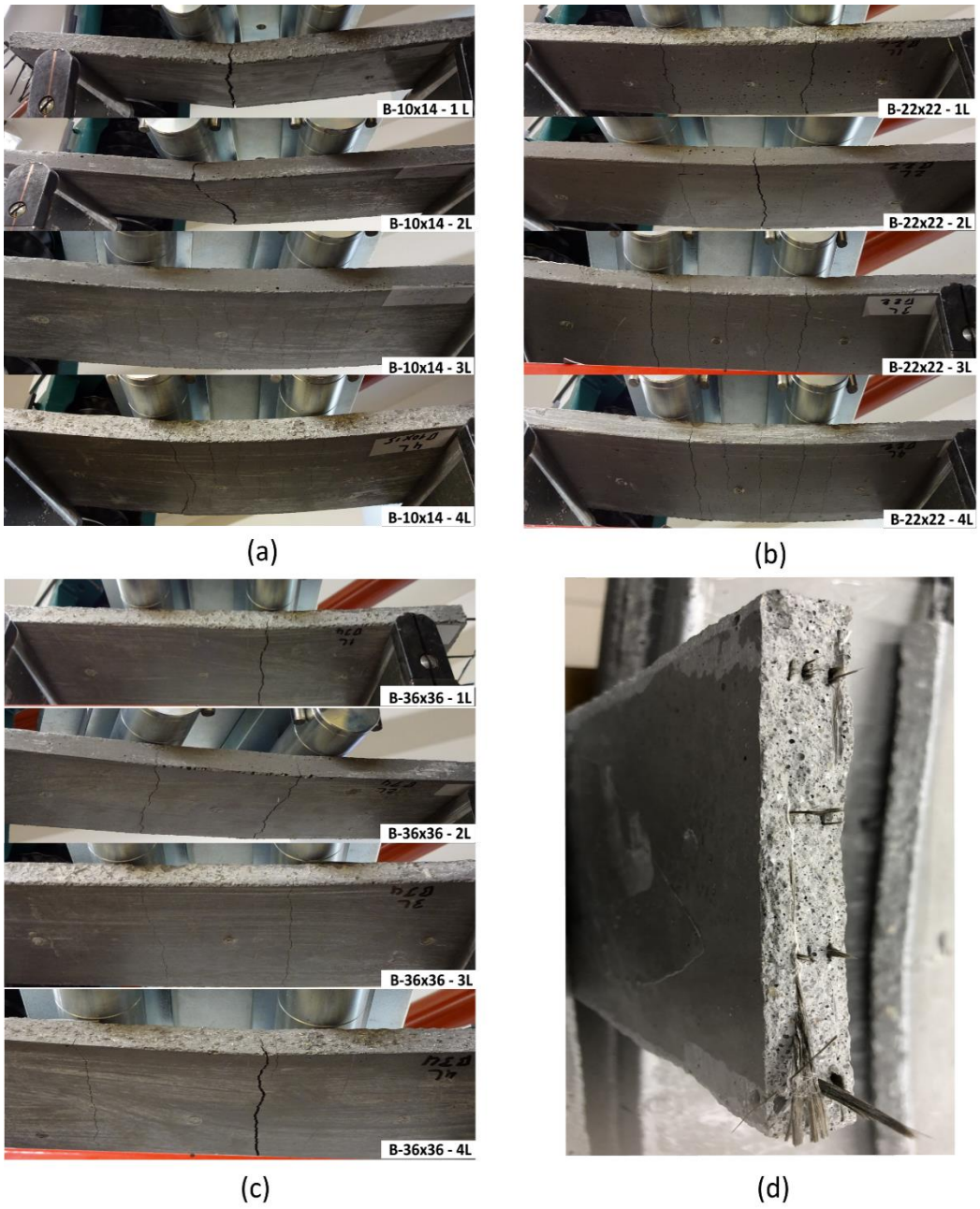

Figure 5.13 Photographs of the failure modes of the BRG specimens: (a) basalt textile of a small net size of 10 x 14 mm^2; (b) basalt textile of a middle net size of 22 x 22 mm^2; (c) basalt textile of a big net size of 36 x 36 mm^2; (d) rupture failure of the tested BRG specimen.

5.4 Summary

- The specimen production phase also plays an important role in the first-crack strength of these composite. The subjectivity in the specimen production can lead to the BRG specimens having many cavities at the interface between mortar matrix and fiber yarn which result in a decrease of the mechanical strength of the BRG specimens.
- With the increasing number of textile layers, the mechanical properties of the BRG specimens were improved significantly, especially with the BRG specimens reinforced with basalt mesh having a small net size.
- There is no impact on the mechanical strength of the BRG reinforced with basalt mesh of big net size, failure of these BRG specimens is due to localization of the first-crack. It can be concluded that using basalt mesh of big net size as reinforcement is not helpful. So, the author suggests that only basalt textile of small net size should be used to reinforce in specimens due to reinforcement effectiveness; or in case of using basalt mesh of big net size, fiber yarn should be resized to its size by the way that such fiber yarn should be made of more filaments to improve its low tensile strength.
- All the BRG specimens have the same failure mode by flexural failure due to rupture of fiber yarn in mortar matrix and no debonding of fiber yarn or a gradual peeling process of mortar matrix happed during testing.
- When the BRG specimens were exposed at longer ageing times (60, 90, 150, 180, 365 days), degradation of the mechanical strength with the increasing ageing time was revealed. The obvious loss of durability is after 150 days of ageing time. This reduction happed in both the mortar specimens and the BRG specimens, so it can be attributed to the presence of basalt fiber in geopolymer.

6. FLEXURAL PERFORMANCE OF VARIOUS CARBON FIBER MESHES REINFORCED GEOPOLYMER MORTAR.

This part investigates the effect of carbon fiber meshes on the flexural performance of textile reinforced geopolymer mortar. Three types of carbon mesh described in the previous part are used as a reinforcement in geopolymer mortar, and the flexural performance of textile geopolymer mortar composite was analyzed based on several key factors as follows: three different types of textile reinforcement inclusion various reinforcement ratio, geomortar type and arrangement of the position of textile mesh layer in the specimens.

6.1 The effect of textile type and reinforcement ratio on flexural performance

6.1.1 The flexural behavior of the CRG specimens

The influence of the textile type and the reinforcement ratio on the flexural behavior of the CRG composites is shown through means of flexural load-displacement curves in Figure 6.1–Figure 6.3. In general, geopolymer composite reinforced with carbon fiber meshes produced a displacement-hardening behavior and the load-displacement response of these specimens varies differently which depends on mechanical properties of the fiber yarn and reinforcement ratio.

The effect of the different layers of the C-10x15 textile on the flexural performance of the composites over flexural load-displacement curves is described in Figure 6.1. For one-layer reinforced specimens, the curve response with three different stages was clear. After reaching maximum load-bearing capacity, the specimens were broken down smoothly characterized by a gradual decrease of the curve in load and reduced to roughly 0.6 times of their maximum load capacity. Then theses composites can still maintain load capacity with increasing displacement after being. This phenomenon is attributed to the gradual pull out of the BF in a matrix, which allowed for the ductile failure of the composite. When using two to three reinforcing layers, the stiffness of the CRG specimens improved significantly as seen through the absence of stage 2 and higher slope of stage 3. Using a high reinforcement ratio is one of the factors causing the absence of stage 2 which was mentioned in previous literature [88]. The ending of stage 3 is marked by a sudden drop in

load almost to zero along with loud noise. This was found that the C-10x15 composites with higher reinforcement ratio lead to more catastrophic brittle failure, this means that the geomortar cover thickness between textile layers is not thick enough and strong to avoid the catastrophic failure despite the presence of the BF in the matrix. The reason for this failure mode is that the amount of energy that specimens absorb will be released as much as when the specimens are destroyed; thus the greater the amount of accumulative energy, the more catastrophic failure of the specimens. In this case it can be concluded that the stiffness of the composites was governed by the stiffness of the geopolymer matrix, material characteristic of fiber yarn, and reinforcement ratio. It found that the absence of stage 2 results in the maximum flexural strength and stiffness. Similar to the C-10x15 composites, the positive effect of the different layers of the two remaining types of carbon textiles on the flexural behavior of the CRG specimens can generally be seen in Figure 6.2 – Figure 6.3. With the increasing reinforcement ratio, the CRG specimens obviously have a higher load-bearing capacity. On the other hand, by comparing the flexural behavior between C-21x21 composites and C-34x34 composites, it was found that the mechanical properties of the fiber yarn have a strong effect on the response of flexural load-displacement curves which leads to interesting results of the mechanical properties of the TRG composites (Figure 6.4Figure 6.6). As mentioned in Table 3.1, although the tensile strength of the fiber yarns has similar values (only considering fiber yarns in the lengthways direction – the load-bearing direction), the fiber yarns of the C-21x21 textile show a lower Young's modulus and higher elongation than those of the C-34x34 textile; thus, as a result, the C-21x21 composites will tend to exbibit more pseudo-ductile behavior in bending, compared to those reinforced with C-34x34 textile, as proven by lower slope and less oscillation in stage 2. In addition, in stage 3, soon before and after reaching maximum load-bearing capacity, the C-21x21 composites almost maintain the unchanged load-bearing capacity with the increasing displacement (see in Figure 6.2). In other words, it should be noted that by comparing the development of stage 1 between tested specimens, the slope of the first stage of the curve is nearly the same for all tested CRG specimens but the first-crack load value does not follow a logic rule. This phenomenon is attributed to the presence of textile reinforcement in the matrix. The stiffness and the value of the first-crack load in this stage are governed predominantly by the stiffness of the matrix. However pre-existing micro-cracks, especially at the matrix/fiber interface, that can be formed during manufacturing, curing, and setting-up of the specimens also contribute to the reduction in the first-crack

load. The higher the reinforcement ratio, the greater the probability of the presence of more micro-cracks in the matrix.

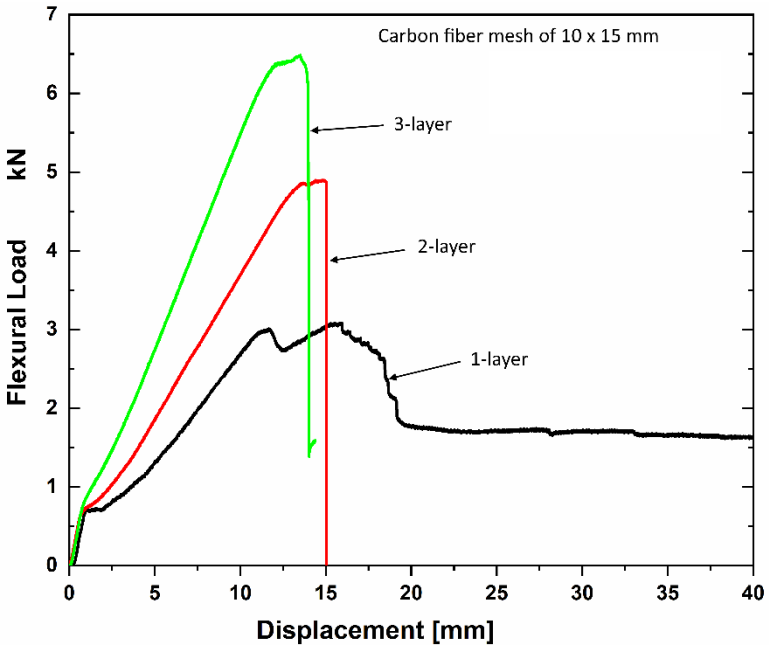

Figure 6.1 Flexural load-displacement curves of the specimens reinforced with the carbon fiber textile having a net size of 10 x 15 mm.

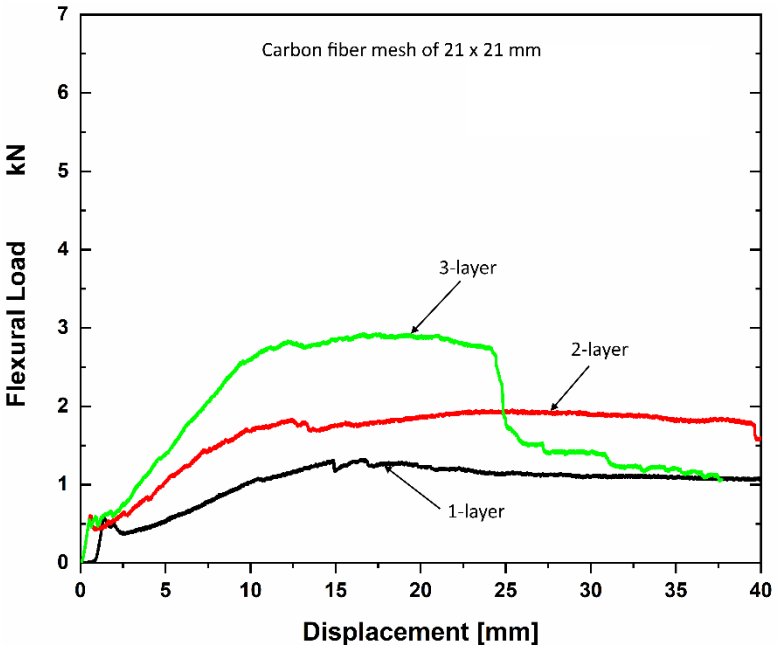

Figure 6.2 Flexural load-displacement curves of the specimens reinforced with the carbon fiber textile having a net size of 21 x 21 mm.

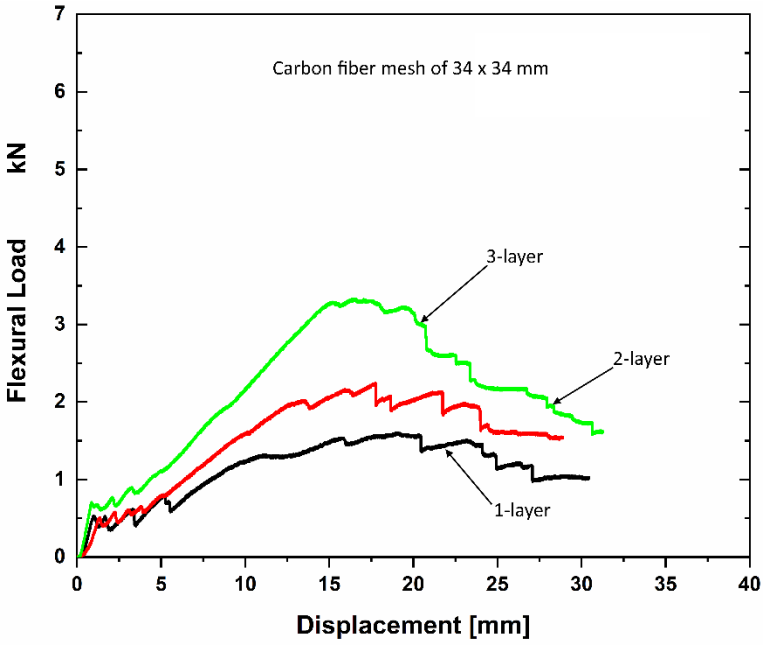

Figure 6.3 Flexural load-displacement curves of the specimens reinforced with the carbon fiber textile having a net size of 34 x 34 mm.

6.1.2 Mechanical properties of the CRG specimens

Table 6.1 The results of flexural behavior of the CRG specimens corresponding to reinforcement ratio and textile type.

Sample		F_1 [kN]	R_{mo1} [MPa]	F_2 [kN]	R_{mo2} [MPa]	y [mm]	Toughness [kN.mm]	Cr. [-]	Rr. [%]
C-10x15	1L	0.79 ±0.05	10.55 ±0.90	3.03 ±0.14	40.36 ±1.88	15.89 ±1.76	31.12 ±0.87	14.67	0.96
	2L	0.79 ±0.03	10.53 ±0.52	4.79 ±0.52	63.94 ±6.88	14.19 ±0.71	38.71 ±3.22	15.33	1.93
	3L	0.89 ±0.06	11.87 ±0.76	6.47 ±0.72	86.30 ±5.65	13.10 ±0.43	46.92 ±2.95	16.00	2.89
C-21x21	1L	0.65 ±0.08	8.67 ±0.84	1.44 ±0.21	19.18 ±2.77	15.48 ±1.73	12.99 ±0.36	3.66	0.45
	2L	0.69 ±0.02	9.24 ±0.79	1.99 ±0.10	26.62 ±1.33	23.86 ±7.09	34.82 ±14.2	6.33	0.96
	3L	0.74 ±0.03	9.89 ±0.47	3.13 ±0.27	41.76 ±3.61	18.21 ±0.25	72.80 ±8.07	8.67	1.45
C-34x34	1L	0.64 ±0.06	8.56 ±0.84	1.61 ±0.15	21.41 ±2.05	17.48 ±2.91	17.93 ±3.89	6.66	0.36
	2L	0.61 ±0.06	8.13 ±0.76	2.33 ±0.21	31.07 ±2.77	18.83 ±0.78	25.65 ±1.38	9.33	0.72
	3L	0.78 ±0.09	10.43 ±1.20	3.29 ±0.17	43.88 ±2.26	17.85 ±2.42	66.98 ±5.61	11.33	1.08

The effect of the reinforcement ratio and the textile type on the flexural strength, the flexural toughness, the displacement, and the crack number of the TRG specimens is presented in Table 6.1and Figure 6.4 – Figure 6.7. It should be noted that due to using the geopolymer matrix with the same recipe for all the tested specimens, the different comparison of the first-crack strength between tested specimens is not mentioned, and a difference in the first-crack strength observed between tested specimens was discussed above. In general, the mechanical strength improved significantly with the increasing reinforcement ratio. The superiority of the reinforcement ratio in the C-10x15 composites makes them achieve remarkably higher flexural strength, compared to those reinforced with C-21x21 textile and C-34x34 textile (Figure 6.4). Even the composites reinforced with three layers of the C-21x21 and C-34x34 textiles almost have the similar flexural strength achieved by the C-10x15 composites reinforced only with one-layer. When comparing flexural strength between C-21x21 composites and C-34x34 composites, the mechanical properties (Young's modulus and elongation) of the fiber yarn have a significant influence on the composite strength. Although the C-21x21 composites apparently have a higher reinforcement ratio than the C-34x34 those (considering for the same reinforcing layer), they could not produce a higher value in flexural strength. At this point, we can confirm the fact that a higher reinforcement ratio does not necessarily result in higher composite strength. For the C-10x15 textile, the specimens reinforced with two and three layers

increased in flexural strength by 58,42% MPa, 113.83% MPa, respectively, compared to the one-layer reinforced specimens. For C-21x21 textile and C-34x34 textile, specimens reinforced with two and three layers increased in ultimate flexural strength by 38.79%, 45.12%, and 117.73%, 102.62%, respectively. Figure 6.5 shows the results of the flexural toughness of the CRG specimens. It was observed that when the specimens reinforced with three layers of the textile are considered, the C-21x21 composites show the highest value of the flexural toughness. It can be explained by the fact that the high elongation of the C-21x21 textile affected positively to the CRG composite ductility (see in Figure 6.6), which compensates for the low flexural strength; as a result, the flexural toughness was improved. This reveals that using both reasonable reinforcement ratio and the textile type make composites possible to enhance significantly the flexural toughness. Figure 6.7 shows that the number of cracks increased with the increasing number of textile layers. Based on this result we also see that the stiffness of the composites is related to the number of cracks. The composites with higher stiffness will delay the propagation of cracks longer, which results in the reduction in the crack width and increase in the number of the cracks at tension edge.

Figure 6.8 showed the strength development of the CRG specimens at different periods of time. In general, with increasing time the bending strength tends to decrease, but the reduction in strength between the CRG specimens at the time after a half-year is not negligible. As shown in Figure 6.8, compared to the 28-day samples the bending strength of the 180-day samples decreased by 8.89%, but the 365-day samples showed a decrease in strength by 1.74% when compared to the 180-day samples.

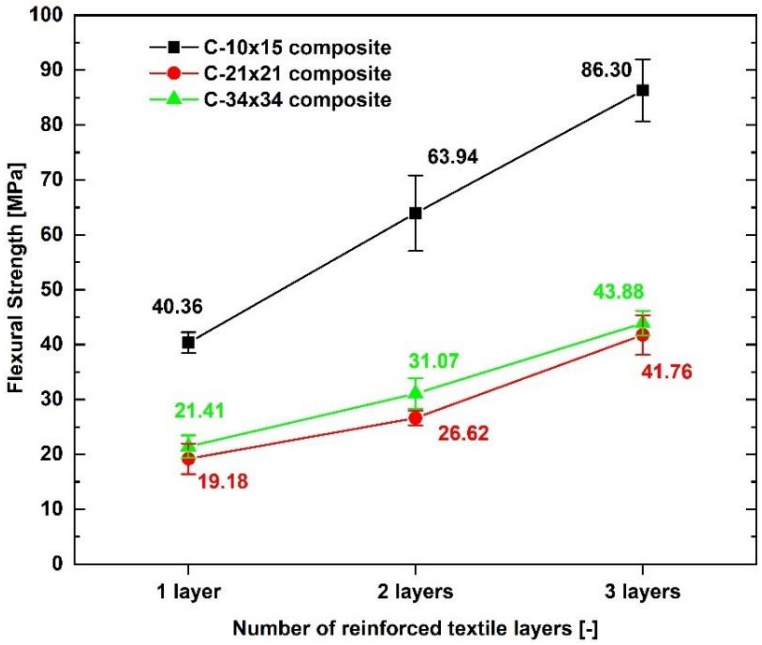

Figure 6.4 Average value of the ultimate four-point bending strength of the CRG specimens corresponding to reinforcement ratio and textile type.

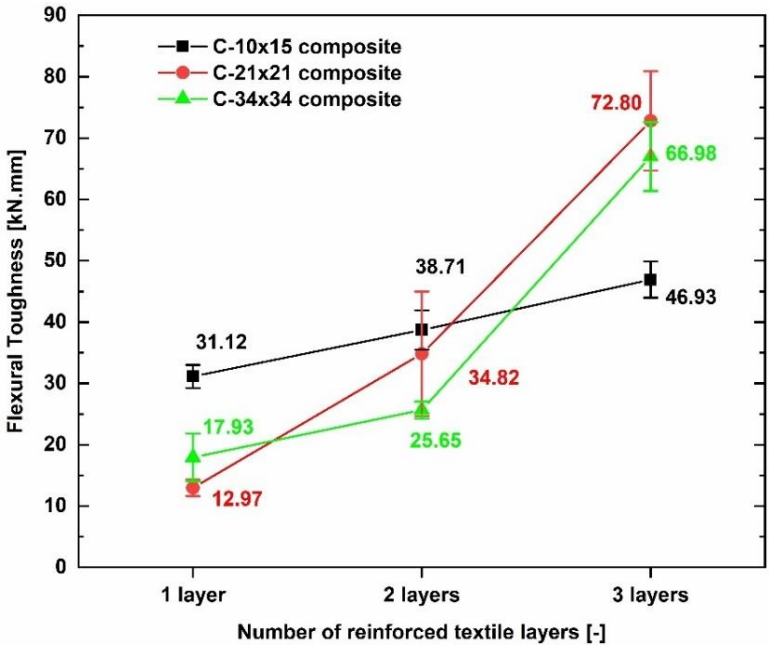

Figure 6.5 Average value of the bending toughness of the CRG specimens corresponding to reinforcement ratio and textile type.

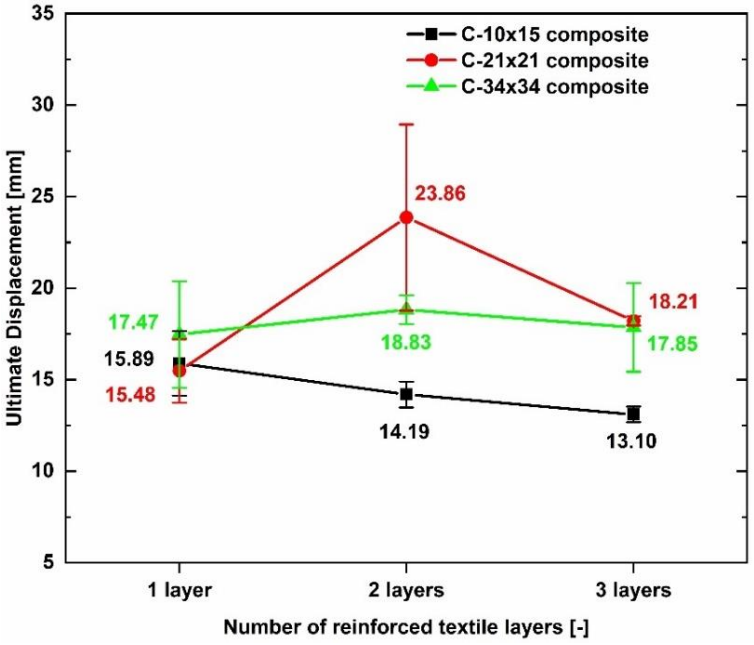

Figure 6.6 The average value of the ultimate displacement of the CRG specimens corresponding to reinforcement ratio and textile type.

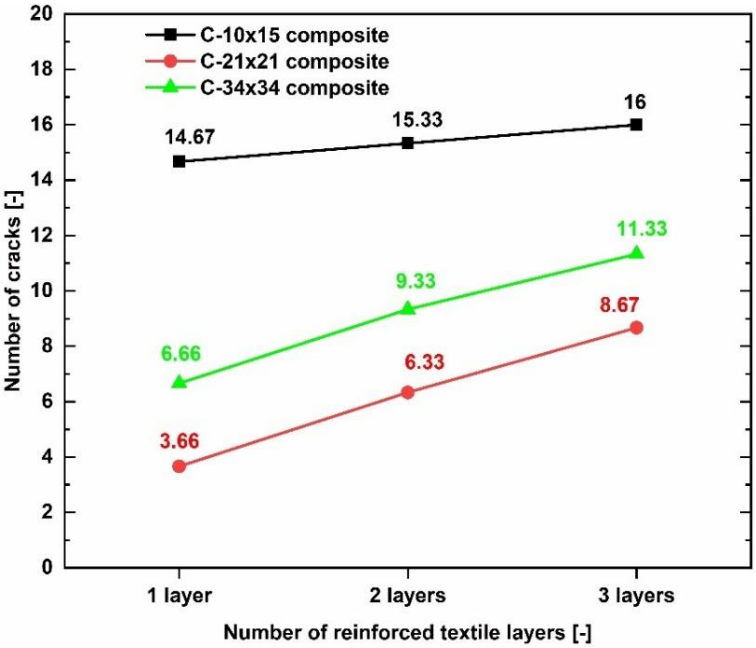

Figure 6.7 The number of the cracks of the CRG specimens corresponding to reinforcement ratio and textile type.

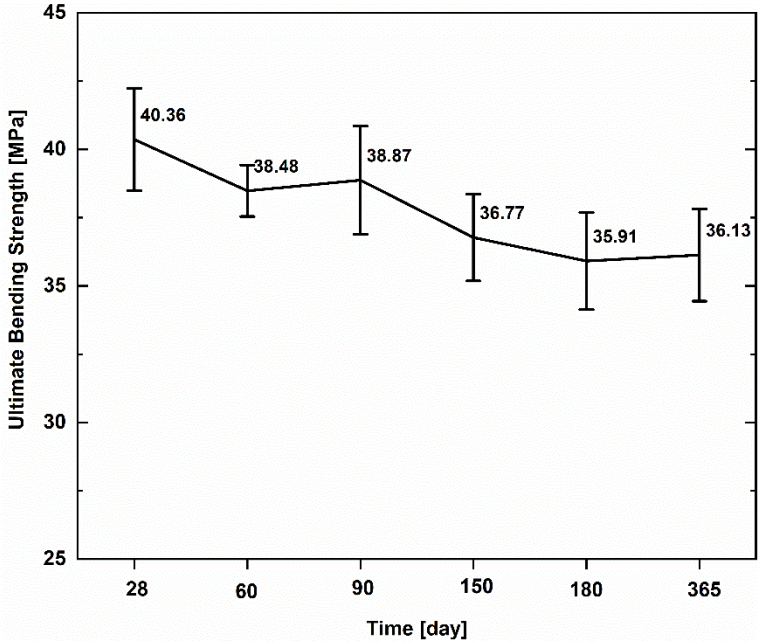

Figure 6.8 Development of flexural strength of the CRG specimens at various periods of time.

6.1.3 Failure modes of the CRG specimens

The flexural failure modes of the TRG composites are displayed in Figure 6.9. It was observed that the CRG specimens could be exhibited two different types of the bending failure: i) the loss of bonding strength at the matrix/fiber interface along with the partial rupture of the filaments at outer layer leads to the slippage of the fiber yarns within mortar matrix resulting in pure flexural failure, ii) the initiation of the failure process is the same like the failure mode of type 1, then as soon as the CRG specimens reach their maximum load-bearing capacity, a sudden debonding process and the catastrophic collapse occurred almost simultaneously with loud noises. As seen in Figure 6.9, all CRG specimens almost have the same failure mode of type 1, while those reinforced with 2 – 3 layers of the C-10x15 textile have the failure mode of type 2.

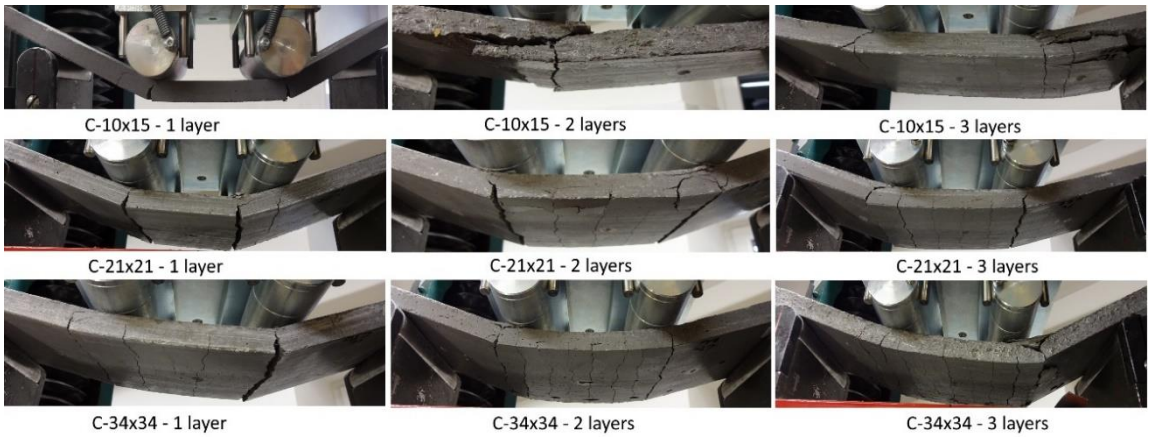

Figure 6.9 Failure modes of the CRG specimens corresponding to the textile type and a different number of the textile layers.

6.2 Effect of mortar type on flexural performance

Geomortar 1 with label GM-0.2S and geomortar 2 with label GM-0.2S0.1F5B (see in Table 3.2) were used to study the influence of the mortar strength on the flexural behavior of the C-10x15 textile composites. In comparison to geomortar 1, the geomortar 2 showed approximately 1.39 times and 1.45 times higher flexural strength and compressive strength, respectively. For both geomortars, composites were reinforced with 1 – 3 layers of the C-10x15 textile. Representative load-displacement curves of the C-10x15 textile composites with geomortar 1 and geomortar 2 are demonstrated in Figure 6.10. In stage 1, both geomortars show a similar linear elastic behavior and the same stiffness. However, there is a clear difference between two types of geomortar affecting the composites when comparing them at stages 2 and 3. In comparison to composites with geomortar 2, the composites with geomortar 1 indicated significantly lower stiffness resulting from the lower slope of these two stages. Also, despite the increased reinforcement ration, the oscillation of the loading curve at stage 2 and non-linearity of this curve during stage 3 still occur which was not found in composites with geomortar 2. This is attributed to the low bond at the interface of matrix and fiber yarn due to less compact in the structure of geomortar 1. In other words, from load-displacement curves, all the composites are characterized by a significant sudden drop (disastrous failure) in the load almost to zero after reaching the maximum load-bearing capacity, except for one reinforcing layer composite with geomortar 2. This is attributed to the fact that the presence of the BF in geomortar 2 along with the reasonable reinforcement ratio of textile helps the composite

avoid catastrophic failure. The role of the BF on the flexural behavior of the textile geopolymer composite will be presented in the next part.

It is clearly evident from Table 6.2 and Figure 6.11, Figure 6.12 the using geomortar 2 drastically improves the mechanical properties of the C-10x15 textile composites. By the increasing geomortar strength, first-crack strength, ultimate strength, and toughness were increased. At the same time, the deformation rate of the composites has decreased, meaning that the composite stiffness increases. For example, the C-10x15 textile composites with geomortar 2 almost show an approximately 2 times higher value of ultimate bending strength compared to those with geomortar 1 at the same reinforcement ratio. Especially for bending toughness value, the geomortar 2 make composite have a better effect on this parameter, especially when comparing composite between 2 and 3 layers, wherein bending toughness increased by 21.21 %, while this value for composite used geo-mortar 1 only increased by 8.94 % (see in Figure 6.12).

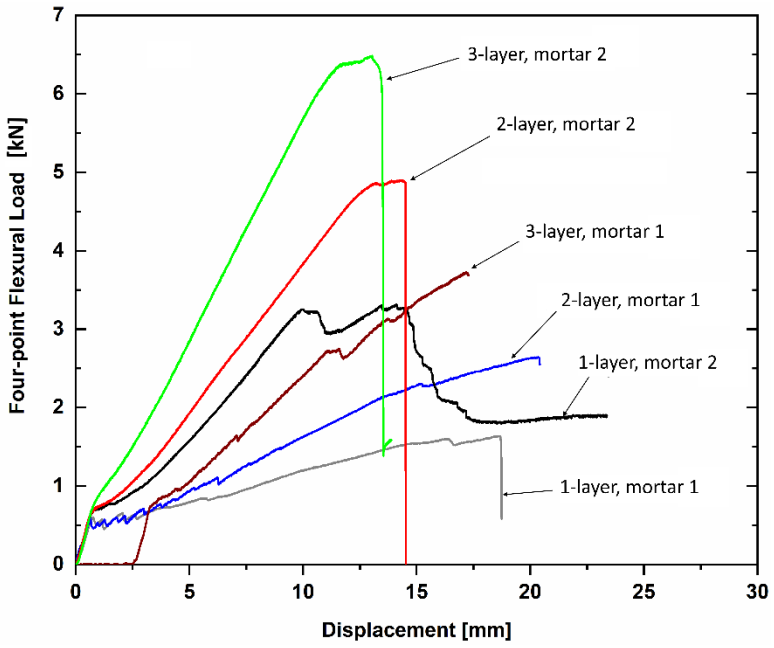

Figure 6.10 Effect of geomortar strength on flexural load-displacement curves of the C-10x15 textile composites.

Table 6.2 Effect of geo-mortar strength on the flexural behavior of C-10x15 textile composites.

Sample		F_1 [kN]	R_{mo1} [MPa]	F_2 [kN]	R_{mo2} [MPa]	y [mm]	Toughness [kN.mm]	Cr. [-]	Rr. [%]
Mortar 1	1L	0.42 ±0.07	5.61 ±1.16	1.62 ±052	21.59 ±2.12	18.94 ±2.42	21.03 ±1.56	7.33	0.96
	2L	0.54 ±0.04	7.23 ± 0.40	2.73 ±0.40	36.41 ±4.32	19.89 ±1.79	32.87 ±0.56	14.33	1.93
	3L	0.72 ±0.02	9.62 ± 0.22	3.75 ±0.55	50.01 ±5.91	17.28 ±1.28	35.81 ±1.82	14.67	2.89
Mortar 2	1L	0.79 ±0.05	10.55 ±0.90	3.03 ±0.14	40.36 ±1.88	15.89 ±1.76	31.12 ±0.87	14.67	0.96
	2L	0.79 ±0.03	10.53 ±0.52	4.79 ±0.52	63.94 ±6.88	14.19 ±0.71	38.71 ±3.22	15.33	1.93
	3L	0.89 ±0.06	11.87 ±0.76	6.47 ±0.72	86.30 ±5.65	13.10 ±0.43	46.92 ±2.95	16.00	2.89

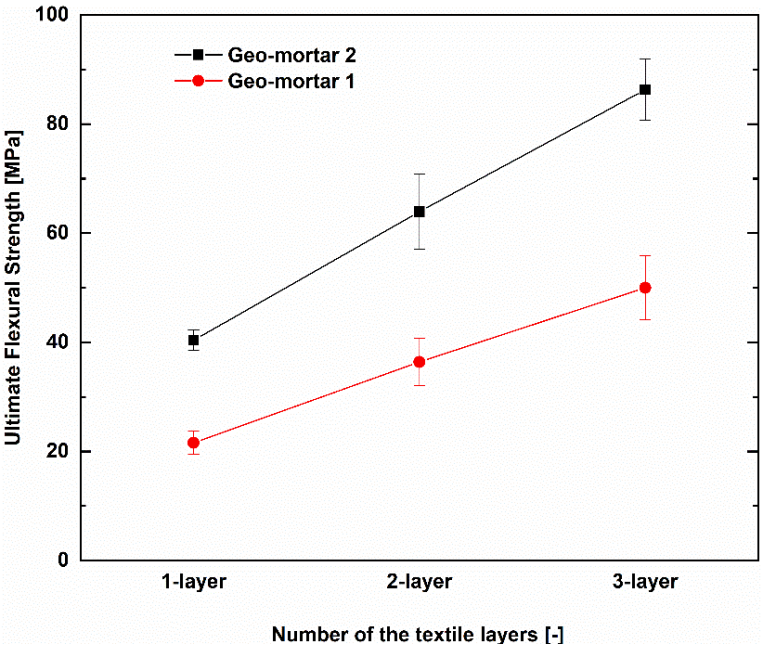

Figure 6.11 Comparison of flexural strength of the C-10x15 textile composites considering the use of the different geomortar.

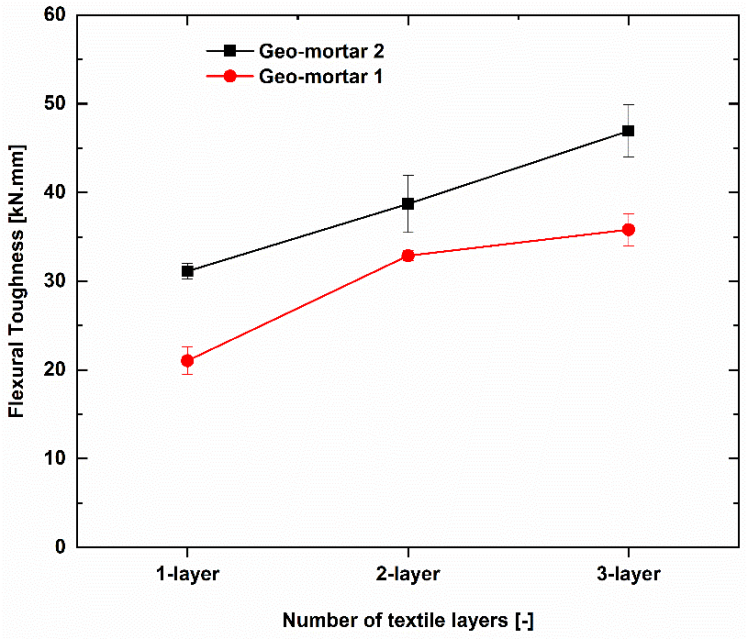

Figure 6.12 Comparison of flexural toughness of the C-10x15 textile composites considering the use of the different geomortar.

6.3 Effect of the position arrangement of the textile layer in the specimen

One of the advantages of TRC composite is that textile reinforcement can be placed at the positions where stress is required respect to ensuring the anchoring capability of textiles. It was observed that when the textile is positioned closer to the tension edge, the composites show a higher load-bearing capacity due to the utilization of the textile used. In this section, the influence of the position of the textile layer in specimens will be investigated and four different kinds of textile positions consisting of 3 mm, 5 mm, 7 mm, and 9 mm were applied. 3 mm value implies the textile layer was placed in the specimen at a distance of 3 mm from a tension edge, and the higher this value is the closer this distance to compressive edge is. Figure 6.13 shows the influence of the position of the textile layer on the flexural behavior of the CRG specimens, whereas the mean values of the experimental results are represented in Table 6.3 and Figure 6.14 – Figure 6.16. It can be observed from Figure 6.13 that the thin cover layer leads to an increment of tension element (textile layer) that brings higher stiffness and higher bearing capacity. This phenomenon can be explained by the fact that when the cover layer thickness guarantees the anchoring capability of the textile in the matrix, the specimens with thinner cover layer will delay the development of the crack

width as long as possible, due to the tension efficiency of the textile. This results in both geopolymer mortar and textile undergoing collectively better bearing capacity under loading. Also, in terms of displacement, when the textile layer tends to be placed away from tension edge the samples will become more deformed due to lower specimen stiffness; thus, the displacement value is higher. It can be seen that, in comparison with the specimens having a cover thickness of 9 mm, the ultimate stress of the specimens having a cover thickness of 7 mm, 5 mm and 3 mm, increases by 67.32%, 96.85%, and 115.13%, respectively. Figure 6.17 shows the photo of failure modes of the CRG specimens respect to the position of the textile layer. All the specimens behaved the same failure as a pure bending failure due to the slipping of fiber yarns in the matrix.

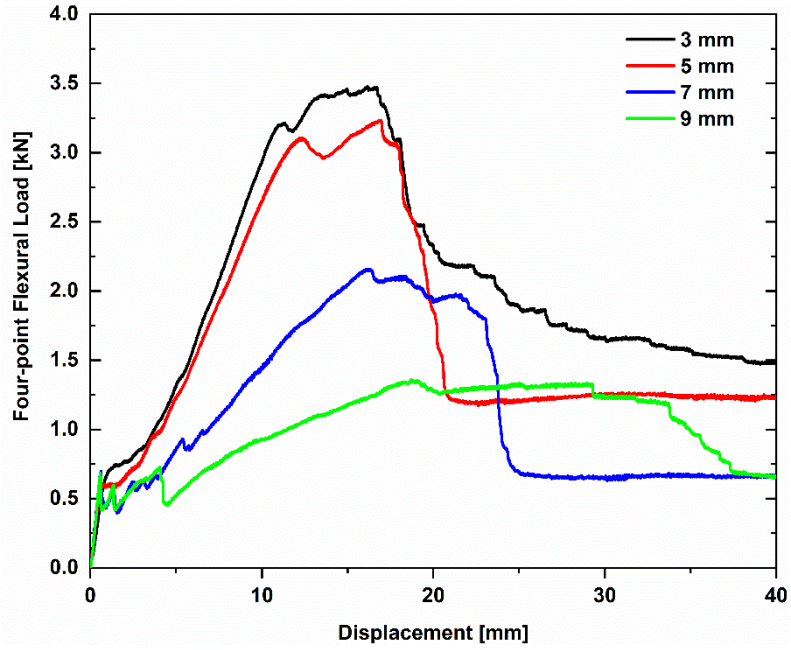

Figure 6.13 Flexural load-displacement curves of the TRG composites with respect to the position of the textile layer in specimens.

Table 6.3 The results of the flexural behavior of the CRG specimens with one reinforcing layer corresponding to the position of the textile layer in specimens.

Sample	Value	F_2 [kN]	R_{mo2} [MPa]	y [mm]	Toughness [kN.mm]	Cr. [-]	Rr. [%]
C-10x15 textile composite	**3 mm**	3.59 ± 0.22	47.90 ± 2.97	16.19 ± 1.65	34.83 ± 1.80	15.67	0.96
	5 mm	3.23 ± 0.15	43.05 ± 1.95	16.27 ± 0.15	31.87 ± 3.24	14.67	0.96
	7 mm	2.29 ± 2.60	32.67 ± 2.87	18.66 ± 2.31	27.09 ± 5.20	11.50	0.96
	9 mm	1.40 ± 0.06	18.69 ± 0.79	18.84 ± 0.30	16.19 ± 0.28	4.67	0.96

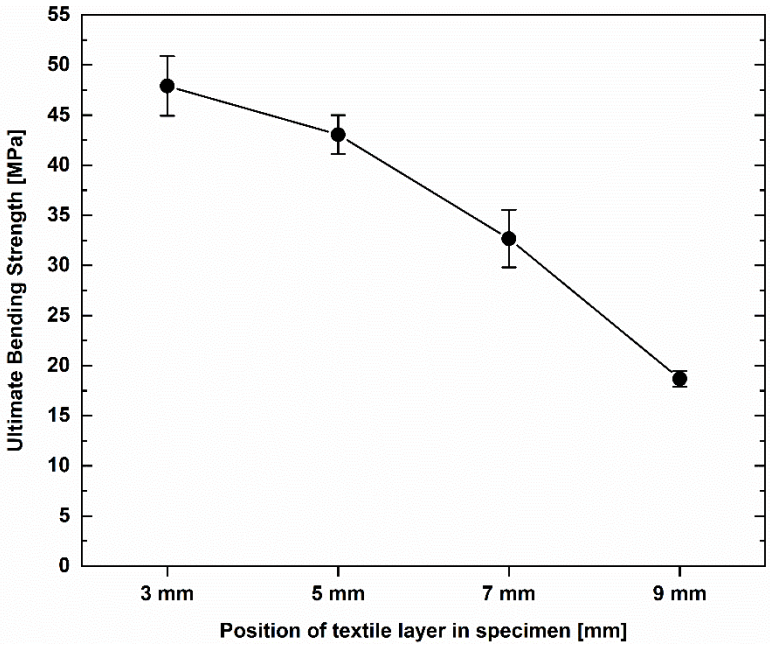

Figure 6.14 The flexural strength of CRG specimens with one reinforcing layer regarding the position of the textile layer in specimens.

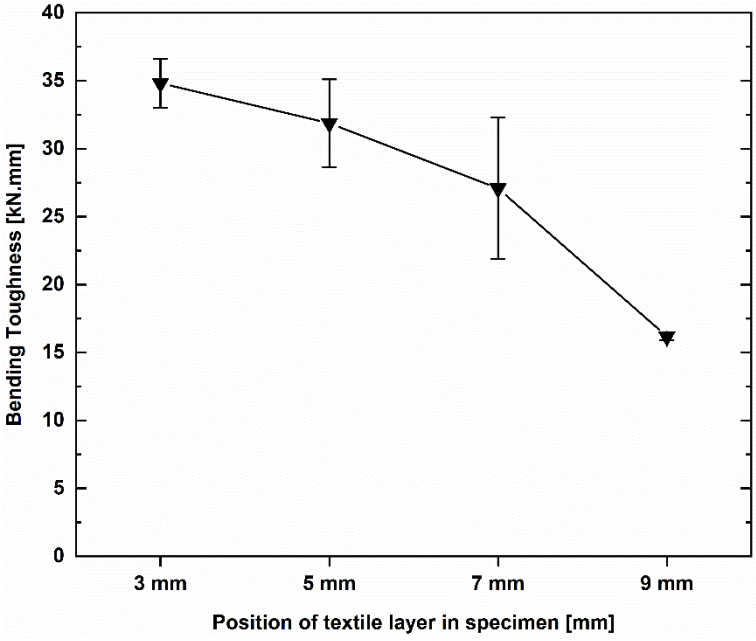

Figure 6.15 Bending toughness of CRG specimens with one reinforcing layer regarding the position of the textile layer in specimens.

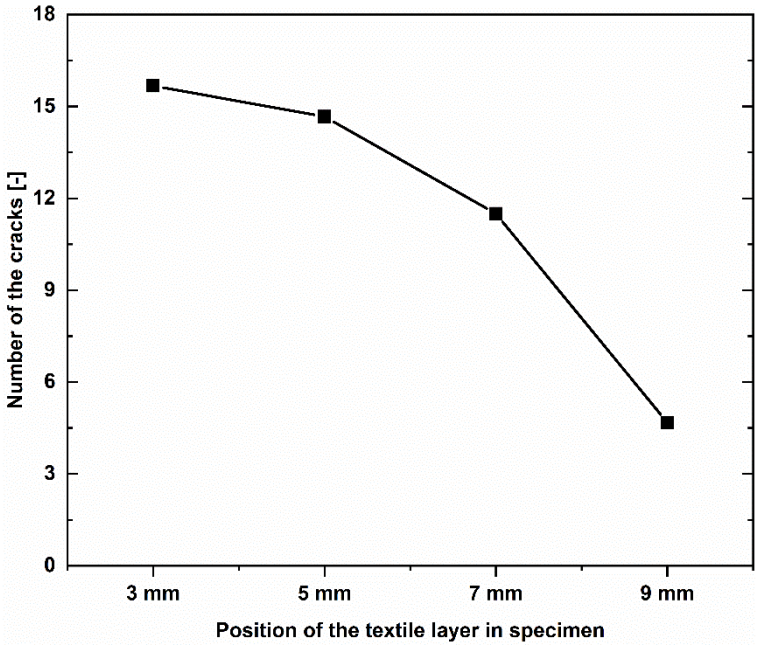

Figure 6.16 Number of cracks of CRG specimens with one reinforcing layer regarding position of the textile layer in specimens.

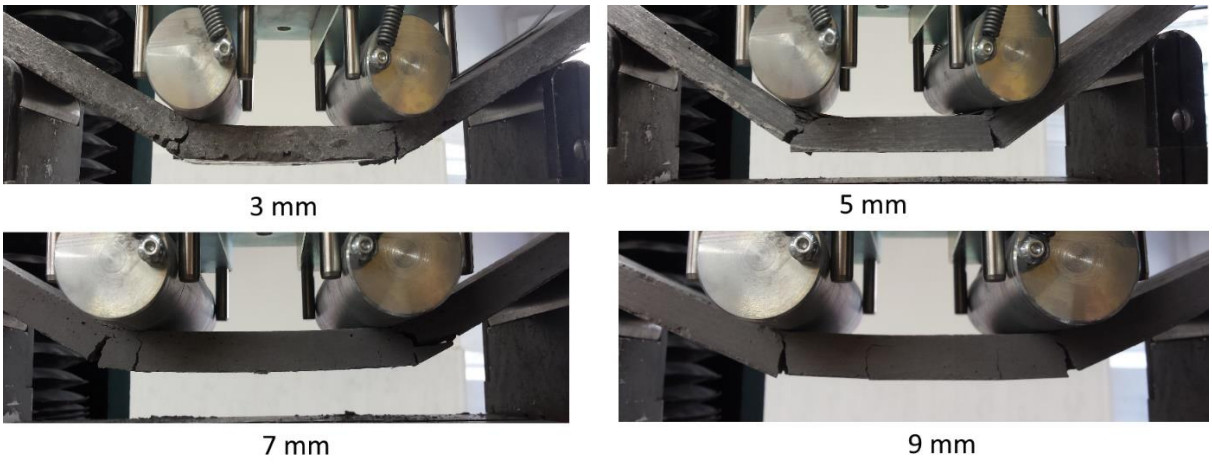

Figure 6.17 Failure modes of the C-10x15 composite with one reinforcing layer regarding the position of the textile layer in specimens.

6.4 Summary

- With the increasing reinforcement ratio, the flexural strength of the CRG specimens was improved significantly. In other words, the CRG specimens reinforced with one-layer of the C-10x15 textile almost have a similar flexural strength achieved by those reinforced with three layers of the C-21x21 textile and the C-34x34 textile.
- Using a high reinforcement ratio makes the C-10x15 composites achieve the high flexural strength, but they were catastrophically destroyed when compared to the remaining TRG specimens. The debonding and collapse phase have taken place simultaneously.
- Although the C-21x21 composites have a higher reinforcement ratio (considering the same reinforcing layer), they are unable to produce the higher flexural strength than those reinforced with the C-34x34 textiles.
- In contrast to flexural strength, the C-21x21 composites reinforced with three layers achieved the highest flexural toughness while C-10x15 those reinforced with three layers achieved the lowest one. The reason for this was concluded that the higher elongation of the C-21x21 textiles makes the CRG specimens obvious achieve greater ductility, which offsets their low flexural strength; as a result, C-21x21 composites have the greater flexural toughness.

- The results obtained in this experiment suggest that the C-10x15 composites are suitable for high-strength and low ductility applications while the composites reinforced with the remaining two types of carbon textile are useful for high-ductility applications.
- Using the geomortar with higher mechanical strength can significantly improve the mechanical strength of the CRG specimens.
- The fact that when the cover layer thickness guarantees the anchoring capability of the textile in the matrix, the specimens with thinner cover layer will delay the development of the crack width as long as possible, due to the tension efficiency of the textile leading to both geopolymer mortar and textile undergoing collectively better bearing capacity under loading.

7. EFFECT OF CHOPPED BASALT FIBER ON FLEXURAL PERFORMANCE OF TEXTILE REINFORCED GEOPOLYMER

Short fibers added to the cement matrix can help to bridge the micro-cracks and inhibit their growth during the crack formation stage. In the field of the TRC, short fibers randomly dispersed in the matrix can help to increase the stiffness and the load-bearing capacity of the TRC composite compared to the bare TRC because of the effective increase in the reinforcement ratio [89]. The various properties of the TRC are also improved by adding short fibers [90–92]. The composites obtained by using two or more different kinds of fibers in a single matrix are termed as hybrid composites. Hybrid composites have a better all-round combination of properties than composites containing only a single fiber type [93].

This part presents the results of an experimental investigation of mechanical properties of textile reinforced geopolymer mortar containing both low and high dose level of the BF ranging from 0.25% to 7.5%. The C-10x15 textile composite specimen with one layer was chosen. Three kinds of the BF with three different lengths of 6 mm, 12 mm, and 24 mm were used as additional reinforcement. The BF dosage added to the matrix for both doses was clearly described in part 3. The effect of varied dosages and different fiber lengths of the BF on the flexural behavior of textile reinforced geomortar was investigated.

7.1 Influence of high dose of chopped basalt fibers on flexural performance

Two geomortars (GM-0.2S and GM-0.2S0.1F) with different mechanical strengths were used to investigate the influence of the high dose level of the BF dosages on the flexural behavior of the textile geopolymer composites. In comparison to GM-0.2S mix, GM-0.2-0.1F showed an approximately 11.66 % higher flexural strength and 16.69 % higher compressive strength. This means that one has weak mechanical strength other has higher mechanical strength. For each geomortar type, three different dosages with an increment of 2.5, from 2.5 % to 7.5 %, were considered as additional reinforcement in the production of the C-10x15 textile geopolymer composite reinforced with one layer. The BF with a fiber length of 6 mm (6 mm BF) will be chosen to add to geomortar due to its convenience in the mixing process. It should be noted that due to the high amount of the BF added into the mortar, the length of the BF was chopped into smaller dimensions during the mixing. Thus,

the original length of the BF does not affect the mechanical strength of the composite, but the fiber dosage does. The main reason for using two mortar types with different strengths is to better accurately assess the role of the BF in the bending behavior of textile geopolymer composites.

Typical load-displacement curves of textile geocomposites used GM-0.2S and GM-0.2S0.1F mortar are displayed in Figure 7.1. In general, both types of geomortars appear to make composites behave roughly similar in load-displacement response. The textile geocomposites without the addition of the BF can hardly carry the load after the initial failure occurred despite the geomortar type. In contrast, the composites with the BF addition exhibited an extended period of plastic deformation (i.e. pseudoplastic behavior) unlike a short drop at the point of maximum load. These composites are typically characterized by a relatively gradual decrease in load after reaching the maximum load-bearing capacity. This behavior of textile geocomposites can be resulted from the fiber-bridging and sliding after debonding and pulling-out of the BF from the geomortar matrix [94]. Even composites used GM-0.2S0.1F mortar can still maintain load capacity with increasing displacement after being reduced to roughly 0.6 times of their maximum load-bearing capacity (see in Figure 7.1b). Furthermore, there are still two clear differences between the two geomortar types that can be observed for stage 2 of the loading curve and composite stiffness. Due to its higher mechanical strength, GM-0.2S0.1F geomortar helps composites have less oscillation of the curve in stage 2 and higher stiffness during both stages 2 and 3. On the other hand, it can be concluded that the geomortar matrix with the BF addition significantly improved the flexural behavior of the CRG composites. The positive effects of increasing BF dosage on the load-displacement responses of the composites can be clearly seen through a higher first-crack load, higher maximum load-bearing capacity, less fluctuation in stage 2, and higher stiffness, compared to those without the BF addition. The improvement in the mechanical properties of the textile-reinforced composite resulting from the BF addition could be explained as follows: i) the randomly distributed fibers in the matrix will help to reduce the overall shrinkage strains, thus decreasing the internal flaws in the matrix. On the other hand, if they do occur, the fibers could reduce their development which induces the formation of micro-cracks [95]; ii) due to the bridge effect of the chopped fiber at the micro-cracks, the geomortar matrix has higher mechanical properties since the shift from micro-cracks to macro-cracks demands higher stress. Moreover, the connection between the fiber yarns of the textile and the

geopolymer mortar is also promoted due to this bridging effect. In this case, it could be said that the chopped fiber contributes to enhancing the efficiency of the textile in the reinforcement as well.

The average mechanical properties of the CRG specimens containing various dosages of chopped basalt fiber are compared in Table 7.1, whereas Figure 7.2 – Figure 7.3 gives a clear view of the flexural strength and bending toughness corresponding to various BF content. It can be seen that a clear trend of increasing strength from samples with increasing BF dosage. The CRG composites with the BF addition confirm the high-quality advancement in the aspect of the bending strength and flexural toughness. However, there is also a high variability of the measured values for this composite. This variability does not follow a clear rule. For example, considering the CRG specimen containing 7.5 % BF, while the GM-0.2S mix makes the CRG specimens obtained the average bending strength with low standard deviation, the CRG specimens using the GM-0.2S0.1F mix achieved the average bending strength with higher standard deviation. This can be attributed to two reasons: i) the sampling error occurred during sample fabrication (but all the samples were fabricated according to the same technique); ii) initial damage of fiber yarns occurred during the production of the textile meshes.

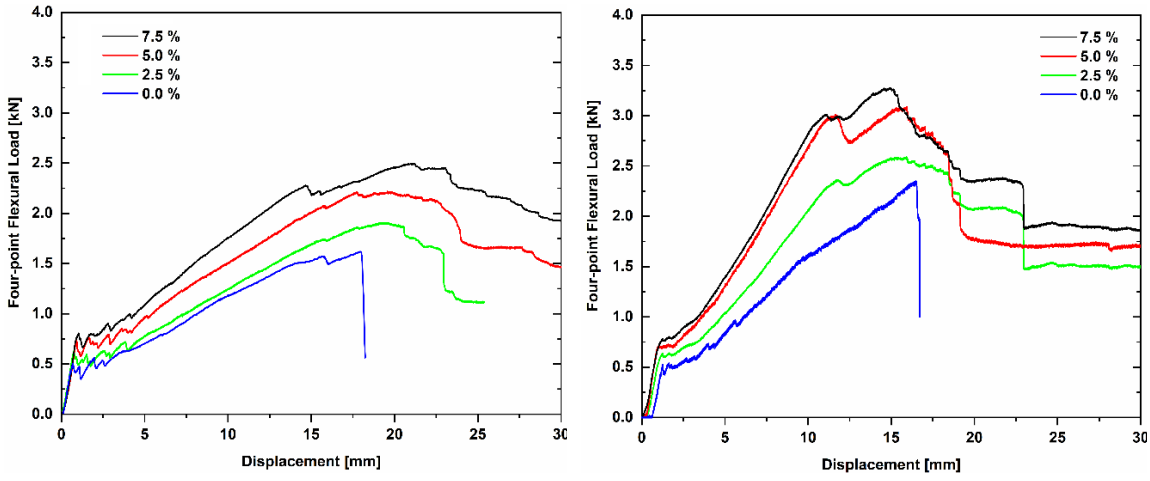

Figure 7.1 Typical flexural load-displacement curves of the C-10x15 textile composite containing varied fiber dosages of 6 mm BF: (a) GM-0.2S mix; (b) GM-0.2S0.1F mix.

Table 7.1 The result of the flexural behavior of the CRG specimens corresponding to various dosages (0.0 %, 2.5 %, 5.0 %, 7.5 %) of chopped basalt fiber.

Sample	Value	F_1 [kN]	F_2 [kN]	R_{mo1} [MPa]	R_{mo2} [MPa]	y [mm]	Toughness [kN.mm]	Cr. [-]	Rr. [%]
GM-0.2S	**0.0 %**	0.42 ± 0.07	1.62 ± 0.52	5.61 ± 1.16	21.59 ±2.12	18.94 ±2.42	21.03 ±1.56	7.33	0.96
	2.5 %	0.68 ± 0.11	2.05 ± 0.40	9.02 ± 1.60	26.72 ±4.07	18.01 ±2.93	23.74 ±2.99	11.33	0.96
	5.0 %	0.72 ± 0.06	2.25 ± 0.31	9.63 ± 0.80	29.99 ±4.11	20.03 ±2.61	27.93 ±5.90	13.67	0.96
	7.5 %	0.80 ± 0.11	2.57 ± 0.14	10.67 ±1.40	34.24 ±1.88	21.85 ±1.83	34.39 ±4.51	14.33	0.96
GM-0.2S0.1F	**0.0 %**	0.53 ± 0.09	2.26 ± 0.71	7.04 ± 1.15	30.14 ±1.29	16.59 ±2.65	24.43 ±2.57	8.66	0.96
	2.5 %	0.71 ± 0.07	2.57 ± 0.34	9.48 ± 0.9	34.26 ±2.79	17.79 ±1.41	28.15 ±2.15	11.33	0.96
	5.0 %	0.79 ± 0.05	3.03 ± 0.34	10.55 ± 0.9	40.36 ±2.38	15.89 ±2.88	31.12 ±3.82	14.67	0.96
	7.5 %	0.83 ± 0.07	3.21 ± 0.16	11.16 ± 1.4	42.79 ±4.13	16.59 ±1.99	35.87 ±4.72	14.67	0.96

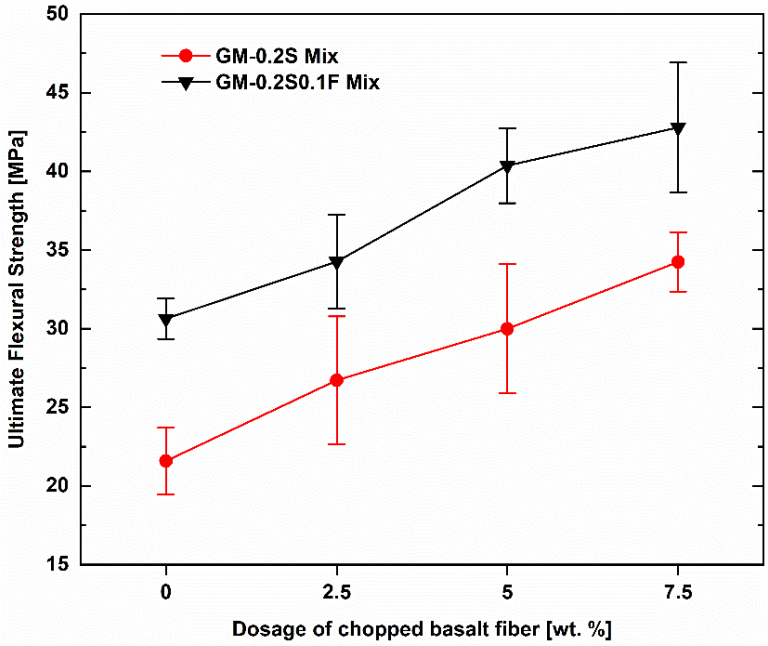

Figure 7.2 The average value of the ultimate flexural strength of the CRG composites with regarding varied dosage of the BF at the high dose level.

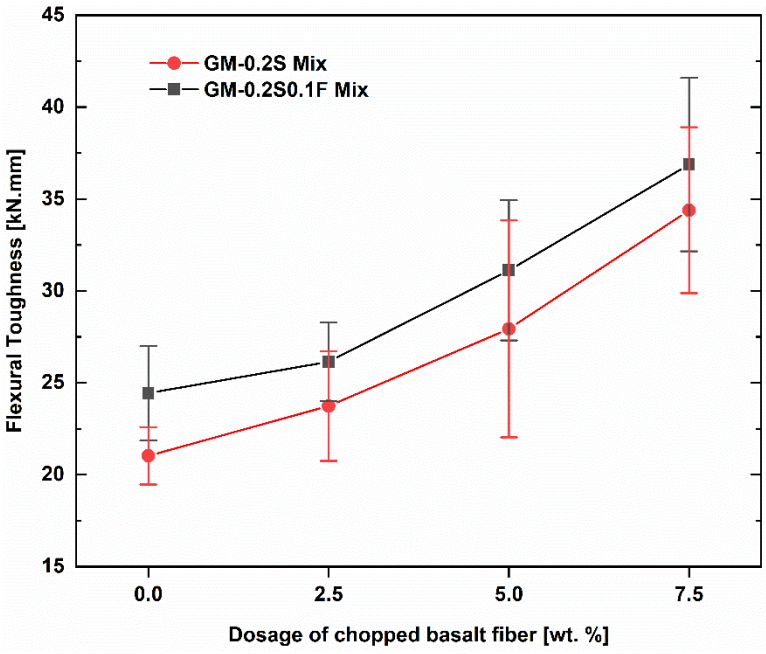

Figure 7.3 The average value of the flexural toughness of the CRG composites with regarding the varied dosage of the BF at the high dose level.

In addition to improving the mechanical properties, the BF addition at high dose level also impacts strongly on the failure mode of the CRG specimens as seen in Figure 7.11. There are two different types of failure modes which demonstrated for the general failure modes of all the CRG specimens. For the CRG specimens without BF addition, the poor bonding performance between the textile layer and geomortar matrix leads to the gradual peeling process of the fiber yarns occurs out from the matrix, followed by collapsing of the matrix due to reaching maximum load-bearing capacity. It was found that although the using GM-0.2S0.1F mix had significantly higher geomortar strength than GM-0.2S mix, both types of geomortar still induce the CRG specimens without the BF addition to have the same failure mode as debonding phase within the matrix occurred. Textile reinforced specimens with BF addition, on the contrary, result in the pure flexural failure without the debonding phase due to the slipping of fiber yarn within the matrix. It can be said that the use of chopped basalt fibers in the production of the geopolymer mortar has markedly improved the rigidity of the matrix structure and has also promoted the cohesion of the fiber yarns of the carbon textile in the matrix. This result confirms that the BF adding into geomortar matrix impacts positively on the failure mode of the CRG specimens, and the use one-layer of textile reinforcement is strong insufficient to peel off the geomortar matrix.

without addition of chopped basalt fiber

7.5% addition of chopped basalt fiber

(a) Mortar type: GM-0.2S

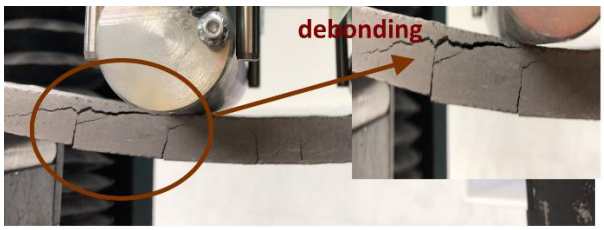

without addition of chopped basalt fiber

7.5% addition of chopped basalt fiber

(b) Mortar type: GM-0.2S0.1F

Figure 7.4 Typical failure modes of textile geopolymer composite.

7.2 Influence of low dose of chopped basalt fibers on flexural performance

At low dose level three kinds of the BF corresponding to three fiber lengths (6 mm BF, 12 mm BF, 24 mm BF) are used to add to geomortar. Also, three different dosages with an increment of 0.25, from 0.25 % up to 0.75 %, were applied for each BF type; except for the 6 mm BF up to 1.0 %. The difference from the high dose level described in the previous section is that the effect of low dose level on the flexural behavior of textile gepcomposites is studied based on varying fiber lengths. The geomortar with GM-0.2S0.1F mix was used as a matrix in the production of C-10x15 textile composites reinforced with one layer.

Figure 7.5 - Figure 7.7 show typical load-displacement curves obtained from four-point bending tests of the CRG specimens with the varied dosage of the BF addition. It is apparent from the diagrams that the BF addition at the low dose level also was efficient in increasing the load-bearing capacity of the CRG specimens compared to those without BF additions. Although there is some variation in the behavior of the individual curves, the general load-displacement response is roughly similar for all the composites. After reaching the

maximum load, almost the specimens are virtually impossible to continue to carry the load anymore. A significant flattening of the load-displacement curves around the point of maximum load associated with inelastic deformation is displayed for all the specimens except to specimens without the BF addition. In some cases, the bending test was ended immediately after reaching the maximum load. In other cases the bending load decreased slowly in a short duration with the displacement.

Table 7.2 and Figure 7.8 - Figure 7.11 provide the information about the result of the flexural tests of all the CRG specimens. The first-crack bending strength of all the CRG specimens with the BF adding was higher compared to those without BF adding (see in Figure 7.8). The CRG composites without the BF adding have the average ultimate flexural strength of 30.14 MPa. The highest value of ultimate bending strength was 41.33 MPa for the CRG composite with 1.0% adding of the 6 mm BF. The next good values of bending strength were 39.07 MPa, 38.51 MPa for the CRG composites with 0.75% adding of the 24 mm BF, the 12 mm BF, respectively, considering higher variability of measured values of the strength. It can be seen that for all three different fiber lengths of the BF, the specimens obtained the highest bending strength with the most BF content. However, keeping in mind that due to the fact that the high BF content makes it difficult to mix the fresh geomortar and resulted in the marked occurrence of clusters of fibers. This reason answers why the author does not want to continue increasing BF content. In other words, the effect of the BF at the low dose level on the bending toughness of the specimens is unclear. From experimental results it can be seen that the specimens with higher flexural strength do not always indicate higher bending toughness than those with lower flexural strength and vice versa. The reason for this is that the toughness value of the specimens depends on both their load capacity and their displacement. For some CRG specimens with an increase in flexural strength, on the other hand, there is a significant reduction in displacement leading to the lower toughness value, compared to those without the BF addition (see in Table 7.2 and Figure 7.10).

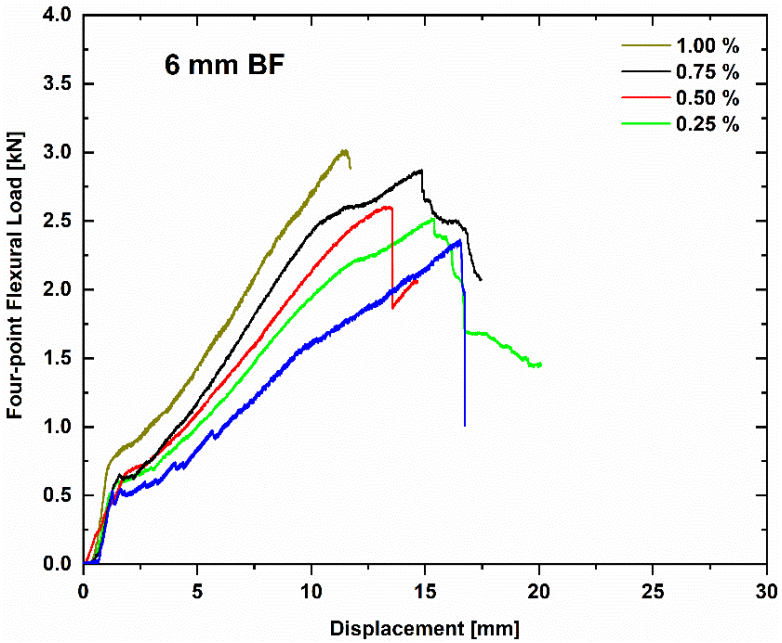

Figure 7.5 Representative load-displacement curves of the CRG composites containing varied fiber dosages of the 6 mm BF.

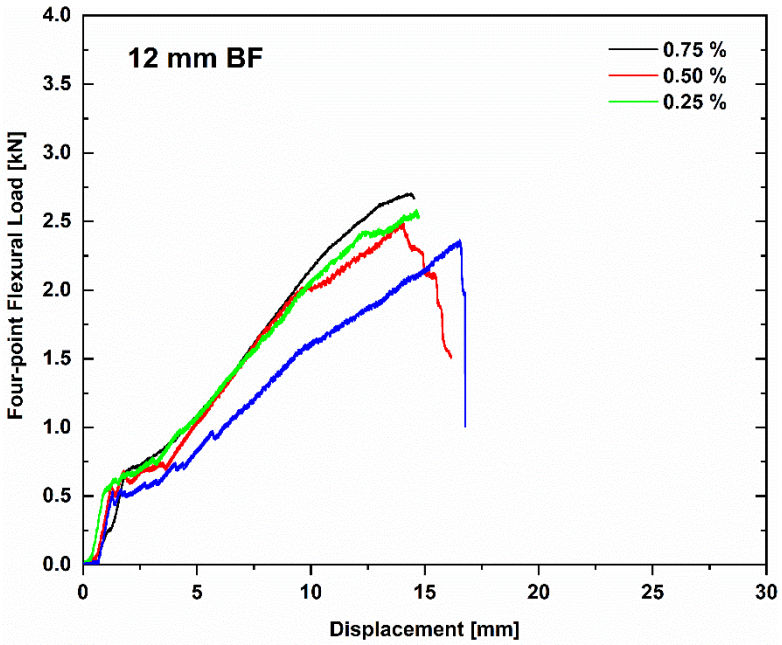

Figure 7.6 Representative load-displacement curves of the CRG composites containing varied fiber dosages of the 12 mm BF.

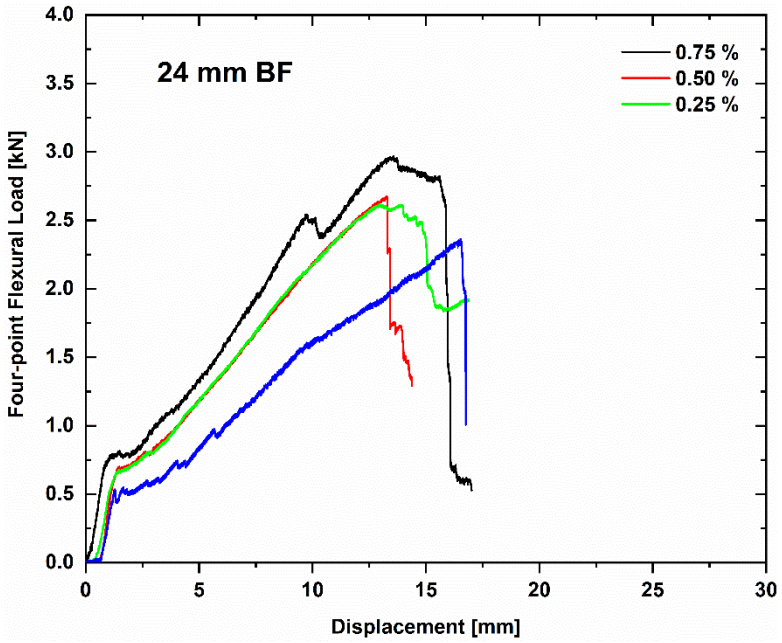

Figure 7.7 Representative load-displacement curves of the CRG composites containing varied fiber dosage of the 24 mm BF.

Table 7.2 The result of flexural tests of the CRG specimens containing three different types of chopped basalt fibers (6 mm BF, 12 mm BF, and 24 mm BF).

Sample	Value	F_1 [kN]	F_2 [kN]	R_{mo1} [MPa]	R_{mo2} [MPa]	y [mm]	Toughness [kN.mm]	Cr. [-]
	0.00 %	0.53 ± 0.09	2.26 ± 0.71	7.04 ± 1.15	30.14± 1.29	16.59± 2.65	23.43± 2.57	8.66
6 mm BF	**0.25 %**	0.61 ± 0.04	2.69 ± 0.44	8.13± 0.50	34.74± 1.72	14.47± 1.27	23.71± 1.49	11.33
	0.50 %	0.56 ± 0.04	2.75 ± 0.28	7.44± 0.49	36.65± 3.77	13.73± 1.19	21.37± 1.78	12.33
	0.75 %	0.63± 0.02	2.93± 0.18	8.34± 0.24	39.01± 2.36	15.03± 1.08	27.36± 3.37	11.67
	1.00 %	0.63 ± 0.04	3.10 ± 0.11	8.41±0.52	41.33± 1.41	12.83± 2.30	23.13± 5.30	13.33
12 mm BF	**0.25 %**	0.57 ± 0.06	2.69 ± 0.18	7.63 ±0.85	35.94± 2.45	15.65± 2.51	23.98± 3.86	12.00
	0.50 %	0.58 ± 0.09	2.57 ± 0.12	7.69 ± 1.33	34.87± 1.65	14.68± 1.61	22.63± 2.49	12.00
	0.75 %	0.64 ± 0.04	2.81 ± 0.24	8.60 ±0.50	38.51± 3.24	14.72± 1.34	24.97± 4.76	12.67
24 mm BF	**0.25 %**	0.64 ± 0.02	2.77 ± 0.22	8.54 ± 0.25	37.04± 2.93	15.28± 1.91	26.21± 5.40	13.33
	0.50 %	0.65 ± 0.02	2.74 ± 0.29	8.77 ±0.25	36.47± 3.88	13.65± 1.18	22.02± 4.13	11.67
	0.75 %	0.66 ± 0.04	2.93 ± 0.27	8.79 ± 0.55	39.07± 3.57	13.41± 1.43	22.77± 4.35	13.67

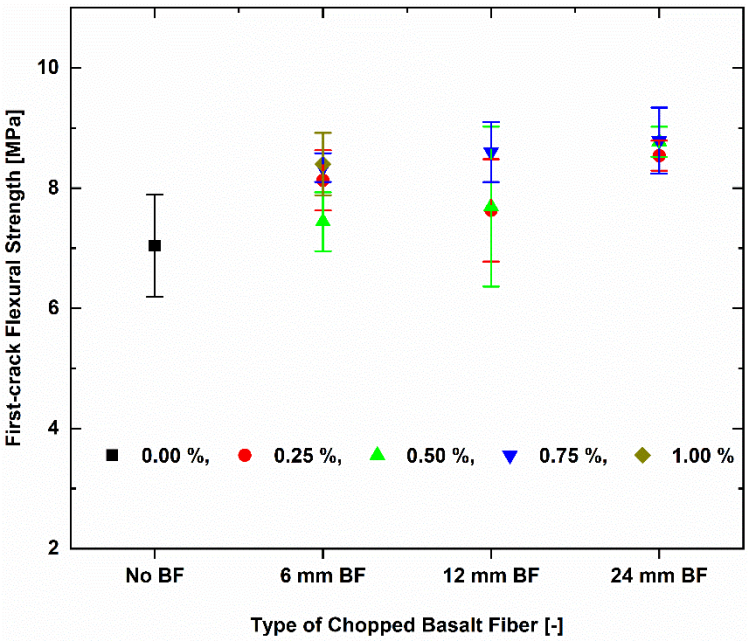

Figure 7.8 The average value of the first-crack flexural strength of the CRG composites with reinforcing one layer regarding fiber lengths and varied dosage of the BF.

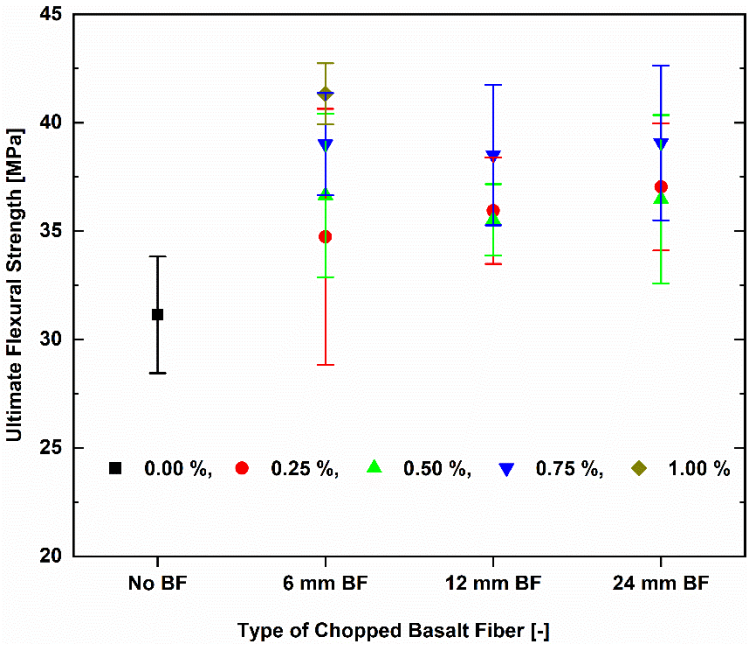

Figure 7.9 The average value of the ultimate flexural strength of the CRG composites with reinforcing one layer regarding fiber lengths and varied dosage of the BF.

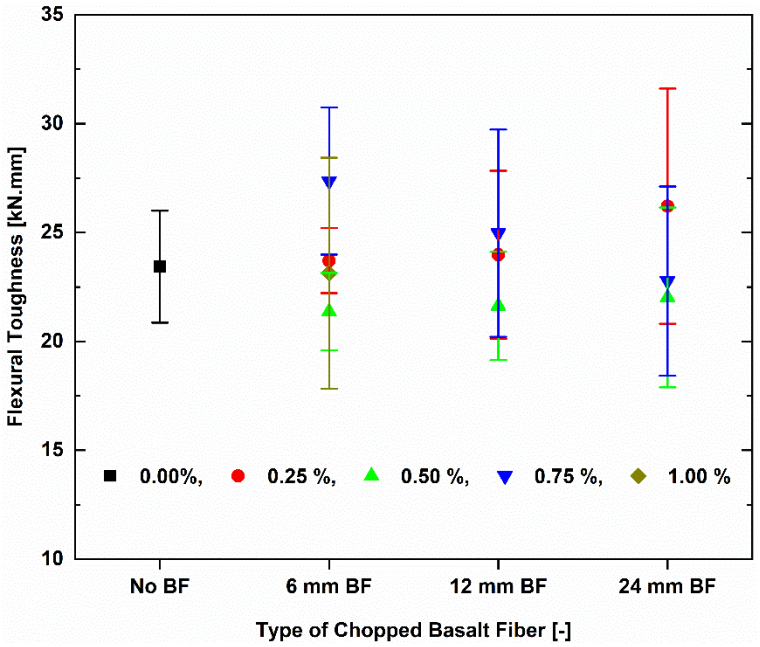

Figure 7.10 The average value of the flexural toughness of the CRG composites with reinforcing one layer regarding fiber lengths and varied dosage of the BF.

Photographs of typical failure observations for these composite specimens are shown in Figure 7.11. Unlike pure flexural failure mode of textile geocomposites with the BF adding at high dose level due slipping of fiber yarns within the matrix, the results from Figure 7.11 showed clearly that the composites with the BF addition at low dose level failed in a catastrophic manner which demonstrated by the process of debonding or debonding and collapse after reaching the maximum bearing-load capacity. In some cases the specimens failed due to the occurrence of debonding along with the matrix-textile interface. In other cases when specimens failed, the geomortar pieces were broken down, and debonding along the matrix-textile interface did not occur. Finally, these specimens broke down due to the collapse of the matrix. The failure modes indicated that although using the BF at the low dose level could enhance the flexural strength of the textile composite, there is no improvement in failure modes compared to those without the BF addition.

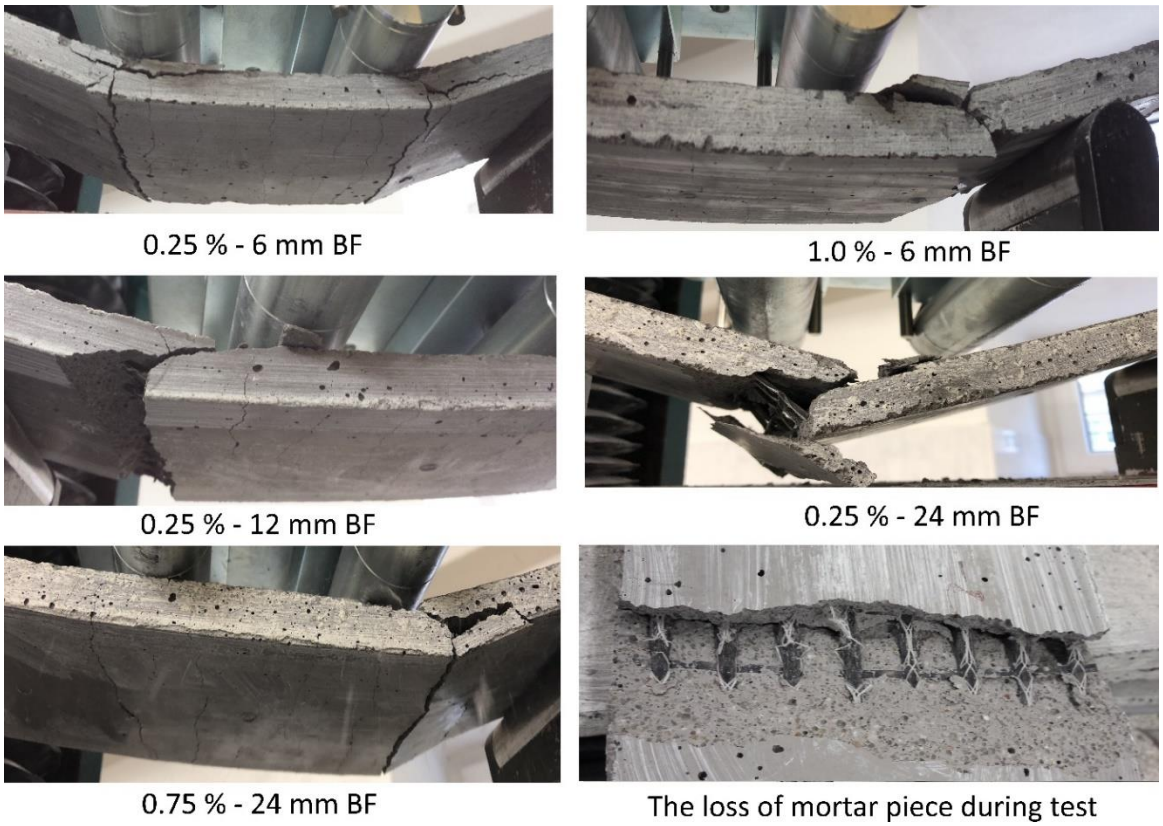

Figure 7.11 Typical failure modes of the CRG composites with reinforcing one layer regarding different fiber lengths and various dosages of the chopped basalt fiber.

7.3 Summary

- The introduction of chopped basalt fiber to geomortar improved significantly the flexural properties of textile geopolymer composites.
- The fact that although using chopped basalt fiber at the low dose level can help to enhance undoubtedly the flexural strength when compared to one without the BF adding, there is no impact on the failure mode of these composites. The typical failure mode of these composites, similar to the specimens without the BF adding, is debonding and collapse after reaching the maximum load capacity.
- Using chopped basalt fiber at the high dose level has a markedly positive effect on the flexural properties and failure mode of textile geopolymer composites. In addition to the significantly improved bending strength, the specimens showed the pure flexural failure without the debonding phase due to the slipping of fiber yarn within the matrix.

8. IMPACT-BENDING PERFORMANCE OF TEXTILE REINFORCED GEOPOLYMER MORTAR

8.1 Introduction

As already mentioned in the previous part geopolymer concretes were have emerged as an alternative to Portland cement-based concretes. In addition to static loads, many concrete structures such as wall panels, hydraulic structures, airport pavements, military structures, and industrial floor overlays may be subjected to dynamic loads in a short duration. These loads originate from sources such as vehicular and ship collisions with structure, rock falls, missile impacts, explosions, machine dynamics, wind gusts, and earthquakes. Concrete subjected to high impact loads will experience significant damage in structural stability and integrity.

The Charpy test was originally established for metals and then was applied to unreinforced polymer and cement-based composites. In terms of the Charpy test the specimen is exhibited to a three-point bending impact loading produced by a swinging pendulum. The amount of energy absorbed by the specimen was defined as the change in potential energy related to the difference in the height of the swinging pendulum before it was released and the maximum height it reached as it passed through the specimen after impact. Sufficient energy was delivered to the specimen to ensure that it was completely fractured during the impact process. The reported Charpy impact strength is determined as this energy divided by the mid-section area [96]. Impact strength is an essential dynamic property of engineering material that gives an indication of its resistance against a suddenly applied load and is expressed in terms of energy. Often measured with the Charpy impact test, which measures the impact energy required to fracture a sample. The impact strength of fiber reinforced polymer is governed by the matrix–fiber interfacial bonding, and properties of matrix and fibers. When the composites experience a suddenly applied load, the impact energy is dispersed by the combination of fiber pull-outs, fiber fracture, and matrix deformation [97]. Charpy impact test was performed on a wide variety of cementitious composites including mortar/concrete without or with fiber reinforcements. The specimen sizes ranged from 10 by 10 by 50 – 55 mm [98–100] to 100 by 100 by 500 mm [101]. In some cases the specimens have a loading span of 40 mm, in other cases they have larger

loading spans [101–103]. Despite a number of studies on the collision resistance of cementitious composites by Charpy impact test, there is no specific standard for such tests.

Fiber addition to concrete improves its ductility, tensile, impact, and flexural strength. The purpose of this part is to present the experimental results of an impact Charpy test on the composite samples of the textile reinforced geomortar. The variables investigated are different dosage and fiber length of chopped basalt fibers and the number of textile layers. The 6 samples with an approximate dimension of 15 x 50 x 120 mm^3 for each recipe were prepared for measurement of the results for the Charpy impact test.

8.2 Influence of dosage and fiber length of the BF on impact strength

Table 8.1 The results of Charpy impact test of the CRG specimens containing three different types of the BF.

No. sample / Value			CRG specimens with varied additions of the BF		
			BF [wt.%]	K [J]	KC [kJ/m²]
C-10x15 textile composite reinforced with one layer		No BF	0.00	46.07 ± 7.27	60.86 ± 09.27
	Low doe	6 mm BF	0.25	51.79 ± 9.10	67.92 ± 12.32
			0.50	54.67 ± 10.33	72.12 ± 14.04
			0.75	56.63 ± 8.94	73.81 ± 12.54
			1.00	56.13 ± 6.22	74.23 ± 08.16
		12 mm BF	0.25	59.49 ± 7.04	78.90 ± 08.63
			0.50	56.17 ± 9.80	73.11 ± 12.66
			0.75	58.92 ± 4.07	77.32 ± 08.46
		24 mm BF	0.25	58.96 ± 6.90	76.90 ± 11.10
			0.50	56.50 ± 10.07	74.59 ± 14.07
			0.75	59.13 ± 7.64	78.26 ± 8.53
	High dose	6 mm BF	2.50	58.38 ± 5.98	76.41 ± 06.71
			5.00	61.46 ± 6.42	80.55 ± 08.74
			7.50	61.17 ± 8.32	79.26 ± 09.10

The experimental results of Charpy impact tests for CRG specimens with the addition of various dosages and fiber lengths of the BF were reported in Table 8.1 and Figure 8.1 – Figure 8.2. The composites without BF addition show the lowest average impact strength with value of 60.86 kJ/m^2. After adding varied dosages of the BF to geopolymer composite, the average impact strength ranges from 67.92 kJ/m^2 to 80.55 kJ/m^2 which is increased by

11.66 % to 32.35 %, depending on the added BF dosage. This finding confirmed that the BF also improves the significantly mechanical strength of textile geomortar composites under dynamic load. However, an observation in the value of standard deviation also indicated confusing variability. As shown in Table 8.1 at the low dose level, the geocomposites with an addition at a dosage of 0.25 % and 0.75 % for all three BF kinds showed a smaller standard deviation compared to those at 0.5 %. The resulting strength of the samples for each fiber type at each dosage was generally unpredictable. For example, while the geocomposites with the 12 mm BF addition at 0.25% showed the highest impact strength compared to those at other two percentages, the highest impact strength for geocomposites with the 24 mm BF addition achieved at a dosage of 0.75%. This result can be attributed to the fabrication process. Since all the specimens were fabricated according to the same technique and from the same materials, this behavior can be attributed to the presence of several clusters of fibers in the mixture during mixing resulting in a non-homogenous structure of hardened geomortar. In other words, from the results in Table 8.1 and Figure 8.1 it can be observed that the geocomposites with 6 mm BF show lower impact strength value compared to those with the other two BFs. This result is not consistent with results in the static loading test (four-point bending test) of these geocomposites, where the highest strength value achieved for geocomposites with 6 mm BF at 1 %. This finding shows that the failure mechanism of fiber geocomposites is different under static and impact loading.

The average impact strength of the composites with varied addition of the 6 mm BF is compared in Table 8.1 and Figure 8.2. With increasing the BF content, the composites showed an increased trend in strength. However, the BF addition at high dose level appears to have composites achieve more homogeneous strength within each recipe due to a smaller value of standard deviation, compared to a low dose level. This can be attributed to the BF amount added to geomortar. If the amount of the BF added still ensures good workability of fresh mortar and mechanical strength of hardened mortar, the more the BF added, the more homogeneous mortar is.

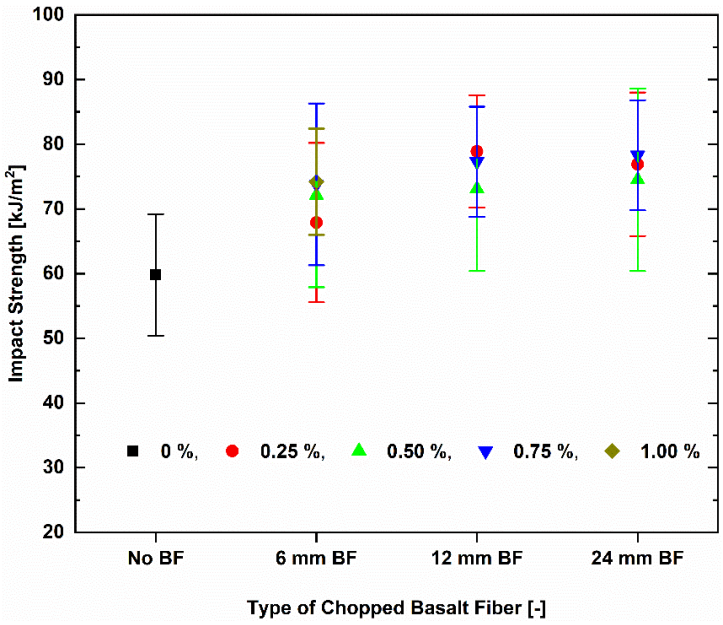

Figure 8.1 The result of the bending impact of carbon fiber mesh reinforced geomortar containing the various types of chopped basalt fibers.

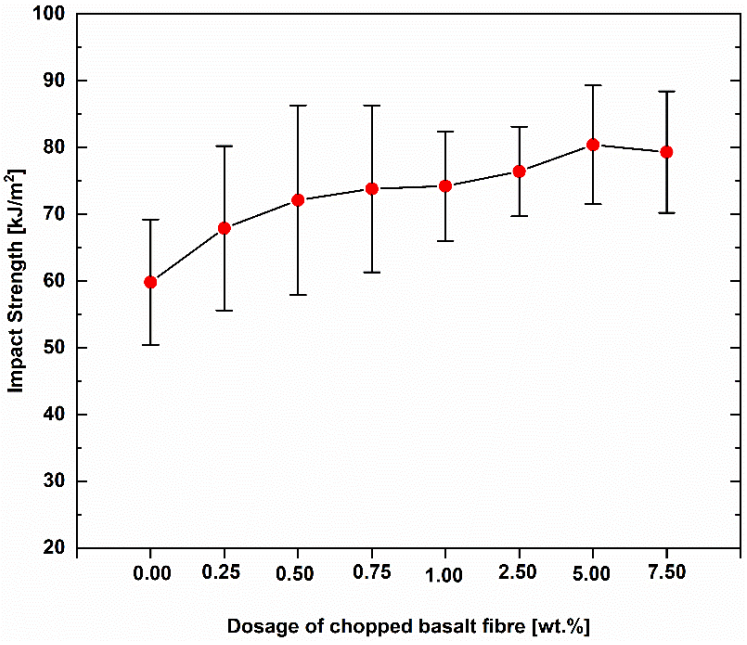

Figure 8.2 The result of the bending impact of carbon fiber mesh reinforced geomortar containing the various dosages of the 6 mm BF.

8.3 Influence of textile type and number of textile layers

The experimental results of impact Charpy tests for the composites reinforced with a number of textile layers of C-10x15 and B-10x14 textile were reported in Table 8.2 and Figure 8.3 – Figure 8.5. From Table 8.2 we can see that the non-reinforced sample without the BF addition achieved impact strength of 4.16 kJ/m^2, which showed ~1.47 times higher average strength compared to non-reinforced sample with 5 % BF addition (6.1 kJ/m^2). The BF also enhanced the energy absorption capacity of textile composite samples considering the same reinforcement ratio, when compared to those without the BF adding. For example, in the case of B-10x14 textile, the composites with 5 % BF reinforced with 1 – 4 layers increased in impact strength by 1.59 times, 1.41 times, 1.39 times, and 1.42 times, respectively, compared to those without BF adding. For C-10x15 textile, the composites with 5 % BF reinforced with 1 – 3 layers increased by 1.32 times, 1.30 times and 1.24 times, respectively, compared to those without BF adding. It is also observed that the higher average strength is accompanied by a higher standard deviation of measured strength. This problem of standard deviation has the same situation with the textile geocomposites under the four-point bending test. The experimental results showed that a clear improvement for textile reinforced specimens was observed with increasing reinforcement ratio. On the other hand, the much higher impact strength of the C-10x15 composite is attributed to the higher mechanical strength of carbon fiber in comparison to basalt fiber. For example, the highest average strength of 107.55 kJ/m^2 was recorded for C-10x15 textile composites with 2 reinforcing layers, and this value is ~ 2.68 times higher compared to B-10x14 textile composite with 4 reinforcing layers which achieved the highest strength of 40.10 kJ/m^2. It is worth seeing an interesting point when looking at Figure 8.3 and Figure 8.4. The B-10x14 textile composites show an increasing trend when the reinforcement ratio increased from 1 layer to 4 layers. In contrast, the C-10x15 textile composite reinforced with 3 layers do not show a higher average strength value than those reinforced with 2 layers even smaller. However, under static loading test (four-point bending test) the C-10x15 textile composites with 3 reinforcing layers showed much higher flexural strength than those with 2 reinforcing layers. This phenomenon can be attributed to the anchoring capacity of textile reinforcement in geomortar under dynamic loading test. Since the distance between two adjacent textile layers was 2 mm of the geomortar as described in part 3, the cover thickness of this geomortar may not be strong enough to anchor the fiber yarns of textile under impact loads.

Table 8.2 The results of Charpy impact test of the textile reinforced geomortar corresponding to the varied number of textile layers at the age of 28 days.

Value / Sample	No. layer	Geomortar without BF addition		Geomortar with 5% BF addition	
		K [J]	KC [kJ/m^2]	K [J]	KC [kJ/m^2]
Non-reinforced sample	0L	3.14 ± 1.04	04.16 ± 1.35	4.63 ± 1.34	06.10 ± 1.64
B-10x14 composite	1L	19.13 ± 1.97	15.82 ± 1.92	19.13 ± 1.97	25.18 ± 2.81
	2L	23.82 ± 2.63	19.76 ± 4.18	23.82 ± 2.63	27.88 ± 3.18
	3L	26.42 ± 4.06	24.79 ± 5.21	26.42 ± 4.06	34.34 ± 5.71
	4L	31.50 ± 4.83	28.24 ± 6.21	31.50 ± 4.83	40.10 ± 6.11
C-10x15 composite	1L	46.07 ± 7.27	60.86 ± 07.27	61.46 ± 6.42	80.55 ± 8.74
	2L	62.42 ± 13.23	82.67 ± 13.84	82.63 ±13.23	107.55 ± 16.61
	3L	60.59 ± 14.93	81.85 ± 16.58	77.96 ±14.93	101.88 ± 18.69

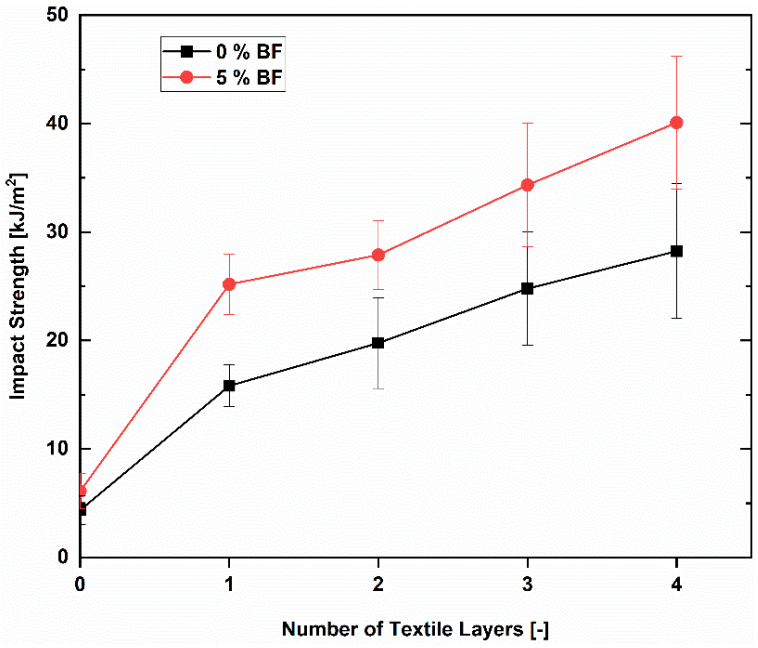

Figure 8.3 The result of the bending impact of fiber mesh reinforced geomortar corresponding to the various number of textile layers.

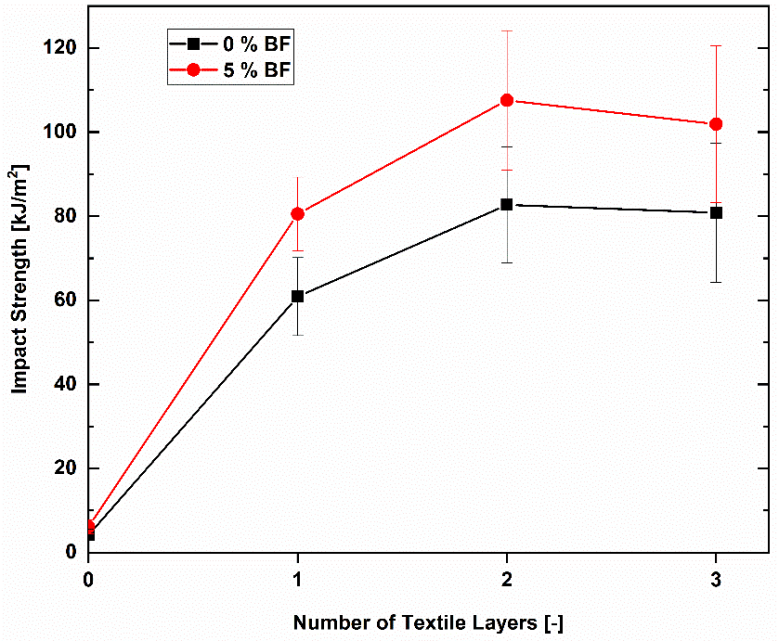

Figure 8.4 The result of the bending impact of fiber mesh reinforced geomortar corresponding to the various number of textile layers.

Table 8.3 summarizes the results of the Charpy impact tests of textile geocomposites at the time period of 365 days, whereas Figure 8.5 provides a comparison of impact strength between 28-day samples and 365-day samples. The B-10x14 textile composites with 4 reinforcing layers and C-10x15 textile composites with 2 reinforcing layers were selected and geomortar without and with 5 % BF were applied to each type of respective textile geocomposite. The results confirmed that the basalt reinforcements adversely affect the impact strength of composites. However, the decrease of composite strength after a year is considered to be negligible.

Table 8.3 The results of the textile geopolymer composite at the age of 365 days.

Sample	BF [wt. %]	K [J]	KC [kJ/m^2]
B-10x14 composite – 4 Layers	**0 %**	16.44 ± 4.21	21.84 ± 5.41
C-10x15 composite – 2 Layers		62.42 ± 8.58	82.67 ± 13.84
B-10x14 composite – 4 Layers	**5 %**	28.26 ± 4.83	34.29 ± 6.71
C-10x15 composite – 2 Layers		73.58 ± 9.26	99.18 ± 13.12

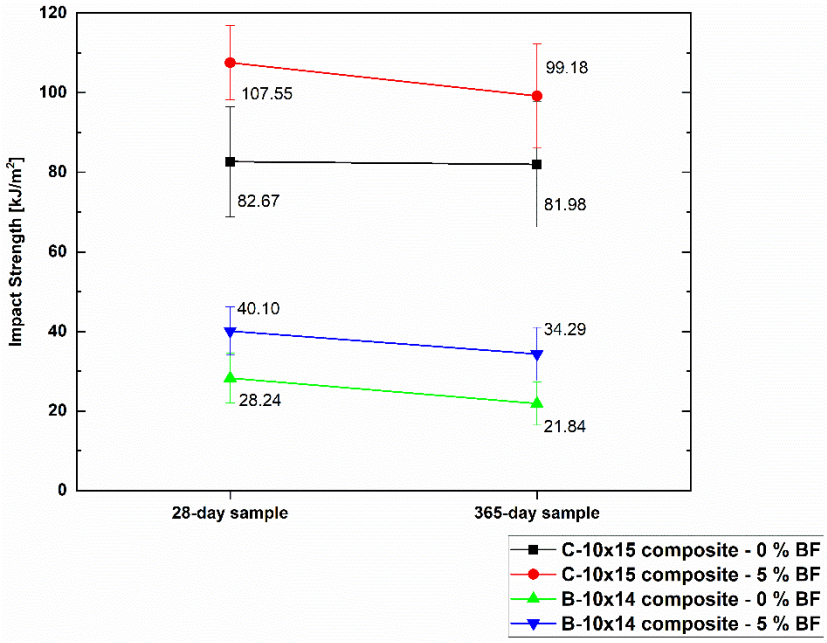

Figure 8.5 Comparison of the impact strength of textile reinforced geomortar between 28-day samples and 365-day samples: (a) BRG specimens; (b) CRG specimens.

8.4 Failure modes of tested specimens

A photo of the typical failure modes of the composite specimens after finishing the Charpy impact test is shown in Figure 8.6. Some important remarks concerning the failure modes should be noted. It could be observed that the specimen without the reinforcing layer was easily broken after the Charpy impact test. For the B-10x14 textile composites, the obvious rupture of fiber yarns of basalt textiles for all the composites is inspected. The specimens were almost broken at the point of central load by the impact of the head of the hammer. In some cases, other cracks at other positions were also displayed from the impact of the hammer. From the failure mode of basalt textile composites, it can be concluded that the anchoring capacity of basalt textile with 2 mm thickness of mortar cover was suitable. This is consistent with the results of impact strength that composite with 4 reinforcing layers is clearly higher than those with 3 reinforcing layers.

For C-10x15 textile composites, the dominating failure mode for these composites was the slip of fiber yarns within the geomortar matrix along with partial damage of multifilament at the outer layer, no bundles were broken. Also, from Figure 8.6 it is observed that the composites with one reinforcing layer have shown a different failure manner compared to

those with 2 – 3 layers. The 1-layer composites were separated into two main parts with a distance themselves of ~ 10 – 15 mm causing by slipping of fiber bundles. In some cases, the specimens fail disastrous other cases specimens fail smooth. On the other hand, the composites with 2 – 3 layers lost their structural geometry and integrity upon reaching the impact energy capacity, which cannot return to its original shape after finishing the test. The specimens bend around the head of the hammer but do not separate due to the flexibility of fiber that was not broken. This evidence showed that one reinforcing layer can receive the collision energy and transmit well, while a higher reinforcement ratio in composites with three reinforcing layers makes the usefulness of textiles not fully utilized.

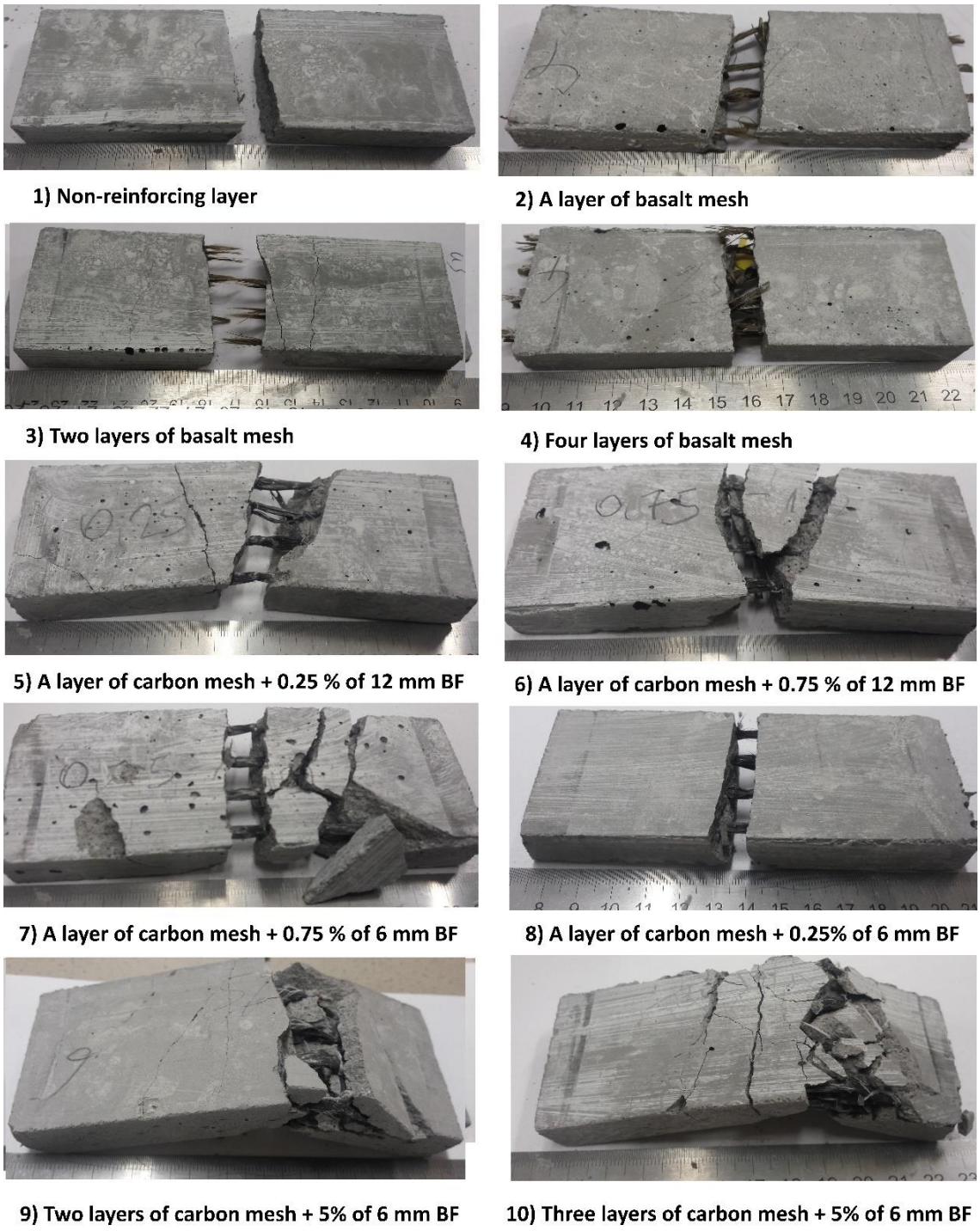

Figure 8.6 Typical failure modes of the textile reinforced geomortar after finishing Charpy impact test.

8.5 Summary

- The experimental results confirmed that the BF also improves the significantly mechanical strength of textile geomortar composites under dynamic load. It is also observed that the geocomposites with 6 mm BF show lower impact strength value compared to those with the other two BFs. This result is not consistent with results in the static loading test (four-point bending test) of these geocomposites, where the highest strength value achieved for geocomposites with 6 mm BFs at 1%. This finding shows that the failure mechanism of geocomposites with the addition of the BF is different under static and impact loading.
- With the increasing reinforcement ratio the B-10x14 textile composites showed a clear increasing trend of the impact strength, but this did not occur for the C-10x15 textile composites. The geocomposites with three layers of carbon textiles showed a lower impact strength value than one with two layers. This phenomenon can be attributed to the fact that the cover thickness of the geomortar may not be strong enough to anchor the fiber yarns of textile under impact loads.
- For the B-10x14 textile composites, the obvious rupture of fiber yarns of basalt textiles for all the composites is inspected. For C-10x15 textile composites, the dominating failure mode for these composites was the slip of fiber yarns within the geomortar matrix along with partial damage of multifilament at the outer layer, no bundles were broken.

9. CONCLUSION AND FUTURE WORK

9.1 Overall Conclusions

The aim of this thesis was the fabrication of composite thin plates made of geomortar matrix and textile reinforcements and the evaluation of their mechanical properties through a four-point bending test and Charpy impact test. The research works included optimization of the geomortar compositions with the highest mechanical strength, effect of textile types and reinforcement ratio on flexural properties of textile geopolymer composites, the effect of chopped basalt fiber on the flexural properties of textile geopolymer composites and also failure modes of relevant composites.

- From experimental results of the optimization of the geomortar it was found that the geomortar incorporating different filler materials with reasonable proportion can achieve relatively high mechanical strength. When adding both micro-particles and chopped fibers in geomortar, the best mixture makes samples to increase flexural strength approximately by 55.44 % and compressive strength by 61.32 % respectively, compared to plain geomortar. The fact that although the chopped basalt fiber addition at the low dose level to geomortar showed a clear increase in flexural strength, there is no clear effect on compressive strength. In contrast, the use of the BF at the high dose level makes geomortar achieve significant improvement in both flexural strength and compressive strength. The reported data on the strength development of the geomortar revealed that the geomortar without the BF additions almost remains unchanged strength over time up to 365 days. In contrast, the mechanical strength of the geomortar with the BF addition has been reduced due to the degradation of the BF in the alkali environment. However, a decrease of the sample strength lasts only up to 150 days, beyond this time the mechanical strength is almost unchanged.
- Under a four-point bending test, all the BRG specimens have the same failure mode by flexural failure due to rupture of fiber yarn in mortar matrix and no debonding of fiber yarn or a gradual peeling process of mortar matrix happed during testing. On the other hand, the specimens reinforced with more textile layers lead to a greater number of cracks resulting in higher specimen stiffness. With the increasing

number of textile layers, the mechanical properties of the BRG specimens were improved significantly, considering for the BRG specimens reinforced with basalt mesh having a small net size and middle net size. There is no impact on the mechanical strength of the BRG reinforced with basalt mesh of big net size, failure of these BRG specimens is due to localization of the first-crack. It can be concluded that using basalt textiles with the big net size is not effective in reinforcement. So, the author suggests that only basalt textile of small net size should be used to reinforce in specimens due to reinforcement effectiveness; or in case of using basalt mesh of big net size, fiber yarn should be resized to its size by way of fiber yarn that should be made of more individual filaments to improve its low tensile strength. In other words, the specimen production phase also plays an important role in the first-crack strength of these composites. The subjectivity in the specimen production can lead to the BRG specimens having many cavities at the interface between mortar matrix and fiber yarn which results in a decrease of the mechanical strength of the BRG specimens.

- Under a four-point bending test, the specimens reinforced with carbon textiles show a markedly positive effect on the mechanical properties of the resulting composites through a displacement-hardening behavior. With the increasing reinforcement ratio, the flexural strength of the CRG specimens was improved significantly especially with the CRG specimens reinforced with the C-10×15 textiles. The CRG specimens reinforced with the one-layer of the C-10×15 textile have an almost similar flexural strength achieved by those reinforced with the three layers of the C-21×21 textile and the C-34×34 textile. Using a high reinforcement ratio makes the C-10×15 composites achieve high flexural strength, but they were catastrophically destroyed when compared to the remaining CRG specimens. The debonding and collapse phase took place simultaneously. Although the C-21×21 composites have a higher reinforcement ratio (considering the same reinforcing layer), they are unable to produce a higher flexural strength than those reinforced with the C-34×34 textiles. In contrast to the flexural strength, the C-21×21 composites reinforced with the three layers (a reinforcement ratio of 1.45 %) achieved the highest flexural toughness while the C-10×15 composite reinforced with three layers (2.89 %) achieved the lowest one. The reason for this is that the higher elongation of the C-21×21 textiles makes the CRG specimens obviously achieve greater ductility, which

offsets their low flexural strength; as a result, the C-21×21 composites have a greater flexural toughness. The failure mode of all the specimens shows either a pure bending failure or a peeling off the geomortar at the matrix/fiber interface due to the rupture of some filaments in the outer layer and the loss of the bonding strength of the fiber yarn in the matrix leading to the slippage of the fiber yarns within the matrix The results obtained in the four-point bending test of carbon textiles reinforced geomortar suggest that the C-10×15 composites are suitable for high-strength and low-ductility applications while the composites reinforced with the remaining two types of carbon textile are useful for high-ductility applications.

- Using the geomortar with higher mechanical strength can significantly improve the mechanical strength of the CRG specimens.
- The fact that when the cover layer thickness guarantees the anchoring capability of the textile in the matrix, the specimens with thinner cover layer will delay the development of the crack width as long as possible, due to the tension efficiency of the textile leading to both geopolymer mortar and textile undergoing collectively better load-bearing capacity under loading.
- In contrast to basalt textiles, the specimens reinforced with carbon textiles provide a much better effect on the mechanical properties of the resulting composites. For example, specimens reinforced with a 1-carbon layer (41 MPa) have achieved flexural strength higher than those with 4-basalt layers (29.72 MPa) reinforced specimens. Although the price of carbon fiber is much higher than basalt fiber, the production of the composite with carbon textile provides a more reinforcing effect and saves much time for sample production.
- The introduction of chopped basalt fiber to geomortar improved significantly the flexural properties of textile geopolymer composites. The addition of the BF to geomortar obviously improved the mechanical strength of the composites, however only the high dose level of the BF can help to improve both the mechanical properties and failure modes. Failure mode can shift from a catastrophic manner due to the debonding and collapse phase to pure bending failure due to the slipping of fiber yarn in the matrix.
- Under the Charpy impact test, textile geomortar composites have shown impressive dynamic shock resistance. For example, non-reinforced composites have an average impact strength of 6.1 kJ/m^2. The composites reinforced with 4-basalt textile layers

and 2-carbon textile layer increased in impact strength approximately by 557% (40.10 kJ/m^2) and 1663% (107.55 kJ/m^2), respectively. Tested results also showed that the impact strength of composite reinforced with 3-carbon layers is not higher than one with 2-carbon layers. However, under static loading test (four-point bending test) the C-10x15 textile composites with 3 reinforcing layers showed much higher flexural strength than those with 2 reinforcing layers. This phenomenon can be attributed to the anchoring capacity of textile reinforcement in geomortar under dynamic loading tests. The thickness of the geomortar layer between textile layers may be reasonable for static loading tests but may not be strong enough to anchor the fiber yarns of textiles under impact loading tests.

- Based on the references and empirical results achieved in this study, it can conclude that although basalt fiber is proved to have partial loss of strength; however, the mechanical strength of the composites at the age of 365 days is still good, compared to those at 28 days.

9.2 Limitations and Future Directions

- Only long-term mechanical strength of basalt fiber geomortar composite was studied in this dissertation. The composite strength was reduced over time due to fiber degradation, but only at a certain period of time. The mechanisms of fiber degradation are not explained. So the investigation on this behaviour needs to be explored in the future.
- C-10x15 textile geomortar composites with 2 – 3 reinforcing layers were displayed high flexural strength. However, accompanied by this value is a catastrophic failure mode despite the BF added to geomortar matrix. This is attributed to the fact that the sample thickness is unreasonable for reinforcing multiple layers. The composite samples with a thickness of 15 mm produced in this study were tested. The investigation on the optimum thickness of the samples when using reinforcing multiple layers of this type of carbon textile should be carried out to improve the failure manner.
- Geopolymers are known to be fire-resistant materials. The investigation on the fire-resistant behaviour of the textile geomortar composites at elevated temperatures should be studied in the future.

- The durability of the construction materials significantly influences their service life. Although the 365-day composite strength exposed at lab temperature remains well compared to 25-day one, the other durability properties such as chloride and sulfuric acid resistance, freezing, and thawing durability should be carried out.

REFERENCES

[1] Verian K. P. and Behnood A. Effects of deicers on the performance of concrete pavements containing air-cooled blast furnace slag and supplementary cementitious materials. Cem. Concr. Compos., July 2018, **90**, 27–41.

[2] Meyer C. The greening of the concrete industry. Cem. Concr. Compos., 2009, **31**(8), 601–605.

[3] Davidovits P. J. Properties of Geopolymer Cements. First Int. Conf. Alkaline Cem. Concr., 1994, 131–149.

[4] Butler M., Lieboldt M., and Mechtcherine V. Application of Textile-Reinforced Concrete (TRC) for structural strengthening and in prefabrication. In: Proceedings of the International Conference on Advanced Concrete Materials (ACM); Stellenbosch, South Africa, 2010, 125–134.

[5] Mechtcherine V. Novel cement-based composites for the strengthening and repair of concrete structures. Constr. Build. Mater. 2013, **41**, 365–373.

[6] Williams Portal N., Flansbjer M., Zandi K., Wlasak L., and Malaga K. Bending behaviour of novel Textile Reinforced Concrete-foamed concrete (TRC-FC) sandwich elements. Compos. Struct., 2017, **177**, 104–118.

[7] Hartig J., Häußler-combe U., and Schicktanz K. Cement & Concrete Composites Influence of bond properties on the tensile behaviour of Textile Reinforced Concrete. Cem. Concr. Compos., 2008, **30**(10), 898–906.

[8] Tysmans T., Adriaenssens S., Cuypers H., and Wastiels J. Structural analysis of small span textile reinforced concrete shells with double curvature. Compos. Sci. Technol., 2009, **69**(11–12), 1790–1796.

[9] Alrshoudi Fahed Abdullah S. Textile Reinforced Concrete : Design Methodology and Novel Reinforcement. PhD Thesis, The University of Leeds, United Kingdom, 2015.

[10] Portal N. W. Sustainability and Flexural Behaviour of Textile Reinforced Concrete. Thesis for the degree of Licentiate of Engineering, Chalmers University of Technology Gothenburg, Sweden, 2013.

[11] Rambo D. A. S., de Andrade Silva F., Toledo Filho R. D., and da Fonseca Martins Gomes O. Effect of elevated temperatures on the mechanical behavior of basalt textile reinforced refractory concrete. Mater. Des., 2015, **65**, 24–33.

[12] Peled A. and Bentur A. Fabric structure and its reinforcing efficiency in textile reinforced cement composites. Composites Part A: Applied Science and Manufacturing, 2003, **34**(2), 107–118.

[13] Barbosa V. F. F., MacKenzie K. J. D., and Thaumaturgo C. Synthesis and characterisation of materials based on inorganic polymers of alumina and silica: Sodium polysialate polymers. Int. J. Inorg. Mater., 2000, **2**(4), 309–317.

[14] Duxson P., Fernández-Jiménez A., Provis J. L., Lukey G. C., Palomo A., and Van

Deventer J. S. J. Geopolymer technology: The current state of the art. J. Mater. Sci., 2007, **42**(9), 2917–2933.

[15] Xu H. and Van Deventer J. S. J. The geopolymerisation of alumino-silicate minerals. International Journal of Mineral Processing, 2000, **59**(3), 247-266.

[16] Komnitsas K. and Zaharaki D. Geopolymerisation : A review and prospects for the minerals industry. Minerals Engineering, 2007, **20**(14), 1261–1277.

[17] Sumajouw D. M. J., Hardjito D., Wallah S. E., Rangan B. V. Fly ash-based geopolymer concrete : study of slender reinforced columns. J Mater Sci, 2007, **42**, 3124–3130.

[18] Higuera I., Varga C., Palomo J. G., Vázquez T., and Puertas F. Mechanical behaviour of alkali-activated blast furnace slag-activated metakaolin blended pastes . Statistical study. Materiales de Construcción, 2012, **62**(306), 163–181.

[19] Duxson P., Provis J. L., Lukey G. C., Mallicoat S. W., Kriven W. M., and Van Deventer J. S. J. Understanding the relationship between geopolymer composition, microstructure and mechanical properties. Colloids Surfaces A Physicochem. Eng. Asp., 2005, **269**(1–3), 47–58.

[20] Duxson P., Mallicoat S. W., Lukey G. C., Kriven W. M., and Van Deventer J. S. J. The effect of alkali and Si / Al ratio on the development of mechanical properties of metakaolin-based geopolymers. Colloids and Surfaces A: Physicochemical and Engineering Aspects, 2007, **292**(1) , 8-20.

[21] Lahoti M., Narang P., Tan K. H., and Yang E. Mix design factors and strength prediction of metakaolin-based geopolymer. Ceram. Int., 2017, **43**(14), 11433–11441.

[22] Kamalloo A., Ganjkhanlou Y., Aboutalebi S. H., and Nouranian H. Research note modeling of compressive strength of metakaolin based geopolymers by the use of artificial. Conference Proceedings, 2010, **23**(2), 145–152.

[23] Rowles M. and Connor B. O. Chemical optimisation of the compressive strength of aluminosilicate geopolymers synthesised by sodium silicate activation of metakaolinite. Journal of Materials Chemistry, 2003, **13**, 1161-1165.

[24] Pan Z., Sanjayan J. G., and Rangan B. V. Fracture properties of geopolymer paste and concrete. Mag. Concr. Res., 2011, **63**(10), 763–771.

[25] Kuenzel C., Vandeperre L. Li, L., Boccaccini A. R., and Cheeseman C. R. Influence of sand on the mechanical properties of metakaolin geopolymers. Construction and Building Materials, 2014, **66**, 442-446.

[26] Wan Q., Rao F., Song S., Cholico-gonz D. F., and Ortiz N. L. Combination formation in the reinforcement of metakaolin geopolymers with quartz sand. Cement and Concrete Composites, 2017, **80**, 115-122.

[27] Çevik A., Alzeebaree R., Humur G., and Eren M. Eff ect of nano-silica on the chemical durability and mechanical performance of fl y ash based geopolymer concrete. Ceramics International , 1 August 2018, **44**(11), 12253-12264.

[28] Duan P., Yan C., and Zhou W. Compressive strength and microstructure of fly ash

based geopolymer blended with silica fume under thermal cycle. Cem. Concr. Compos., 2017, **78**, 108–119.

[29] Shaikh F., Haque S. Effect of nano silica and fine silica sand on compressive strength of sodium and potassium activators synthesised fly ash geopolymer at elevate temperatures. Fire and Materials - Wiley Online Library, April 2018, **42**(3), 324-335.

[30] Jithendra C. and Elavenil S. Effects of Silica Fume on Workability and Compressive Strength Properties of Aluminosilicate Based Flowable Geopolymer Mortar under Ambient Curing. Silicon, 2019, 0–9.

[31] Okoye F. N., Prakash S., and Singh N. B. Durability of fl y ash based geopolymer concrete in the presence of silica fume. J. Clean. Prod., 2017, **149**, 1062–1067.

[32] Nmiri A., Duc M., Hamdi N., Yazoghli-marzouk O., and Srasra E. Replacement of alkali silicate solution with silica fume in metakaolin-based geopolymers. Int J Miner Metall Mater, 2019, **26**, 555–564.

[33] Cheah C. B., Tan L. E., and Ramli M. The engineering properties and microstructure of sodium carbonate activated fly ash / slag blended mortars with silica fume. Compos. Part B, March 2019, **160**, 558–572.

[34] Zawrah M. F., Sawan S. E. A., Khattab R. M., and Abdel-shafi A. A. Effect of nano sand on the properties of metakaolin-based geopolymer : Study on its low rate sintering. Constr. Build. Mater., 2020, **246**, 118486.

[35] Shaikh F. Effect of nano silica and fine silica sand on compressive strength of sodium and potassium activators synthesised fly ash geopolymer at elevated temperatures. Fire and Materials, April 2018, 42(3), 324-335 .

[36] Steinerova M. Mechanical properties of geopolymer mortars in relation to their porous structure. Ceram. - Silikaty, 2011, **55**(4), 362–372.

[37] Kabay N. Abrasion resistance and fracture energy of concretes with basalt fiber," *Constr. Build. Mater.*, 2014, **50**, 95–101.

[38] Ranjbar N. and Zhang M. Fiber-reinforced geopolymer composites : A review. Cem. Concr. Compos., 2020, **107**, 103498.

[39] J. Davidovits. Ceramic-ceramic composite material and production method, US Patent No. 4 888 311, 19 December 1989.

[40] Davidovits J. Alkaline aluminosilicate geopolymeric matrix for composite

materials with fibre reinforcement and method for obtaining same, US Patent No. 5 798 307, 25 August 1998.

[41] Davidovits J. Geopolymers: Inorganic polymeric new materials. Journal of thermal analysis, 1991, 37, 1633–1656.

[42] Rahman A. S. Effects of nano fibers on properties of geopolymer composites. Nanotechnology in Eco-efficient Construction, 2019, 123–140.

[43] Shaikh F. U. A. Deflection hardening behaviour of short fibre reinforced fly ash based geopolymer composites. Mater. Des., 2013, **50**, 674–682.

[44] Lin T., Jia D., Wang M., He P., and Liang D. Effects of fibre content on mechanical properties and fracture behaviour of short carbon fibre reinforced geopolymer matrix composites. Bull Mater Sci, 2009, **32**, 77–81.

[45] Masi G., Rickard W. D. A., Chiara M., and Van Riessen A. The effect of organic and inorganic fibres on the mechanical and thermal properties of aluminate activated geopolymers. Compos. Part B, 2015, **76**, 218–228.

[46] Bhutta A., Farooq M., and Banthia N. Performance characteristics of micro fiber reinforced geopolymer mortars for repair. Constr. Build. Mater., 2019, **215**, 605–612.

[47] Sukontasukkul P., Pongsopha P., Chindaprasirt P., and Songpiriyakij S. Flexural performance and toughness of hybrid steel and polypropylene fibre reinforced geopolymer. Constr. Build. Mater., 2018, **161**, 37–44.

[48] Uddin F., Shaikh, A. and Hosan A. Mechanical properties of steel fibre reinforced geopolymer concretes at elevated temperatures. Constr. Build. Mater., 2016, **114,** 15–28.

[49] Pehlivanli Z. O., Uzun I., and Demir I. Mechanical and microstructural features of autoclaved aerated concrete reinforced with autoclaved polypropylene, carbon, basalt and glass fiber. Constr. Build. Mater., 2015, **96**, 428–433.

[50] Lin T., Jia D., He P., and Wang M. In situ crack growth observation and fracture behavior of short carbon fiber reinforced geopolymer matrix composites. Materials Science and Engineering: A, April 2010, **527**(9), 2404-2407.

[51] Lin T., Jia D., He P., Wang M., and Liang D. Effects of fiber length on mechanical properties and fracture behavior of short carbon fiber reinforced geopolymer matrix composites. Materials Science and Engineering: A, December 2008, **497**(1–2), 181-185.

[52] Alzeer M. and Mackenzie K. Applied Clay Science Synthesis and mechanical properties of novel composites of inorganic polymers (geopolymers) with unidirectional natural flax fibres (phormium tenax). Appl. Clay Sci., 2013, **75–76**, 148–152.

[53] Nair Q. Z. Æ. B. and Balaguru Æ. T. R. Æ. P. Novel geopolymer based composites with enhanced ductility. J Mater Sci, 2007, **42**, 3131–3137.

[54] He P., Jia D., Lin T., Wang M., and Zhou Y. Effects of high-temperature heat treatment on the mechanical properties of unidirectional carbon fiber reinforced geopolymer composites. Ceram. Int., 2010, **36**(4), 1447–1453.

[55] Pernica D., Reis P. N. B., Ferreira J. A. M., and Louda P. Effect of test conditions on the bending strength of a geopolymer-reinforced composite. J Mater Sci, 2010, **45**, 744–749.

[56] Samal S., Thanh P. N., Marvalová B., Petríková I., Katleen A.M. and Stepan V. Correlation of microstructure and mechanical properties of various fabric reinforced geo-polymer composites after exposure to elevated temperature. Ceram. Int., 2015, **41**(9), 12115–12129.

[57] Samal S., Marvalová B., Petríková I., Vallons K. A. M., Lomov S. V, and Rahier H.

Impact and post impact behavior of fabric reinforced geopolymer composite. Constr. Build. Mater., 2016, **127**, 111–124.

[58] Assaedi H., Shaikh F. U. A., and Low I. M. Characterizations of flax fabric reinforced nanoclay-geopolymer composites. Compos. Part B, 2016, **95**, 412–422.

[59] Alomayri, T., Shaikh, F.U.A. and Low, I.M.. Thermal and mechanical properties of cotton fabric-reinforced geopolymer composites. J Mater Sci, 2013, **48**, 6746–6752.

[60] Constancio Trindade A.C., Alcamand H.A., Ribeiro Borges P.H. and de Andrade Silva F. Influence of Elevated Temperatures on the Mechanical Behavior of Jute-Textile- Reinforced Geopolymers Behavior of Jute-Textile-Reinforced Geopolymers. J. Ceram. Sci. Technol., 2017, **398,** 389–398.

[61] Novitskii A. G. High-temperature heat-insulating materials based on fibers from basalt-type rock materials. Refractories and Industrial Ceramics, 2004, **45**, 144–146.

[62] Fiore V., Scalici T., Di Bella G., and Valenza A. A review on basalt fibre and its composites. Compos. Part B Eng., 2015, **74**, 74–94.

[63] Sim J., Park C., and Moon D. Y. Characteristics of basalt fiber as a strengthening material for concrete structures. Compos. Part B Eng., 2005, **36**(6–7), 504–512.

[64] Scheffler C., Förster T., Mäder E., Heinrich G., Hempel S., and Mechtcherine V. Aging of alkali-resistant glass and basalt fibers in alkaline solutions: Evaluation of the failure stress by Weibull distribution function. J. Non. Cryst. Solids, 2009, **355**(52–54), 2588–2595.

[65] Wei B., Cao H., and Song S. Tensile behavior contrast of basalt and glass fibers after chemical treatment. Mater. Des., 2010, **31**(9), 4244–4250.

[66] Williams Portal N., Flansbjer M., Johannesson P., Malaga K., and Lundgren K. Tensile behaviour of textile reinforcement under accelerated ageing conditions. J. Build. Eng., 2016, **5**, 57–66.

[67] Rill E., Lowry D. R., and Kriven W. M. Properties of Basalt Fiber Reinforced Geopolymer Composites. In: Strategic Materials and Computational Design - 34th International Conference on Advanced Ceramics and Composites, ICACC, 2010, **31**, 57–67.

[68] Ronad A., Karikatti V. B., and Dyavanal S. S. A STUDY ON MECHANICAL PROPERTIES OF GEOPOLYMER CONCRETE REINFORCED WITH BASALT FIBER. International Journal of Research in Engineering and Technology, 2016, **5**(7), 474–478.

[69] Arunagiri1 K., Elanchezhiyan P., Marimuthu V., Arunkumar G. and Rajeswaran P. MECHANICAL PROPERTIES OF BASALT FIBER BASED GEOPOLYMER CONCRETE. International Journal of Science, Engineering and Technology Research, April 2017, **6**(4) ISSN: 2278 -7798.

[70] Guo X. and Pan X. Mechanical properties and mechanisms of fiber reinforced fly ash – steel slag based geopolymer mortar. Constr. Build. Mater., 2018, **179**, 633–641.

[71] Shaikh F. and Haque S. Behaviour of Carbon and Basalt Fibres Reinforced Fly Ash

Geopolymer at Elevated Temperatures. Int. J. Concr. Struct. Mater., 2018, **12**, 35.

[72] Ren D., Yan C., Duan P., Zhang Z., Li L., and Yan Z. Durability performances of wollastonite , tremolite and basalt fiber reinforced metakaolin geopolymer composites under sulfate and chloride attack. Constr. Build. Mater., 2017, **134**, 56–66.

[73] Celik A., Yilmaz K., Canpolat O., Al-mashhadani M. M., Aygörmez Y., and Uysal M. High-temperature behavior and mechanical characteristics of boron waste additive metakaolin based geopolymer composites reinforced with synthetic fibers. Constr. Build. Mater., 2018, **187**, 1190–1203.

[74] Li W. and Xu J. Mechanical properties of basalt fiber reinforced geopolymeric concrete under impact loading. Mater. Sci. Eng. A, 2009, **505**(1–2), 178–186.

[75] Dias D. P. and Thaumaturgo C. Fracture toughness of geopolymeric concretes reinforced with basalt fibers. Cement and Concrete Composites, 2005, **27**(1), 49-54.

[76] Kim J. S., Lim J. H., and Huh Y. Melt-spinning basalt fibers based on dielectric heating and steady-state process characteristics. Fibers Polym., 2013, **14**(7), 1148–1156.

[77] Toutanji H. and Deng Y. Comparison between Organic and Inorganic Matrices for RC Beams Strengthened with Carbon Fiber Sheets. Journal of Composites for Construction, October 2007, **11**(5), 35–42.

[78] Tamburini S., Natali M., Garbin E., Panizza M., Favaro M., and Valluzzi M. R. Geopolymer matrix for fibre reinforced composites aimed at strengthening masonry structures. Constr. Build. Mater., 2017,**141**, 542–552.

[79] Vasconcelos E., Fernandes S., De Aguiar J. L. B., and Pacheco-torgal F. Concrete retrofitting using metakaolin geopolymer mortars and CFRP. Constr. Build. Mater., 2011, **25**(8), 3213–3221.

[80] Menna C. Asprone D., Ferone C., Colangelo F., Balsamoa A., Protaa A., Cioffib R., Manfredia G. Use of geopolymers for composite external reinforcement of RC members. Composites Part B: Engineering, 2013, **45**(1), 1667-1676.

[81] Zhang H., Hao X., and Fan W. Experimental study on high temperature properties of carbon fiber sheets strengthened concrete cylinders using geopolymer as adhesive. Procedia Eng., 2016, **135**, 47–55.

[82] Najm H., Secaras J., Balaguru P., and Asce M. Compression Tests of Circular Timber Column Confined with Carbon Fibers Using Inorganic Matrix. Journal of Materials in Civil Engineering, February 2007, **19**(2), 198–205.

[83] Yan H., Yan J., Kodur V., and Cao L. Mechanical behavior of concrete beams shear strengthened with textile reinforced geopolymer mortar. Eng. Struct., 2019, **196**, 109348.

[84] Fahim G., Mirza J., Ismail M., Ghoshal S. K., and Abdulameer A. Geopolymer mortars as sustainable repair material : A comprehensive review. Renew. Sustain. Energy Rev., 2017, **80**, 54–74.

[85] Santarelli M. L., Sbardella F., Zuena M., Tirillò J., and Sarasini F. Basalt fiber

reinforced natural hydraulic lime mortars : A potential bio-based material for restoration. J. Mater., 2014, **63**, 398–406.

[86] Le Chi H., Louda P., Periyasamy A., Bakalova T., and Kovacic V. Flexural Behavior of Carbon Textile-Reinforced Geopolymer Composite Thin Plate. Fibers, 2018, **6**(4), 87.

[87] ASTM C1609. Standard Test Method for Flexural Performance of Fiber-Reinforced Concrete (Using Beam With Third-Point Loading).

[88] Li V. C. Engineered Cementitious Composites (ECC) – Material , Structural , and Durability Performance. In: Nawy, editor. Concrete Construction Engineering Handbook. CRC Press, 2008.

[89] Hinzen M. and Brameshuber W. Improvement of Serviceability and Strength of Textile Reinforced Concrete by using Short Fibres. In Proceedings of the 4th Colloquium on Textile Reinforced Structures, Dresden, Germany, 3–5 June 2009, 261–272.

[90] Barhum R. and Mechtcherine V. Mechanical Behaviour under Tensile Loading of Textile Reinforced Concrete with Short Fibres. In: 6th colloquium on textile reinforced structures (CTRS6), Anwendertagung, Bundesanstalt fu¨r Materialforschung und -pru¨fung. (BAM), Berlin, 19–20 September, 2011, 175–186.

[91] Barhum R. and Mechtcherine V. Influence of short dispersed and short integral glass fibres on the mechanical behaviour of textile-reinforced concrete. Materials and Structures, 2013, **46**, 557–572.

[92] Pakravan H. R., Jamshidi M., and Rezaei H. Effect of textile surface treatment on the flexural properties of cementitious composites. Journal of Industrial Textiles, 2016, **46**(1), 116–129

[93] Kistaiah N., Kiran C. U., Reddy G. R., and Rao M. S. Mechanical characterization of hybrid composites : A review. Journal of Reinforced Plastics and Composites, 2014, **33**(14), 1364–1372.

[94] Yan S., He P., Jia D., Yang Z., and Duan X. Effect of fiber content on the microstructure and mechanical properties of carbon fiber felt reinforced geopolymer composites. *Ceramics International*, May 2016, **42**(6), 7837–7843.

[95] Branston J., Das S., Kenno S. Y., and Taylor C. Influence of basalt fibres on free and restrained plastic shrinkage. Cement and Concrete Composites, November 2016, **74**, 182-190

[96] Caminero M. A., Rodríguez G. P., and Muñoz V. Effect of stacking sequence on Charpy impact and flexural damage behavior of composite laminates. Composite Structures, 2016, **136**, 345–357.

[97] Alomayri T., Shaikh F. U. A., and Low I. M. Synthesis and mechanical properties of cotton fabric reinforced geopolymer composites. Composites : Part B, 2014, **60**, 36–42.

[98] Fujiyama, R., Darwish, F., and Perdra, M. V. Mechanical Characterization of Sisal Reinforced Cement Mortar. Theor. Appl. Mech. Lett., 2014, **4**(6).

[99] Pereira, M. V., Fujiyama, R., Darwish, F., and Alves, G. T. On the Strengthening of Cement Mortar by Natural Fibers. Mater. Res., 2015, **18**(1), 2015, 177–183.

[100] Yalçinkaya, C., Sznajder, J., Beglarigale, A., Sancakoglu, O., and Yazici, H. Abrasion Resistance of Reactive Powder Concrete: The Influence of Water-to-Cement Ratio and Steel Micro-Fibers. Adv. Mater. Lett., 2014, **5**(6), 345–351.

[101] Al-Oraimi, S. K. and Seibi, A. C. Mechanical Characterisation and Impact Behaviour of Concrete Reinforced with Natural Fibers. Compos. Struct., 1995, **32**(1), 165–171.

[102] Gopalaratnam, V. S., Shah, S. P., and John, R. A Modified Instrumented Charpy Test for Cement-Based Composites. Exp. Mech., 1984, **24**(2), 102–111.

[103] Gopalaratnam, V. S. and Shah, S. P. Properties of Streel Fiber Reinforced Concrete Subjected to Impact Loading. ACI J. Proc., 1986, **83**(1), 117–126.

LIST OF AUTHOR'S PUBLICATIONS

1) Hiep Le Chi, Petr Louda, Aravin Prince Periyasamy, Totka Bakalova and Vladimir Kovacic. Flexural Behavior of Carbon Textile-Reinforced Geopolymer Composite Thin Plate. Fibers [online]. 2018, 6(4), 87. ISSN 2079-6439. Available on: https://www.mdpi.com/2079-6439/6/4/87.
2) Hiep Le Chi, Petr Louda, Su Le Van, Lukas Volesky, Totka Bakalova and Vladimir Kovacic. Composite Performance Evaluation of Basalt Textile-Reinforced Geopolymer Mortar. Fibers [online]. 2019, 7(63). ISSN 2079-6439. Available on: https://www.mdpi.com/2079-6439/7/7/63.
3) Hiep Le Chi and Petr Louda. Flexural Performance Evaluation of Various Carbon Fibre Fabric Reinforced Geopolymer Composite. Ceramics-Silikáty [online]. 2020, 64(2), 215–226. ISSN 1804-5847. Available on: http://www.ceramics-silikaty.cz/index.php?page=cs_detail_doi&id=1320.
4) Hiep Le Chi, Pavlína Hájková, Su Le Van, Petr Louda and Lukáš Voleský. Water Absorption Properties of Geopolymer Foam after Being Impregnated with Hydrophobic Agents. Materials [online]. 2019, 12(24), 4162. ISSN 1996-1944. Available on: https://www.mdpi.com/1996-1944/12/24/4162.
5) Hiep Le Chi, Petr Louda, Totka Bakalova and Vladimír Kovačič. Preparation and Mechanical Properties of Potassium Metakaolin Based Geopolymer Paste. Advanced Engineering Forum [online]. 2019, 31(3), 38 – 45. ISSN 2234-991X. Available on: https://www.scientific.net/AEF.31.38.

6) Su Le Van, Pavlína Hájková, Vladimir Kovacic, Totka Bakalova, Voleský Lukáš, Chi Hiep Le, Ceccon Seifert Kevin, Pereira Peres Amanda and Petr Louda. Thermal conductivity of reinforced geopolymer foams. Ceramics-Silikáty [online]. 2019, 63(4), 365 – 373. ISSN 0862-5468. Available on: http://www.ceramics silikaty.cz/index.php?page=cs_detail_doi&id=1288.
7) Petr Louda, Totka Bakalova, Vladimir Kovacic and Hiep Le Chi. Composite Based on Geopolymer Mortar Reinforced Chopped Basalt Fiber and Carbon Textile. In: The 22nd International Conference STRUTEX 2018. 2019, 58 – 62. ISSN 1335-0617.
8) Miroslav Frydrich, Štěpán Hýsek, Ludmila Fridrichová, Su Le Van, Miroslav Herclík, Miroslav Pechočiaková, Hiep Le Chi and Petr Louda. Impact of flax and basalt fibre reinforcement on selected properties of geopolymer composites. Sustainability [online]. 2020, 12(1). ISSN 2071-1050. Available on: https://www.mdpi.com/2071-1050/12/1/118.
9) Štěpán Hýsek, Miroslav Frydrich, Miroslav Herclík, Petr Louda, Ludmila Fridrichová, Su Le Van and Hiep Le Chi. Fire-resistant sandwich-structured composite material based on alternative materials and its physical and mechanical properties. Materials [online]. 2019, 12(9). ISSN 1996-1944. Available on: https://www.mdpi.com/1996-1944/12/9/1432.
10) Štěpán Hýsek, Miroslav Frydrich, Miroslav Herclík, Petr Louda, Ludmila Fridrichová, Petr Louda, Roman Knizek, Su Le Van and Hiep Le Chi. Permeable Water-Resistant Heat Insulation Panel Based on Recycled Materials and Its Physical and Mechanical Properties. Molecules [online]. 2019, 24(18). ISSN 1420-3049. Available on: https://www.mdpi.com/1420-3049/24/18/3300.
11) Szczypinski, Michal M., Louda Petr, Exnar Petr, Le Chi Hiep, Kovačič, Vladimír, Van Su, Le, Voleský, Lukáš, Bayhan, Elif and Bakalova, Totka. Evaluation of mechanical properties of composite geopolymer blocks reinforced with basalt fibres. Journal Manufacturing Technology [online]. 2018, 18(5), 861 – 865. ISSN 1213-2489. Available on: https://arl.ujep.cz/arl-ujep/cs/detail-ujep_us_cat-0265358-Evaluation-of-mechanical-properties-of-composite-geopolymer-blocks-reinforced-with-basalt-fibres/.
12) Louda Petr, Totka Bakalova and Hiep Le Chi. Textile Reinforced Composite Material Based on Inorganic Aluminosilicate Polymer Matrix. Jemná mechanika a optika. 2019, 64(2 – 3), 61 – 68. ISSN 0447-6441.

13) Van Su Le, Michal M. Szczypinski, Pavlína Hájková, Vladimir Kovacic, Totka Bakalova, LukasVolesky, Le Chi Hiep, and Petr Louda. Mechanical properties of geopolymer foam at high temperature. Science and Engineering of Composite Materials [online]. 2020, 27(1), 129 – 138. ISSN: 2191-0359. Available on: https://www.degruyter.com/view/journals/secm/27/1/article p129.xml?rskey=oQs1ZT&result=4.
14) Bakalova Totka, Tunakova Veronika, Le Chi Hiep, Ryvolova Martina, Kavanova and Volesky Lukáš. Geopolymers with Carbon or Basalt grids and Incorporated MgO Nanoparticles for Shielding Electromagnetic Radiation. In: 11th International Conference on Nanomaterials - Research & Application, Hotel Voronez I, Brno, Czech Republic, EU, October 16th - 18th 2019. April 2020, 73 – 79. ISSN 2694-930X.
15) Totka Bakalova, Petr Louda, Lukas Volesky, Hiep Le Chi, Su Le Van and Vladimir Kovacic. Ověřená technologie povrchových úprav pro protipožární ochranu staveb [ověřená technologie]. KMT-2019-Z/OT-01, Technická univerzita v Liberci 2019.
16) Technická univerzita v Liberci, Liberec I-Staré Město. Termoizolační geopolymerní kompozit IPC: C04B18/08, C04B18/14, C04B14/42, C04B14/30. Původci: Petr Louda, Vladimír Kovačič, Pavlína Hájková, Totka Bakalova, Lukáš Voleský, Van Su Le, Chi Hiep Le. Česká republika Užitný vzor PUV 2019-36526. 20.12.2019. Available on: https://isdv.upv.cz/doc/FullFiles/UtilityModels/FullDocuments/FDUM0033/uv033566.pdf.